Highlights from Large High Altitude Air Shower Observatory

Dmitri Semikoz

APC, Paris

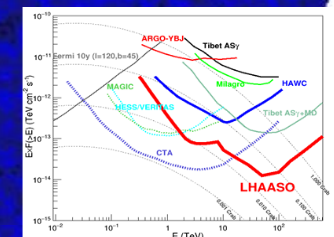

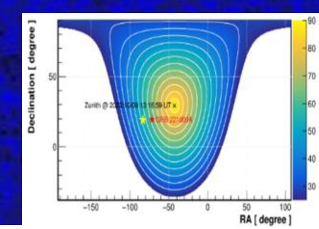

Plan

- Gamma-ray astronomy
- Introduction: LHAASO detector
- Cosmic rays at knee
- First LHAASO catalog of gamma-ray sources
- Diffuse gamma-ray emission from Galaxy
- GRB 221009A
- Cygnus region
- Micro-quasars
- Dark matter limits
- Conclusions

LHAASO detector

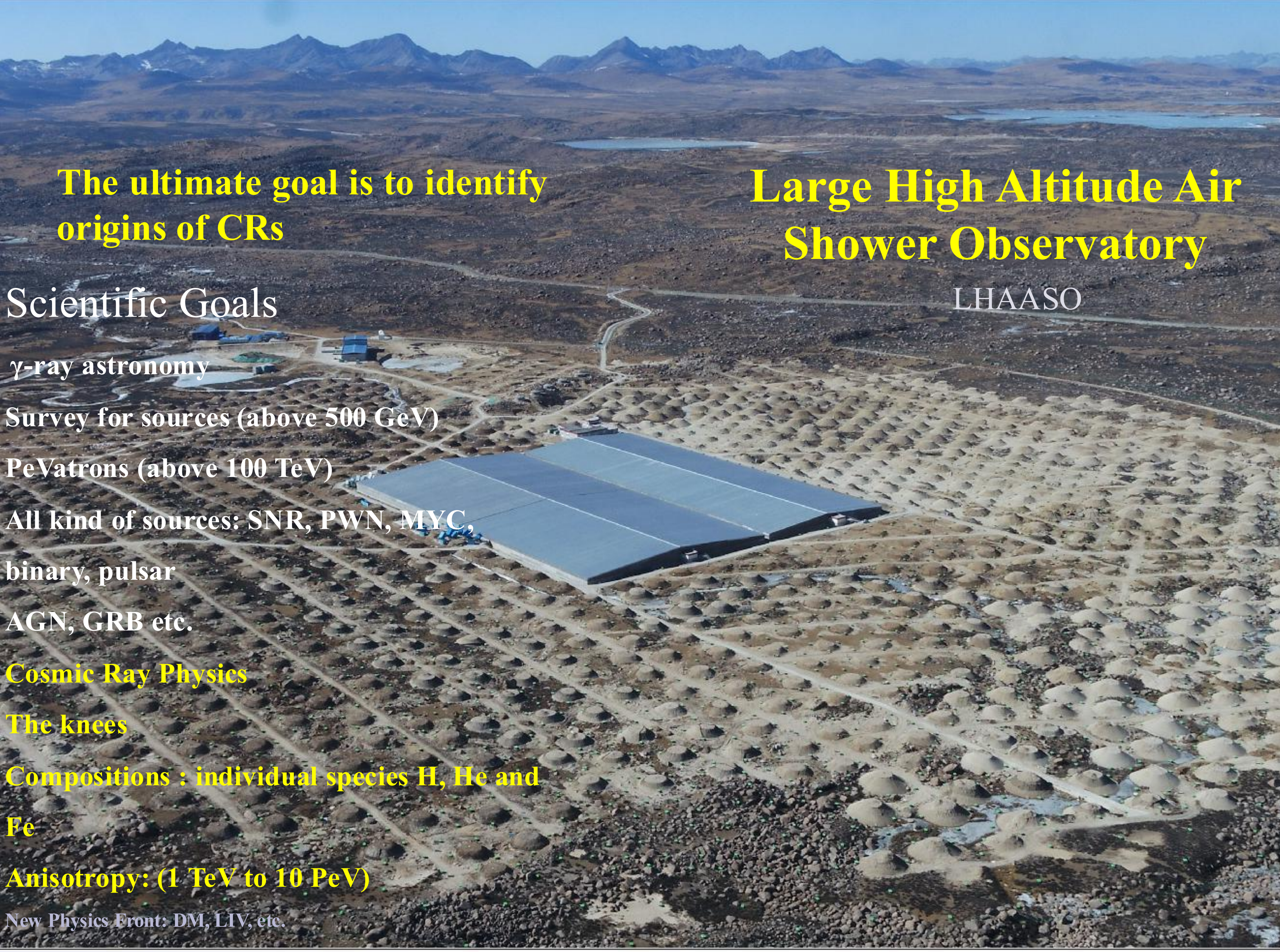

Large High Altitude Air Shower Observatory

LHAASO

The ultimate goal is to identify origins of CRs

Scientific Goals

γ-ray astronomy

Survey for sources (above 500 GeV)

PeVatrons (above 100 TeV)

All kind of sources: SNR, PWN, MYC, binary, pulsar AGN, GRB etc.

Cosmic Ray Physics

The knees

Compositions : individual species H, He and Fe

Anisotropy: (1 TeV to 10 PeV)

New Physics Front: DM, LIV, etc.

LHAASO collaboration

- **316 Scientists**

- **36 institutions**
- **from 5 countries**

Zhen Cao, F. Aharonian, Y.X. Bai, Y.W. Bao, D. Bastieri, X.J. Bi, Y.J. Bi, W. Bian,
A.V. Bukevich, C.M. Cai, W.Y. Cao, Zhe Cao, J. Chang, J.F. Chang, A.M. Chen, E.S. Chen,
G.H. Chen, H.X. Chen, Liang Chen, Long Chen, M.J. Chen, M.L. Chen, Q.H. Chen, S. Chen,
S.H. Chen, S.Z. Chen, T.L. Chen, X.B. Chen, X.J. Chen, Y. Chen, N. Cheng, Y.D. Cheng,
M.C. Chu, M.Y. Cui, S.W. Cui, X.H. Cui, Y.D. Cui, B.Z. Dai, H.L. Dai, Z.G. Dai, Danzengluobu,
Y.X. Diao, X.Q. Dong, K.K. Duan, J.H. Fan, Y.Z. Fan, J. Fang, J.H. Fang, K. Fang, C.F. Feng,
H. Feng, L. Feng, S.H. Feng, X.T. Feng, Y. Feng, Y.L. Feng, S. Gabici, B. Gao, C.D. Gao, Q. Gao,
W. Gao, W.K. Gao, M.M. Ge, T.T. Ge, L.S. Geng, G. Giacinti, G.H. Gong, Q.B. Gou, M.H. Gu,
F.L. Guo, J. Guo, X.L. Guo, Y.Q. Guo, Y.Y. Guo, Y.A. Han, O.A. Hannuksela, M. Hasan, H.H. He,
H.N. He, J.Y. He, X.Y. He, Y. He, S. Hernández-Cadena, B.W. Hou, C. Hou, X. Hou, H.B. Hu, S.C. Hu,
C. Huang, D.H. Huang, J.J. Huang, T.Q. Huang, W.J. Huang, X.T. Huang, X.Y. Huang, Y. Huang,
Y.Y. Huang, X.L. Ji, H.Y. Jia, K. Jia, H.B. Jiang, K. Jiang, X.W. Jiang, Z.J. Jiang, M. Jin, S. Kaci,
M.M. Kang, I. Karpikov, D. Khangulyan, D. Kuleshov, K. Kurinov, B.B. Li, Cheng Li, Cong Li, D. Li,
F. Li, H.B. Li, H.C. Li, Jian Li, Jie Li, K. Li, L. Li, R.L. Li, S.D. Li, T.Y. Li, W.L. Li, X.R. Li, Xin Li, Y. Li,
Y.Z. Li, Zhe Li, Zhuo Li, E.W. Liang, Y.F. Liang, S.J. Lin, B. Liu, C. Liu, D. Liu, D.B. Liu, H. Liu, H.D. Liu,
J. Liu, J.L. Liu, J.R. Liu, M.Y. Liu, R.Y. Liu, S.M. Liu, W. Liu, X. Liu, Y. Liu, Y. Liu, Y.N. Liu, Y.Q. Lou,
Q. Luo, Y. Luo, H.K. Lv, B.Q. Ma, L.L. Ma, X.H. Ma, J.R. Mao, Z. Min, W. Mitthumsiri, G.B. Mou, H.J. Mu,
A. Neronov, K.C.Y. Ng, M.Y. Ni, L. Nie, L.J. Ou, L.J. Ou, P. Pattarakijwanich, Z.Y. Pei, J.C. Qi, M.Y. Qi,
B. J.J. Qin, A. Raza, C.Y. Ren, D. Ruffolo, A. S\'aiz, D. Semikoz, L. Shao, O. Shchegolev, Y.Z. Shen,
C. X.D. Sheng, Z.D. Shi, F.W. Shu, H.C. Song, Yu.V. Stenkin, V. Stepanov, Y. Su, D.X. Sun, H. Sun,
D. Q.N. Sun, X.N. Sun, Z.B. Sun, N.H. Tabasam, J. Takata, P.H.T. Tam, H.B. Tan, Q.W. Tang, R. Tang,
E. Z.B. Tang, W.W. Tian, C.N. Tong, L.H. Wan, C. Wang, G.W. Wang, H.G. Wang, J.C. Wang, K. Wang,
F. Kai Wang, Kai Wang, L.P. Wang, L.Y. Wang, L.Y. Wang, R. Wang, W. Wang, X.G. Wang, X.J. Wang,
G. X.Y. Wang, Y. Wang, Y.D. Wang, Z.H. Wang, Z.X. Wang, Zheng Wang, D.M. Wei, J.J. Wei, Y.J. Wei,
H. T. Wen, S.S. Weng, C.Y. Wu, H.R. Wu, Q.W. Wu, S. Wu, X.F. Wu, Y.S. Wu, S.Q. Xi, J. Xia, J.J. Xia,
I. G.M. Xiang, D.X. Xiao, G. Xiao, Y.L. Xin, Y. Xing, D.R. Xiong, Z. Xiong, D.L. Xu, R.F. Xu, R.X. Xu,
J. W.L. Xu, L. Xue, D.H. Yan, J.Z. Yan, T. Yan, C.W. Yang, C.Y. Yang, F.F. Yang, L.L. Yang, M.J. Yang,
K. R.Z. Yang, W.X. Yang, Z.H. Yang, Z.G. Yao, X.A. Ye, L.Q. Yin, N. Yin, X.H. You, Z.Y. You, Q. Yuan,
L. H. Yue, H.D. Zeng, T.X. Zeng, W. Zeng, X.T. Zeng, M. Zha, B.B. Zhang, B.T. Zhang, C. Zhang, F. Zhang,
M. H. Zhang, H.M. Zhang, H.Y. Zhang, J.L. Zhang, Li Zhang, P.F. Zhang, P.P. Zhang, R. Zhang, S.R. Zhang,
N. S.S. Zhang, W.Y. Zhang, X. Zhang, X.P. Zhang, Yi Zhang, Yong Zhang, Z.P. Zhang, J. Zhao, L. Zhao,
O. L.Z. Zhao, S.P. Zhao, X.H. Zhao, Z.H. Zhao, F. Zheng, W.J. Zhong, B. Zhou, H. Zhou, J.N. Zhou, M. Zhou,
P. P. Zhou, R. Zhou, X.X. Zhou, X.X. Zhou, B.Y. Zhu, C.G. Zhu, F.R. Zhu, H. Zhu, K.J. Zhu, Y.C. Zou, X. Zuo,
(The LHAASO Collaboration)

LHAASO site

- Haizi Mountain, Sichuan province, China
- Location：29º21’ 27.6” N, 100º08’19.6” E
- Altitude：4410 m a.s.l.
- 10 km from Yading Airport

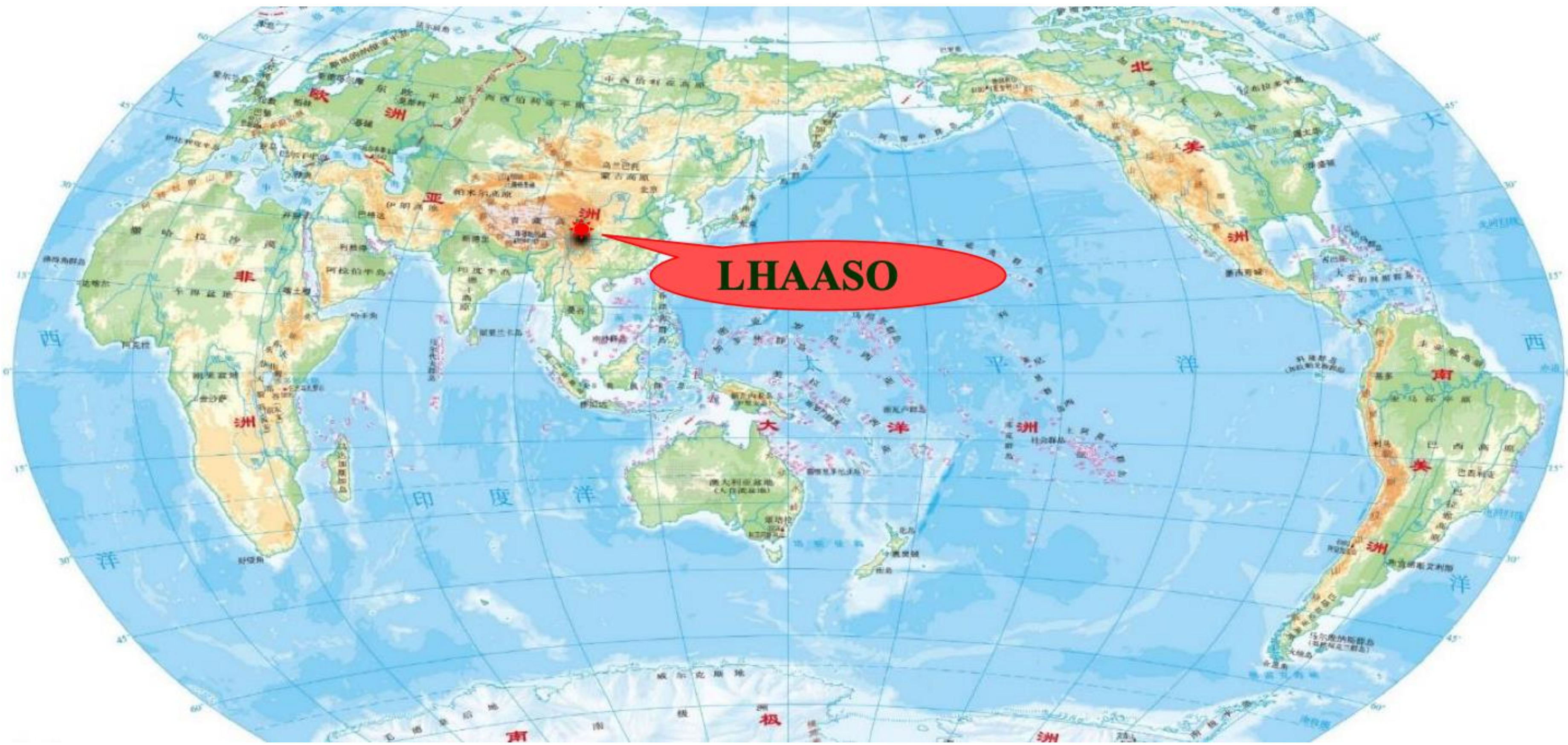

LHAASO Layout

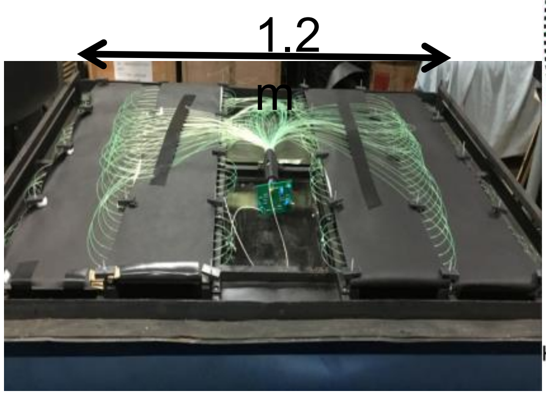

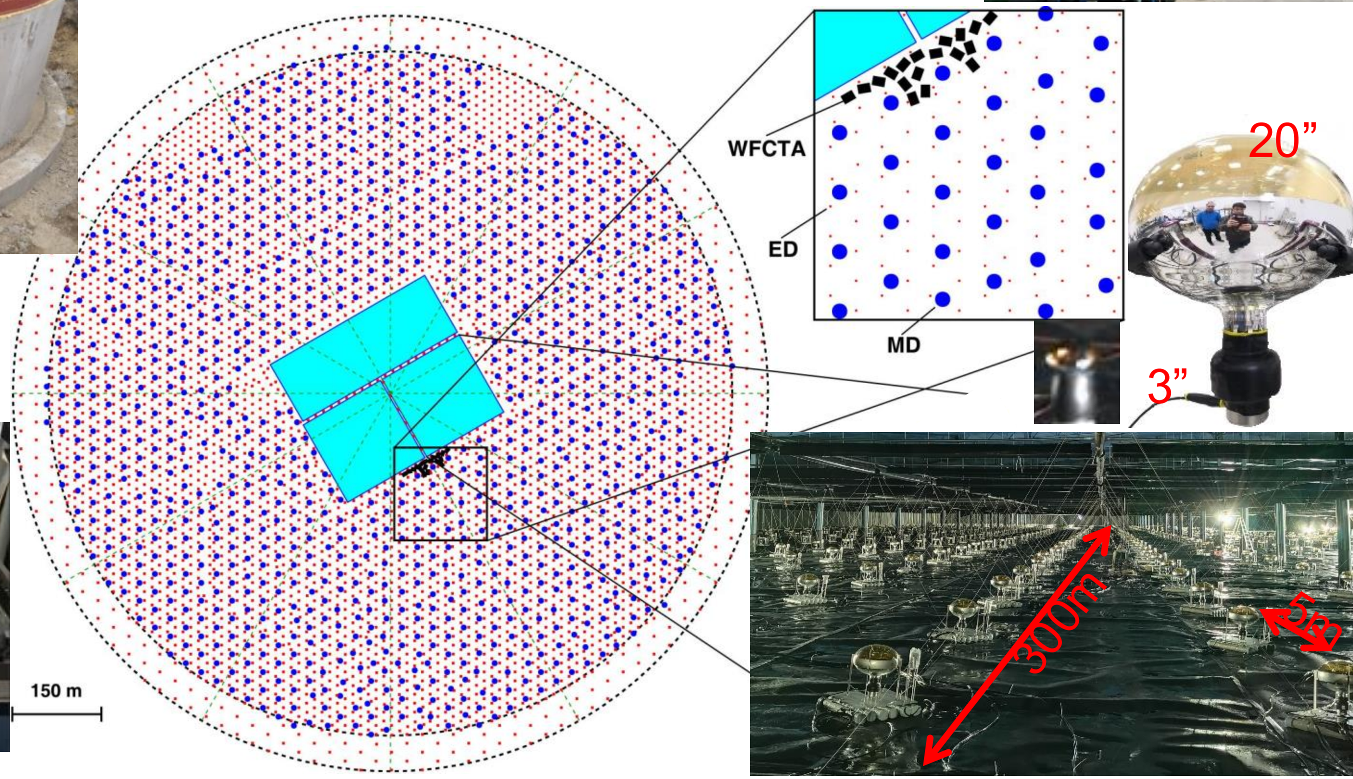

Operation of LHAASO

- KM2A is operated with >99.4% duty cycle and event rate $2x10^8$ /day
- WCDA is operated with 98.4% and event rate $3x10^9$ /day
- Data acquisition time of WFCTA >1400 hrs and number of matched events ~70 million

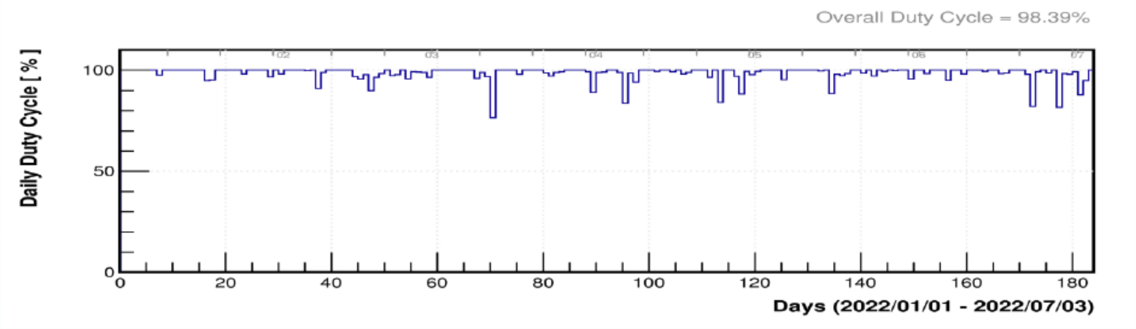

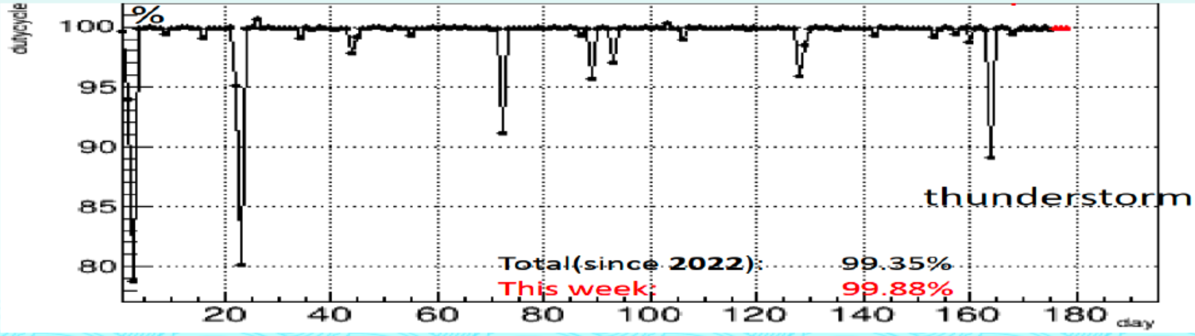

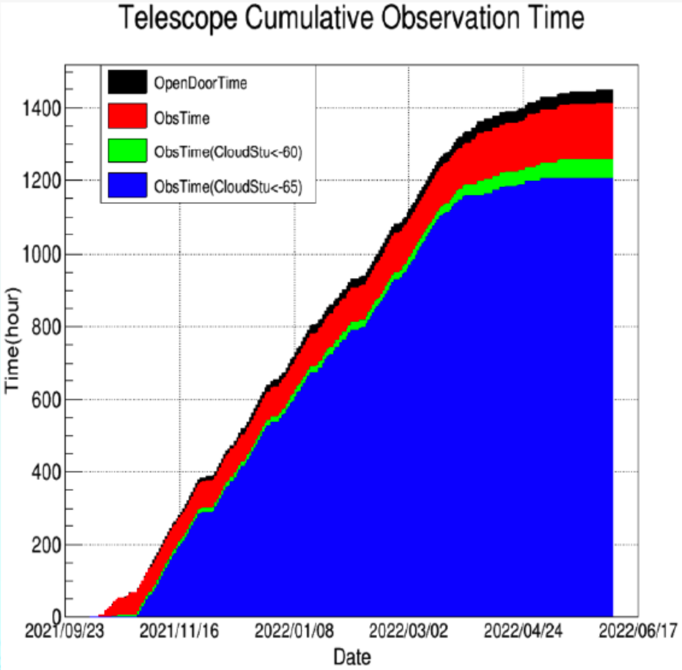

LHAASO-WCDA
Water Cherenkov Detector Array

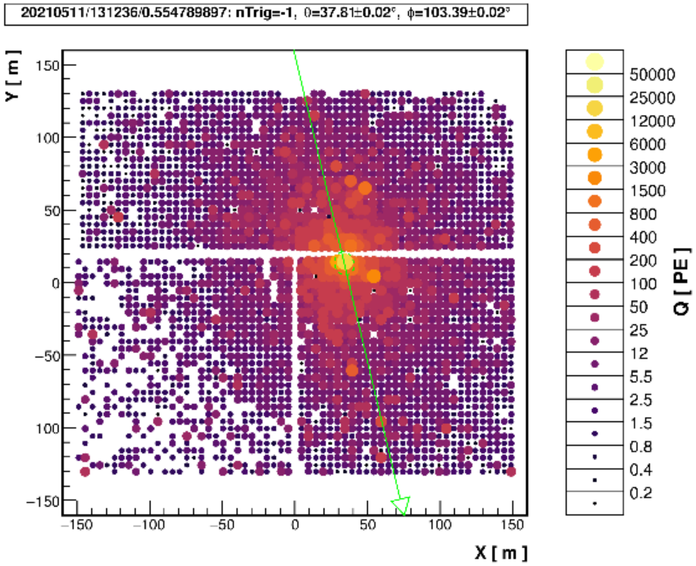

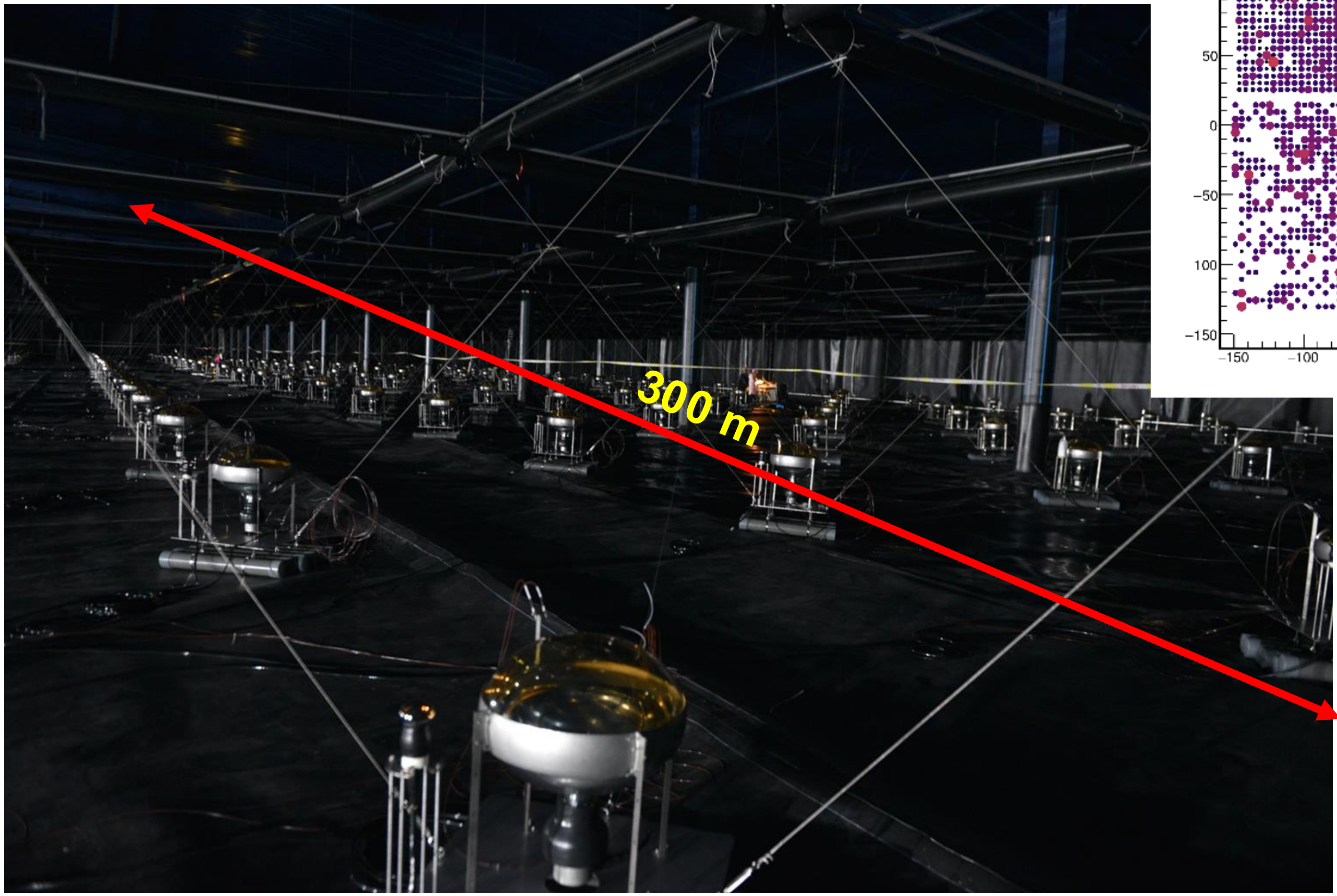

- **Area :** 78,000 m^2
- **Detector units :** 3120
- **Energy Range :** 0.1-10 TeV

LHAASO-KM2A

Selection of γ–rays out of CR background

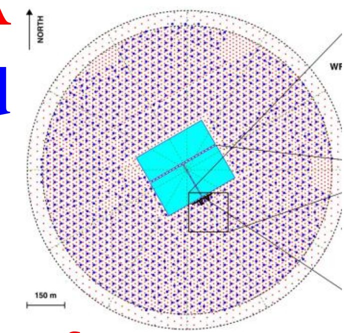

Active Area for Muons vs. Array Area: 4%

~1 PeV CR event: many muons

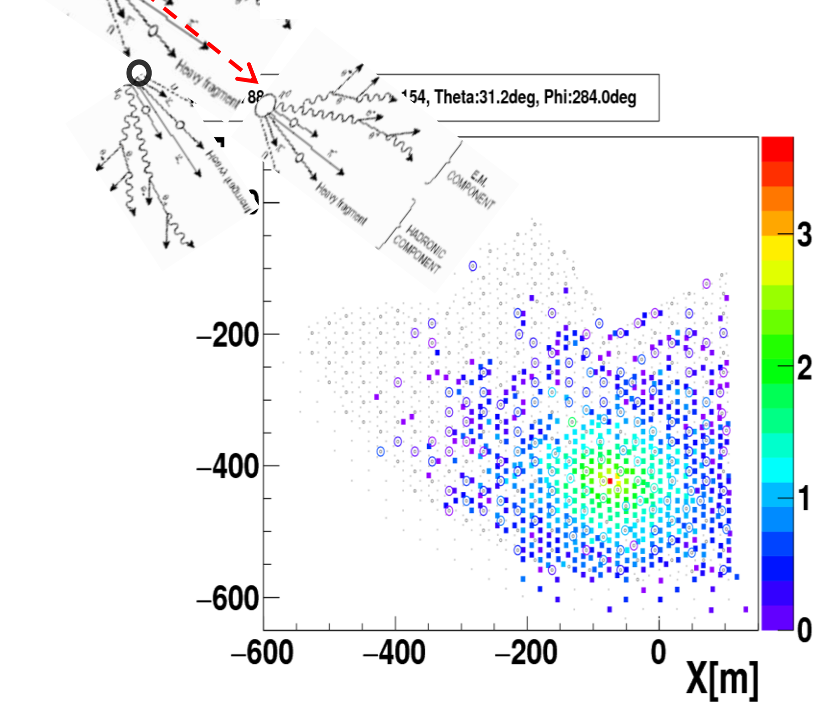

~1 PeV γ–ray event : very few muons

~1 PeV from the Crab

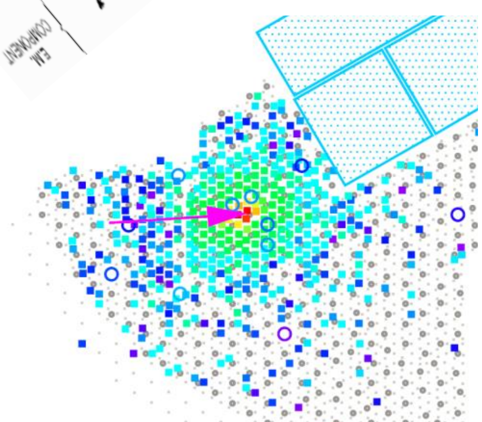

- **Area :** **1.3 km²**
- **Detectors :** **5216 ED** **1188 MD**
- **Energy Range :** **0.01-10 PeV**

LHAASO-WFCTA

Separate of individual CR species & measure the knees

~0.1 PeV CR event

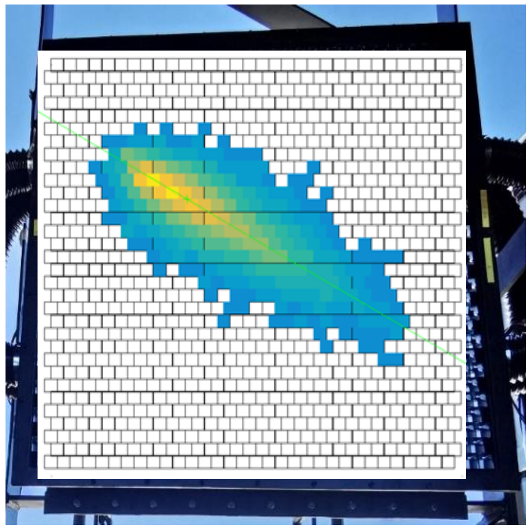

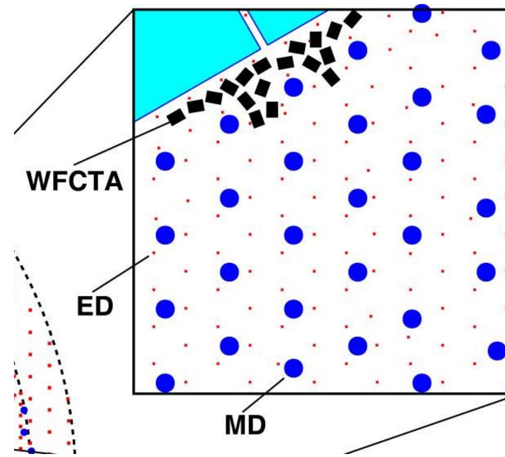

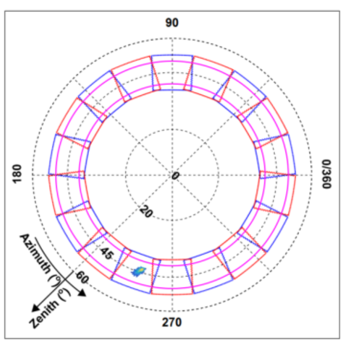

WFCTA: 18 IACTs

- Mirror: 5 m^2
- SiPM camera
- FOV: 16×16°
- Pixel size: 0.5°
- Energy: 0.1-100 PeV

CR Background rejection in WCDA

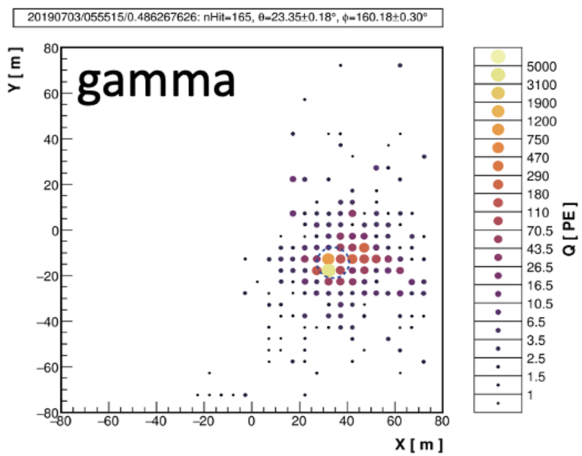

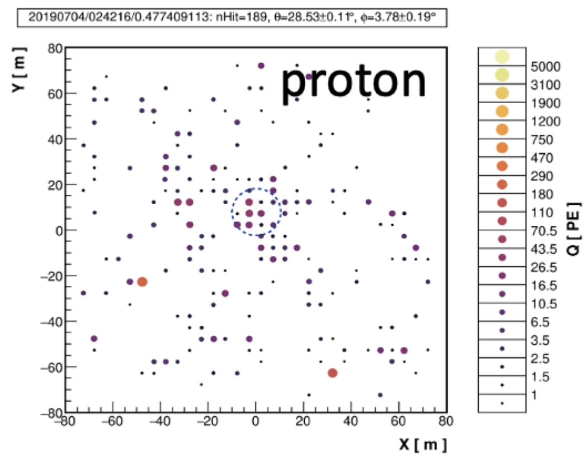

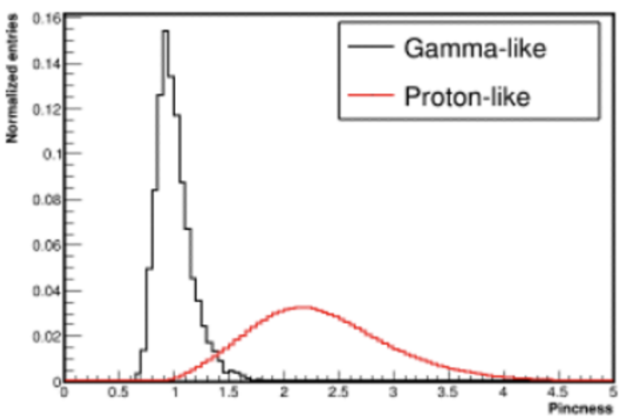

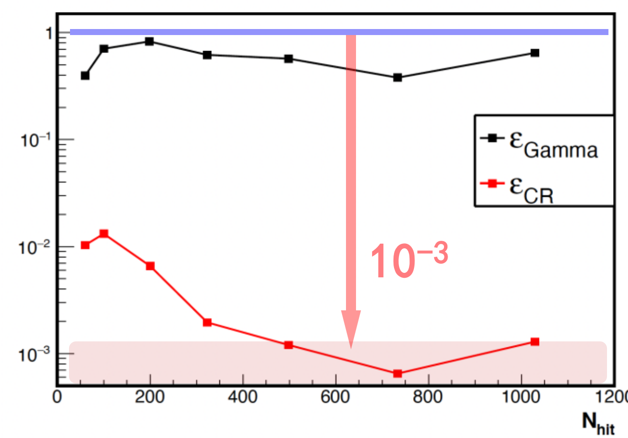

CR background Rejection in KM2A

- Counting number of measured muons in a shower
- Cutting on ratio N_{μ}/N_{e}<**1/230**
- BG-free ($N_{\gamma}>10N_{CR}$) Photon Counting

for showers with E>100 TeV from the Crab

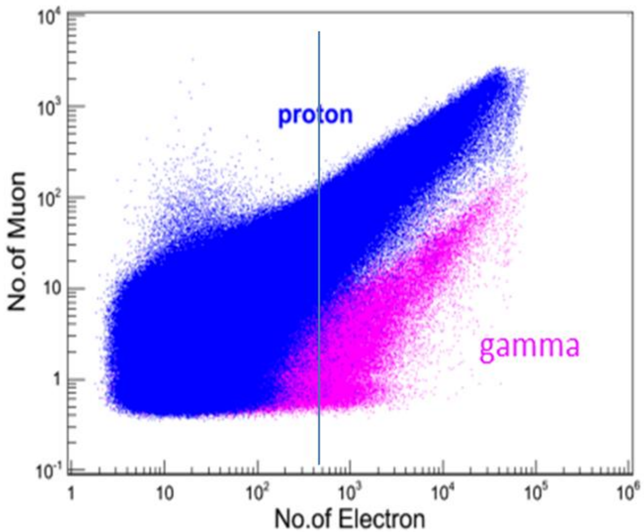

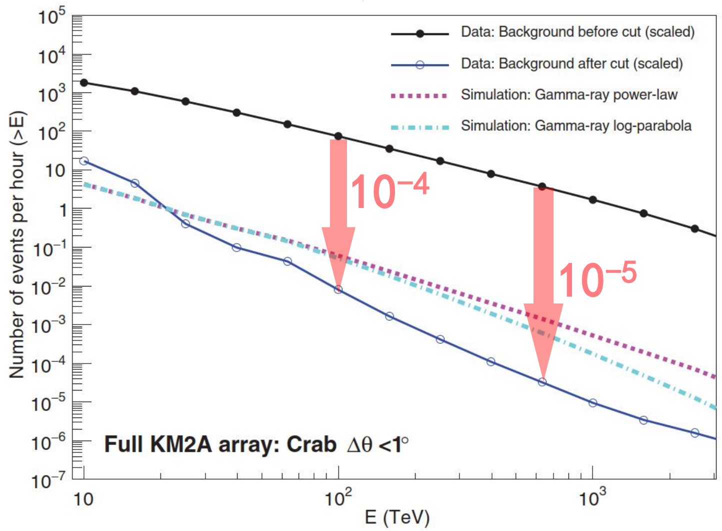

LHAASO Coll., ***Science***, 373, 425 (2021)

LHAASO angular resolution

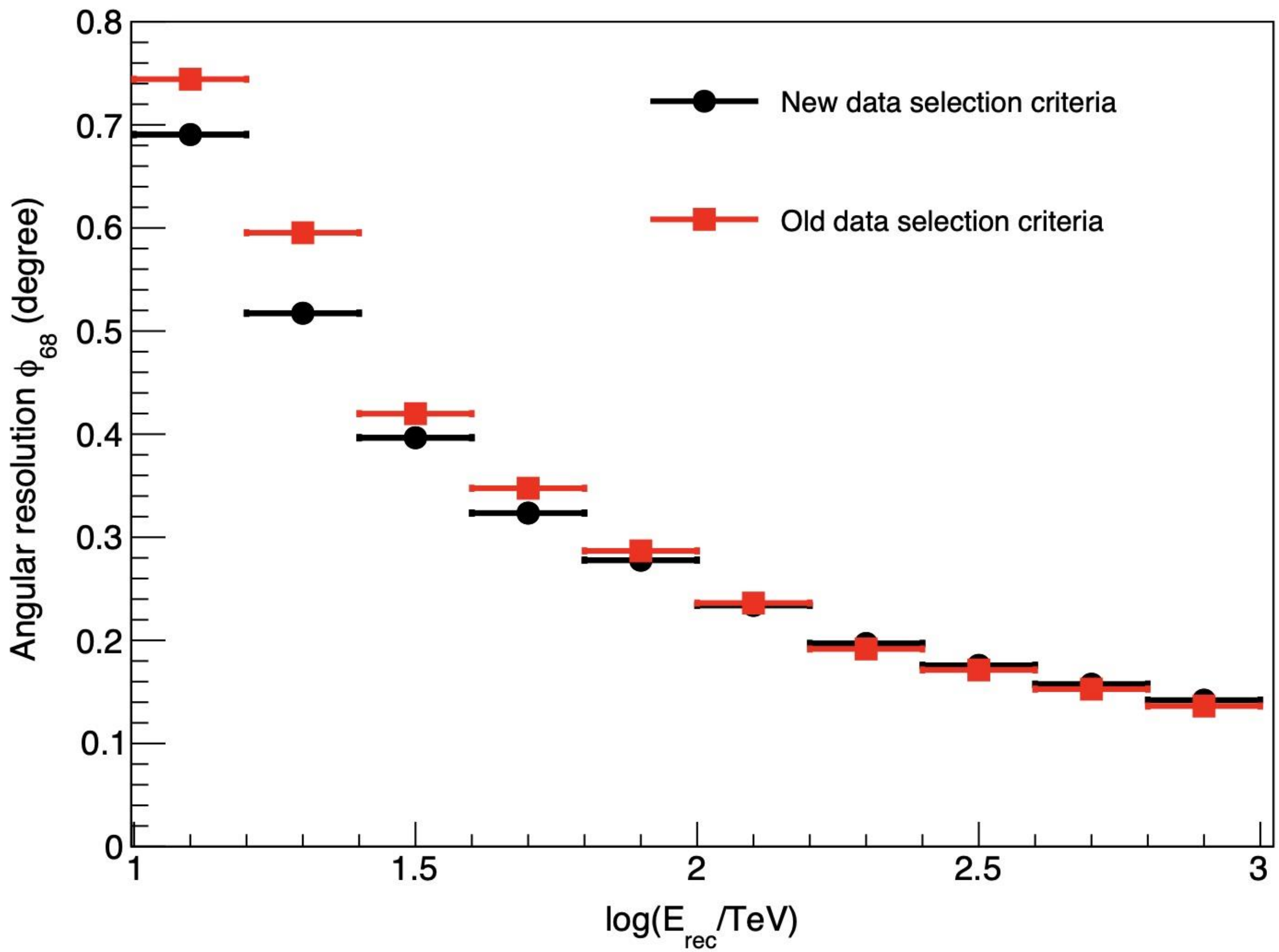

LHAASO Crab study 2401.01038, *Chin.Phys.C* 48 (2024) 6, 065001

LHAASO sensitivity

With large FOV and high sensitivity, LHAASO is an ideal detector for sky survey to search VHE and UHE sources!

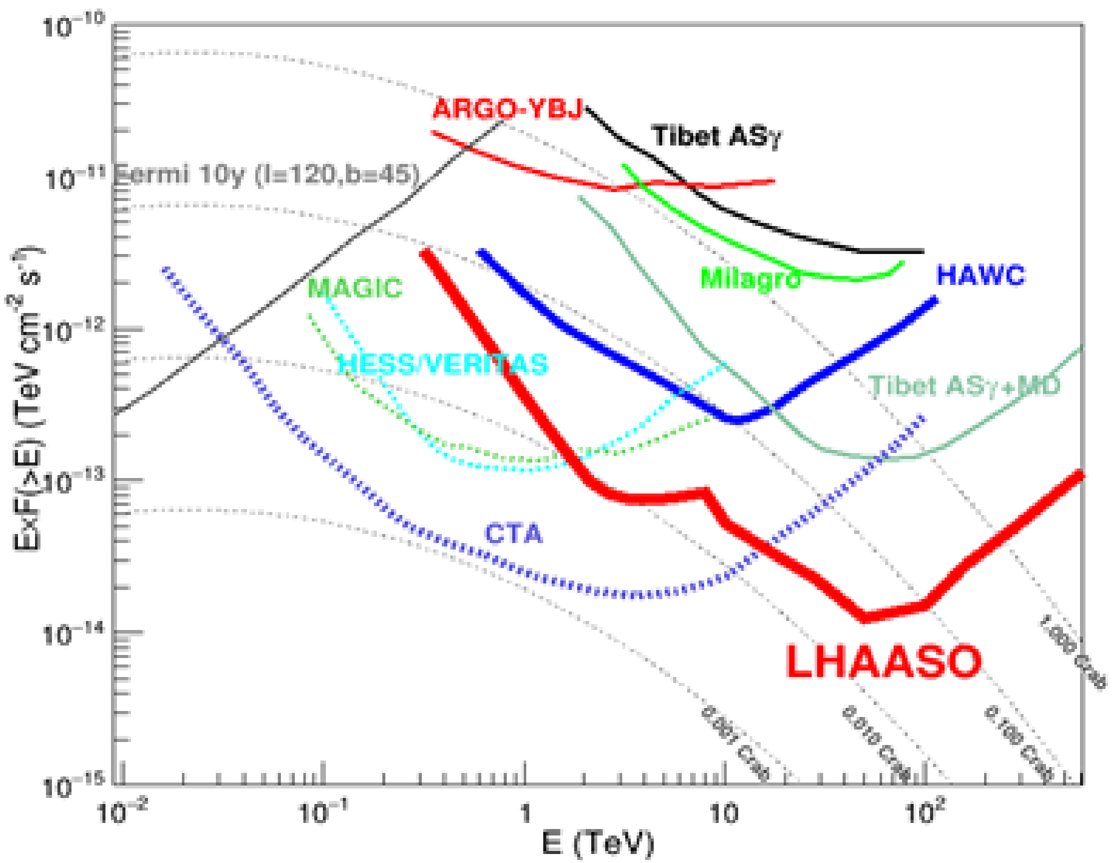

Field of view for GRB/TOO

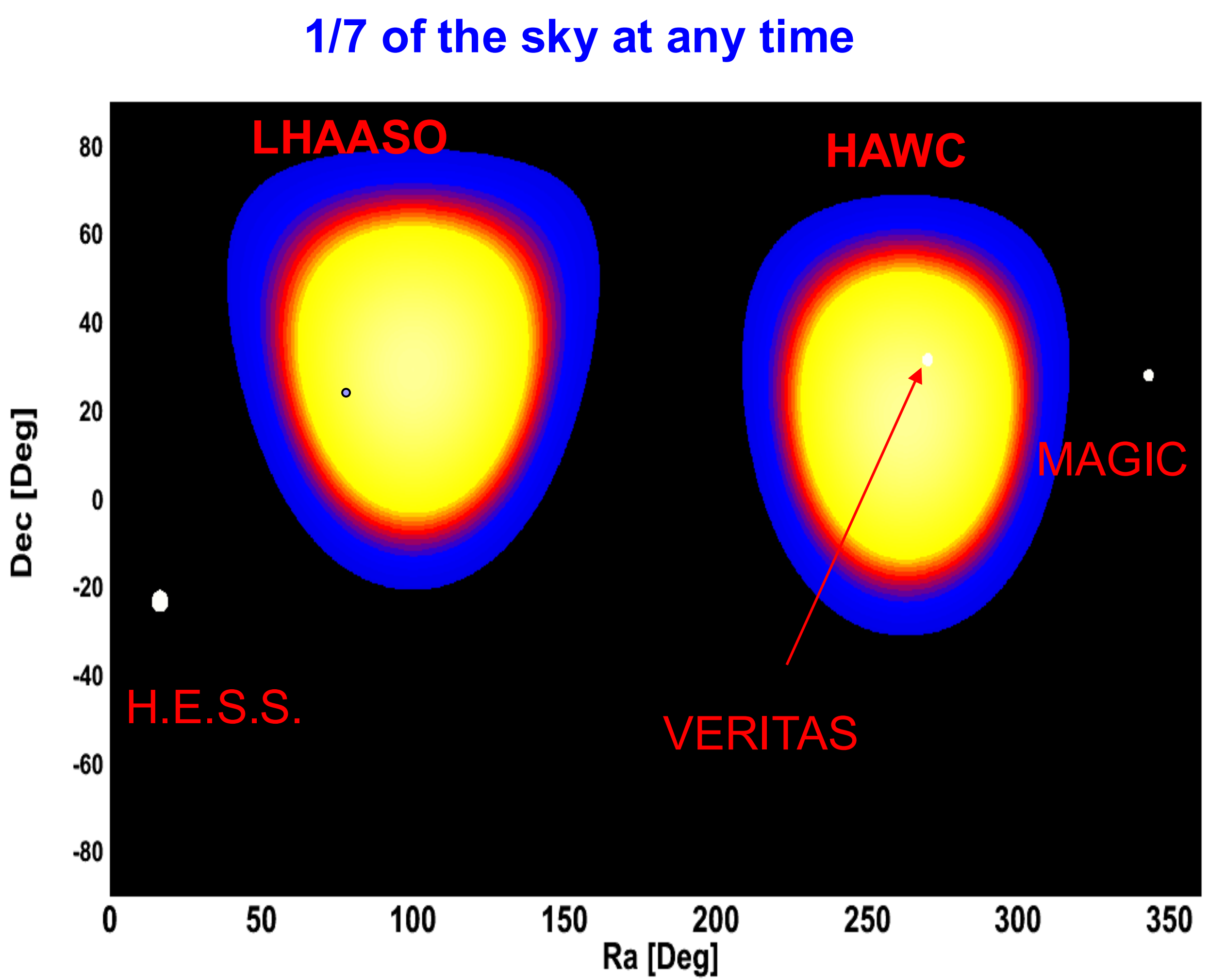

Cosmic rays at knee with LHAASO

Knee-composition

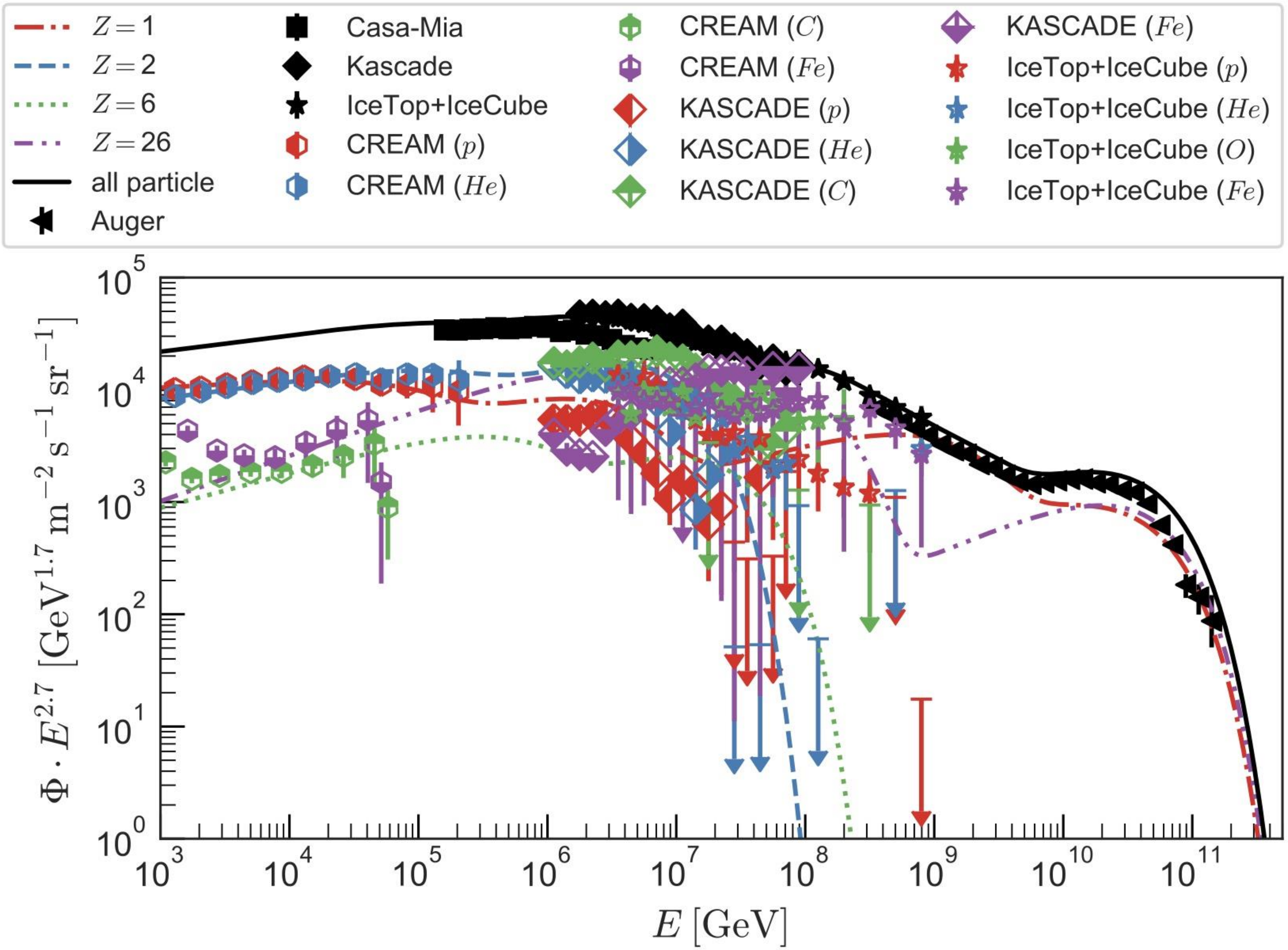

All-particle energy spectrum & <lnA>

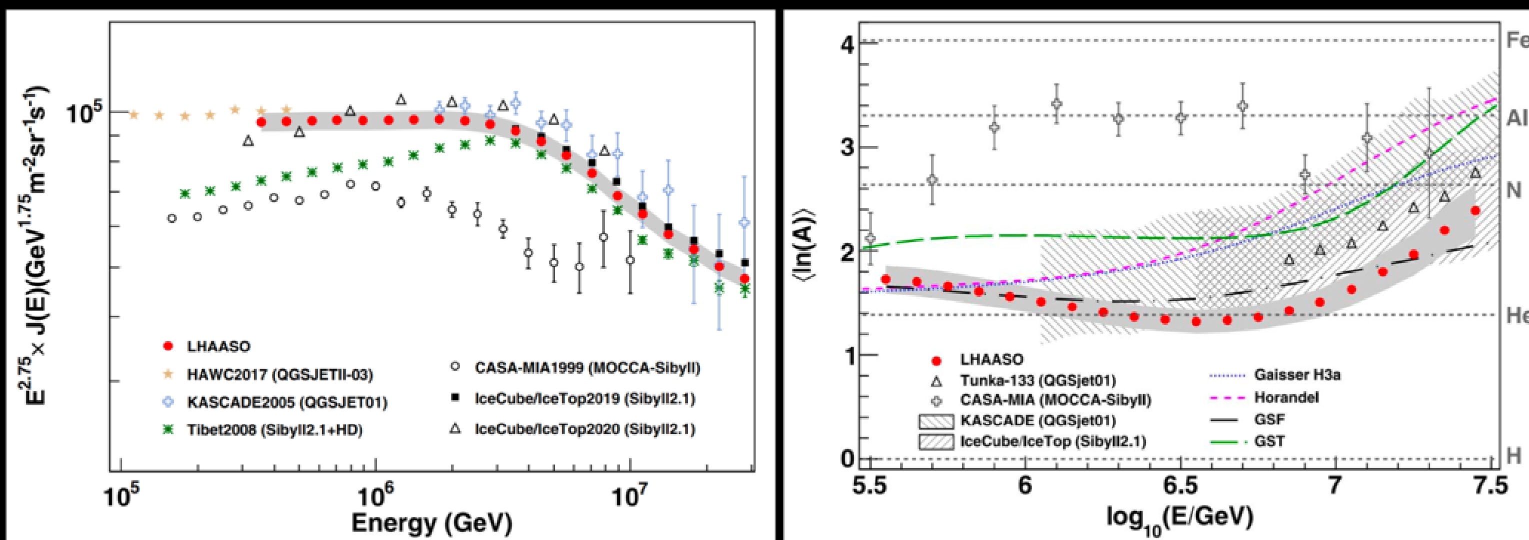

	Flux $J(E)$	$\langle \ln(A) \rangle$
Air preesure	$\pm 3\%$	$\pm 4\%$
Composition models	$\pm 1.5\%$	$\pm 3\%$
Interaction models	$\pm 2.5\%$	$\pm 6\%$

hhh@ihep.ac.cn

• *LHAASO collab.*, Zh.Cao et al, 2403.10010, *Phys.Rev.Lett.* 132 (2024) 13, 131002

From 350%(150%) to 12%

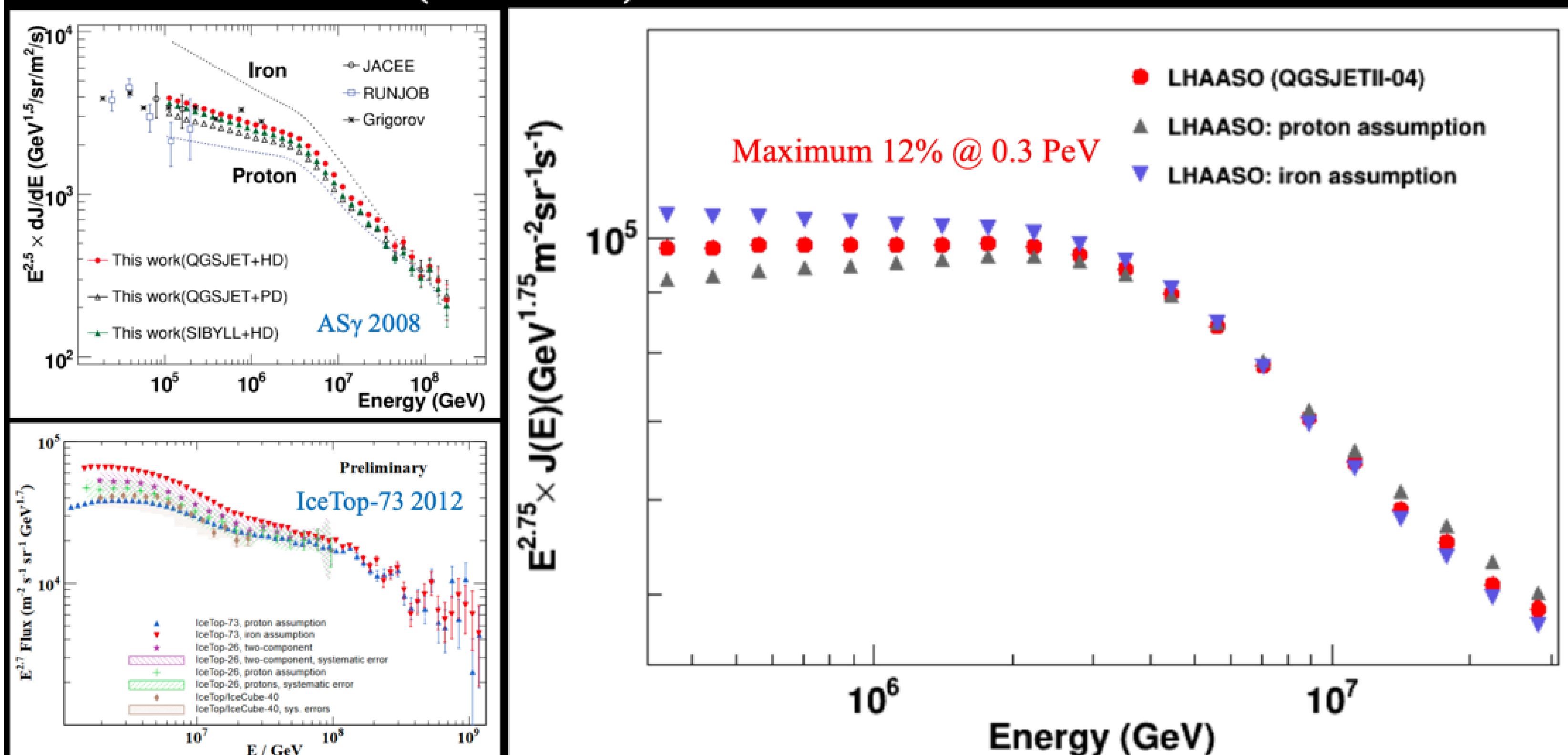

hhh@ihep.ac.cn

TLM: the touchstone for testing if proton spectrum breaks @ knee

- Total logarithmic mass

$$F \equiv \sum_i f_i \quad m \equiv \langle \ln A \rangle \equiv \frac{\sum_i f_i \ln A_i}{\sum_i f_i}$$

$$M \equiv \sum_i f_i \ln A_i = F \times m$$

	P	He	CNO	MgAlSi	Fe
lnA	0	1.39	2.64	3.30	4.03

- More sensitive to structures of heavy nuclei (especially Fe)
- P (lnA=0) doesn't contribute to TLM, thus TLM servs as a touchstone for testing if proton spectrum breaks at the knee
  - No → a similar structure in TLM as in the all-particle energy spectrum
  - Yes → how much does proton contribute to the knee?

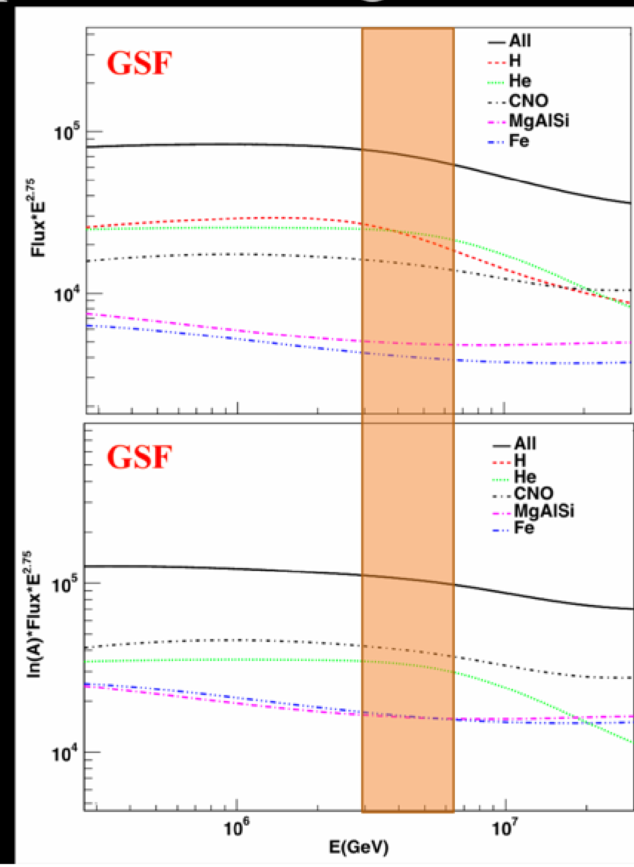

hhh@ihep.ac.cn

The all-particle and TLM spectra by KM2A

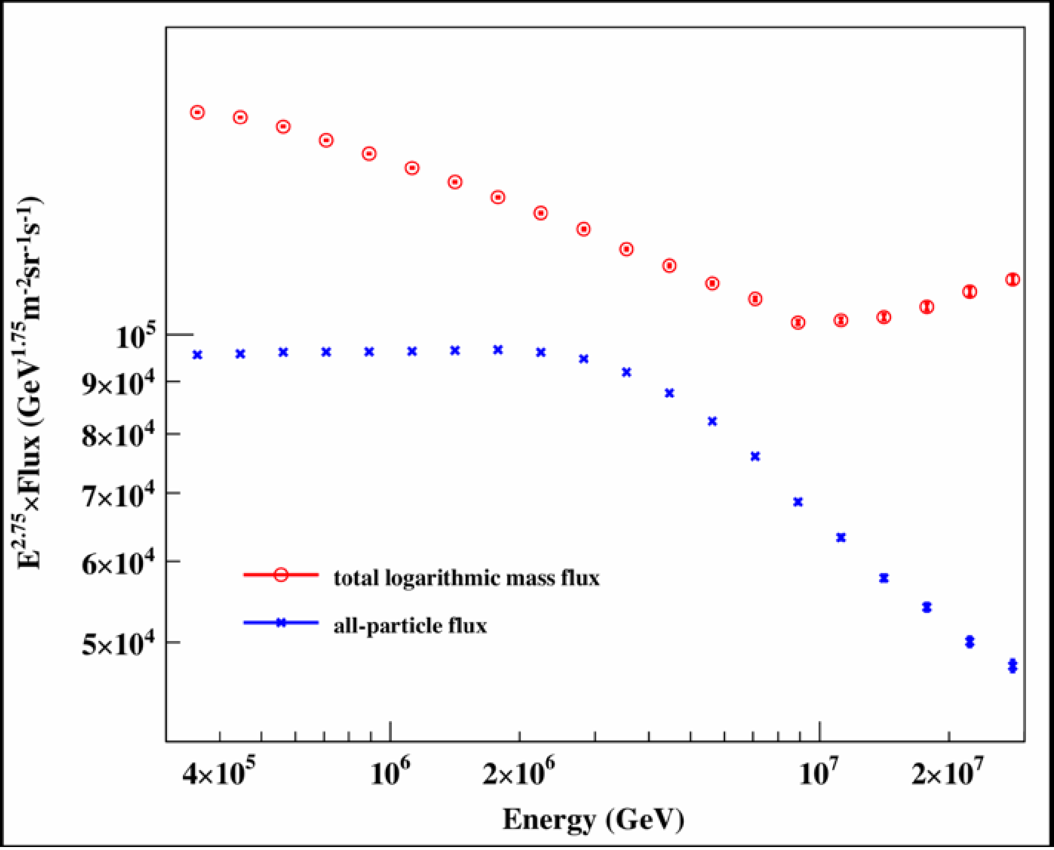

hhh@ihep.ac.cn

Does proton spectrum break at the knee?

- Parameters from LHAASO paper
  - All-particle flux $F' = F_0 \left(\frac{E}{1\ PeV}\right)^{\gamma_F}$
  - <lnA> $m' = m_0 \left(\frac{E}{1\ PeV}\right)^{\gamma_m}$
  - ➢TLM $M' = F' \times m' = F_0 \times M_0 \left(\frac{E}{1\ PeV}\right)^{\gamma_F+\gamma_m}$
- Loss
  - All-particle flux $\Delta F = F' - F$
  - TLM $\Delta M = M' - M$
  - <lnA> of ΔF

$$m_{\Delta F} = \frac{\Delta M}{\Delta F} = q_p \times m_p + (1-q_p) \times m_{\geq He} = (1-q_p) \times m_{\geq He}$$

- TLM anticipation

$$M'' = M' - \Delta F \times m_{\Delta F}$$

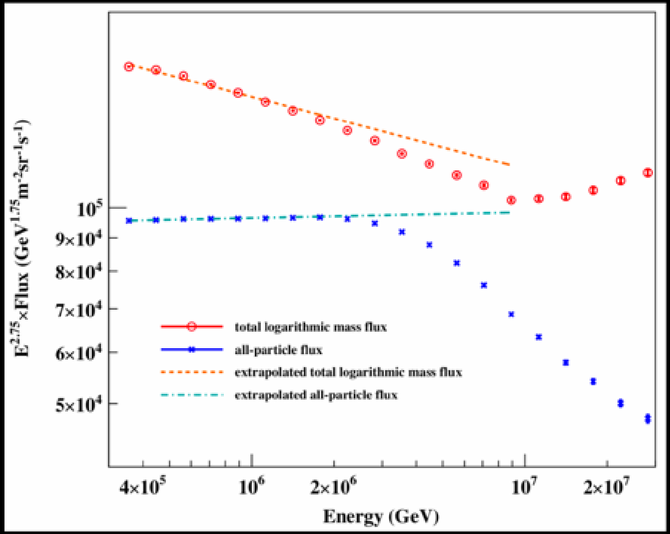

- H_0: no, q_p=0 → best-fit $m_{\Delta F} = \ln 4$
- H_1: yes, q_p>0 → best-fit $m_{\Delta F} = 0.66 \pm 0.02$
- Significance of rejecting H_0: 36.8σ

→Proton spectrum breaks at the knee!

hhh@ihep.ac.cn

Only proton spectrum breaks at the knee?

- H_0: yes, q_p=1
- H_1: no, q_p<1
- Significance of rejecting H_0
  - Paper: 41.8σ
  - 1-10 PeV: 6.3σ

$$m_{\Delta F} = \frac{\Delta M}{\Delta F} = (1 - q_p) \times m_{\geq He}$$

- proton proportion
  - Paper: 52.7%±1.2%≤q_p≤83.7%±0.04%
  - 1-10 PeV: 72.6%±4.5%≤q_p≤90.6%±1.5%

→Proton dominates the knee but it's not the only one whose spectrum breaks!

Features of the proton knee

- $E_p = 3.2 \pm 0.2$ PeV
- Spectral index before the cutoff: -2.6559 ± 0.0009
- Change of spectral index: -0.79 ± 0.03
- Sharpness： 5.1 ± 0.5
- $f_p = 0.43 \pm 0.06$

- Light: $2.35 \pm 0.06 \times 10^{-12}$ /GeV/m²/sr/s
- (all: 3×10^{-12} /GeV/m²/sr/s)

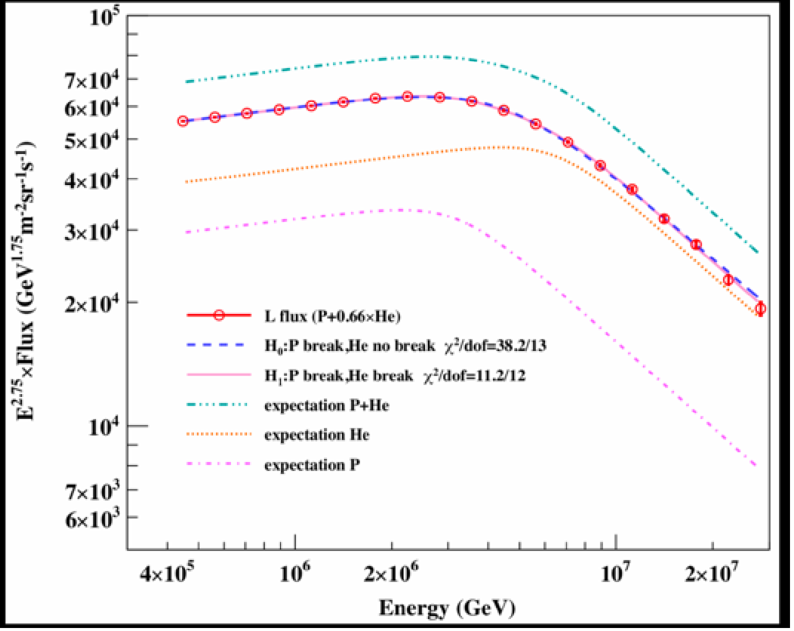

hhh@ihep.ac.cn

Discovery of an ankle-like structure due to Fe

- Break energy: 9.7±0.2 PeV

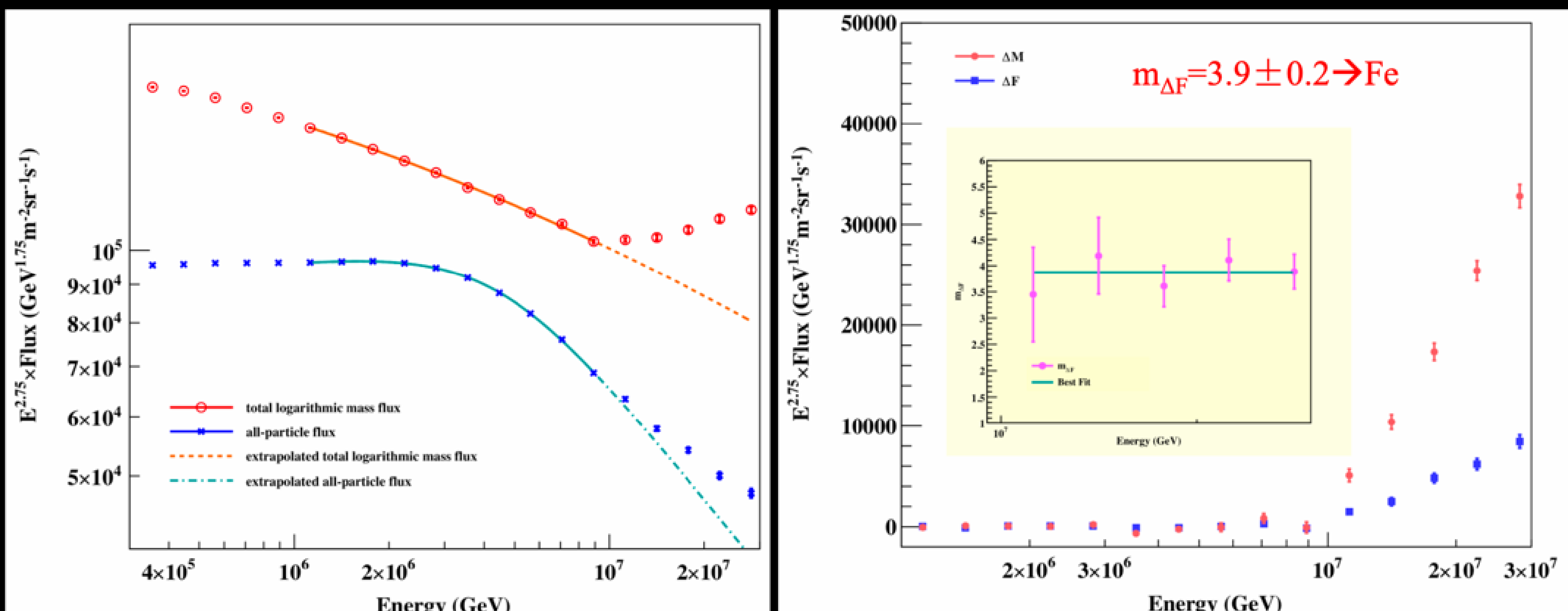

LHAASO proton core

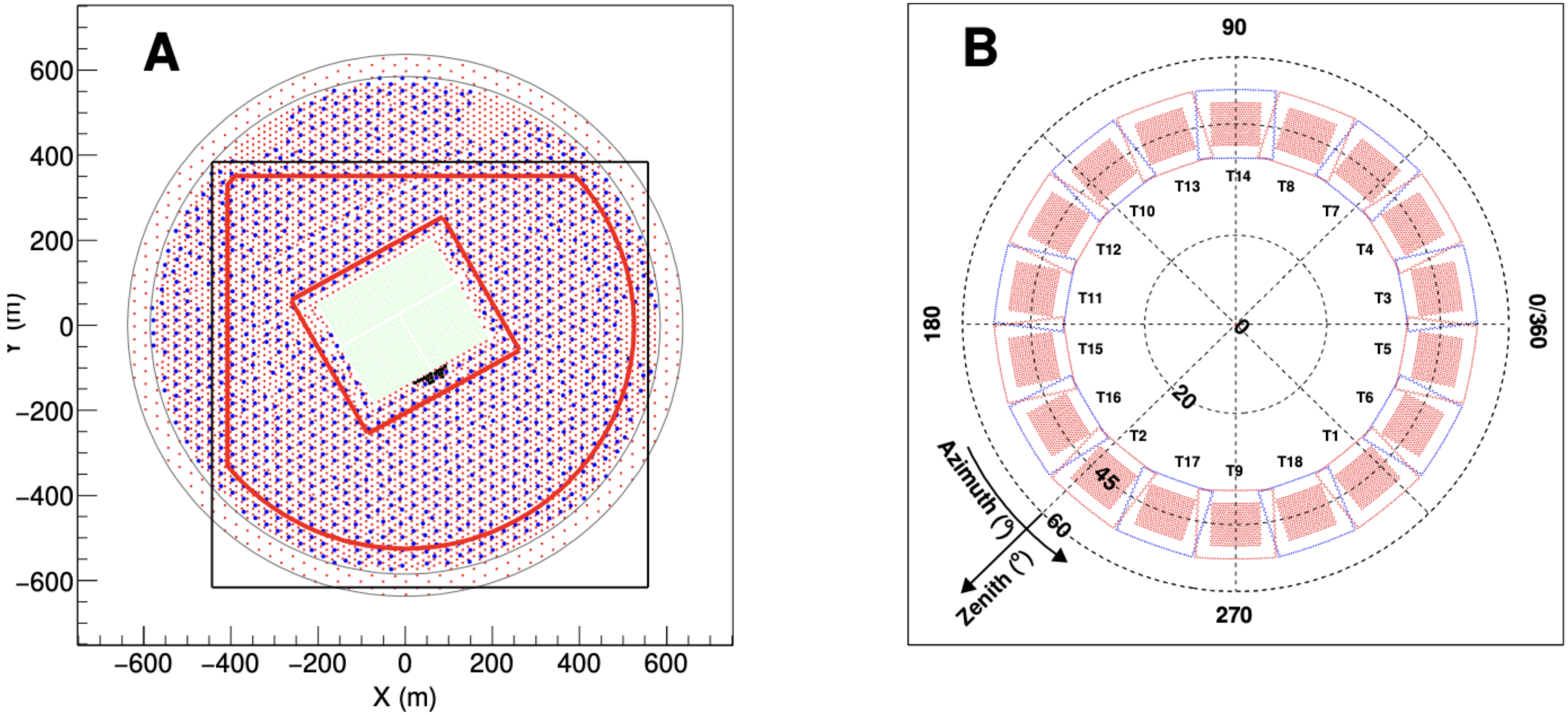

LHAASO collaboration, 2505.14447

KM2a vs WFCT

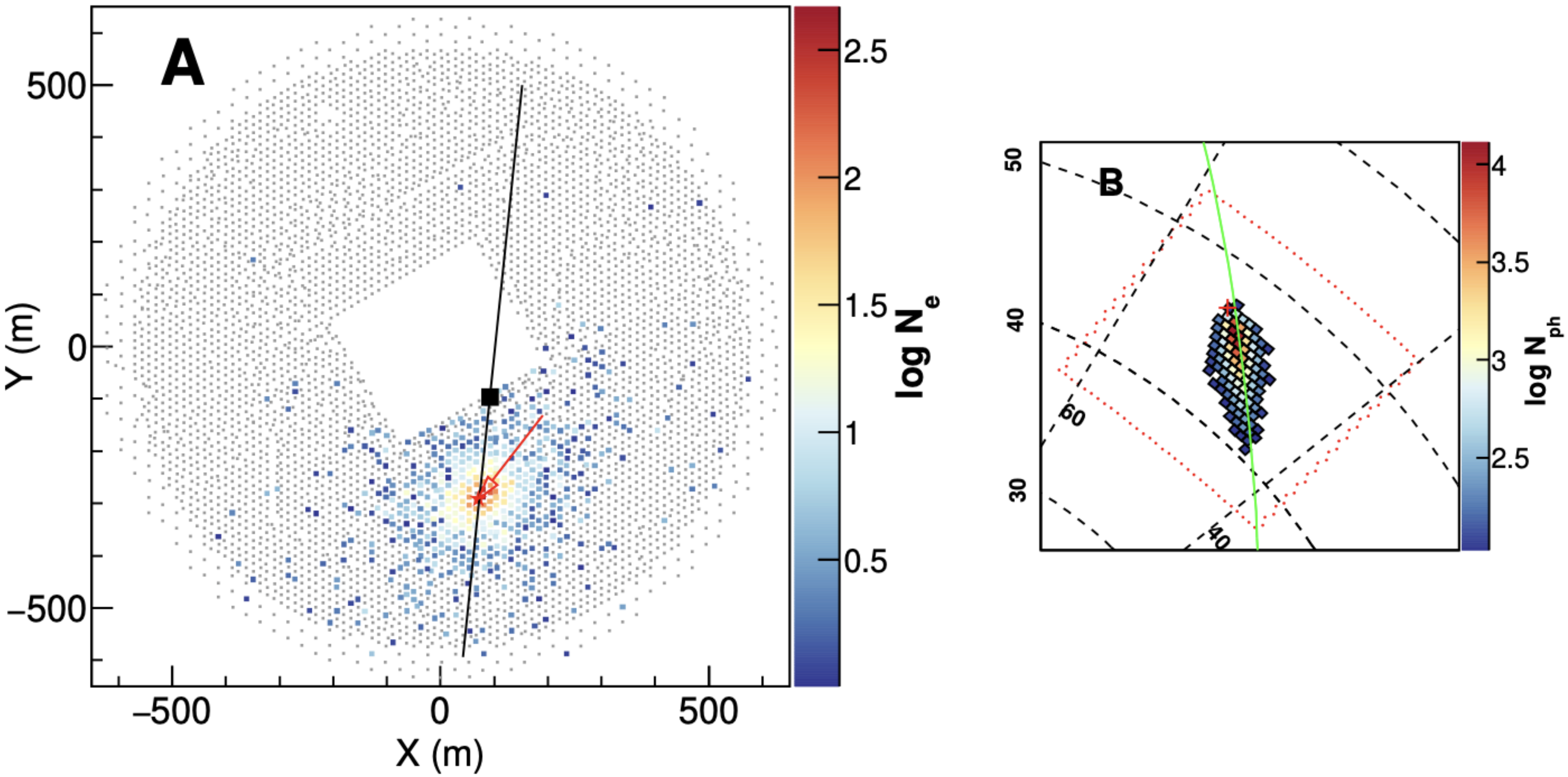

LHAASO collaboration, 2505.14447

Hadronic model systematics

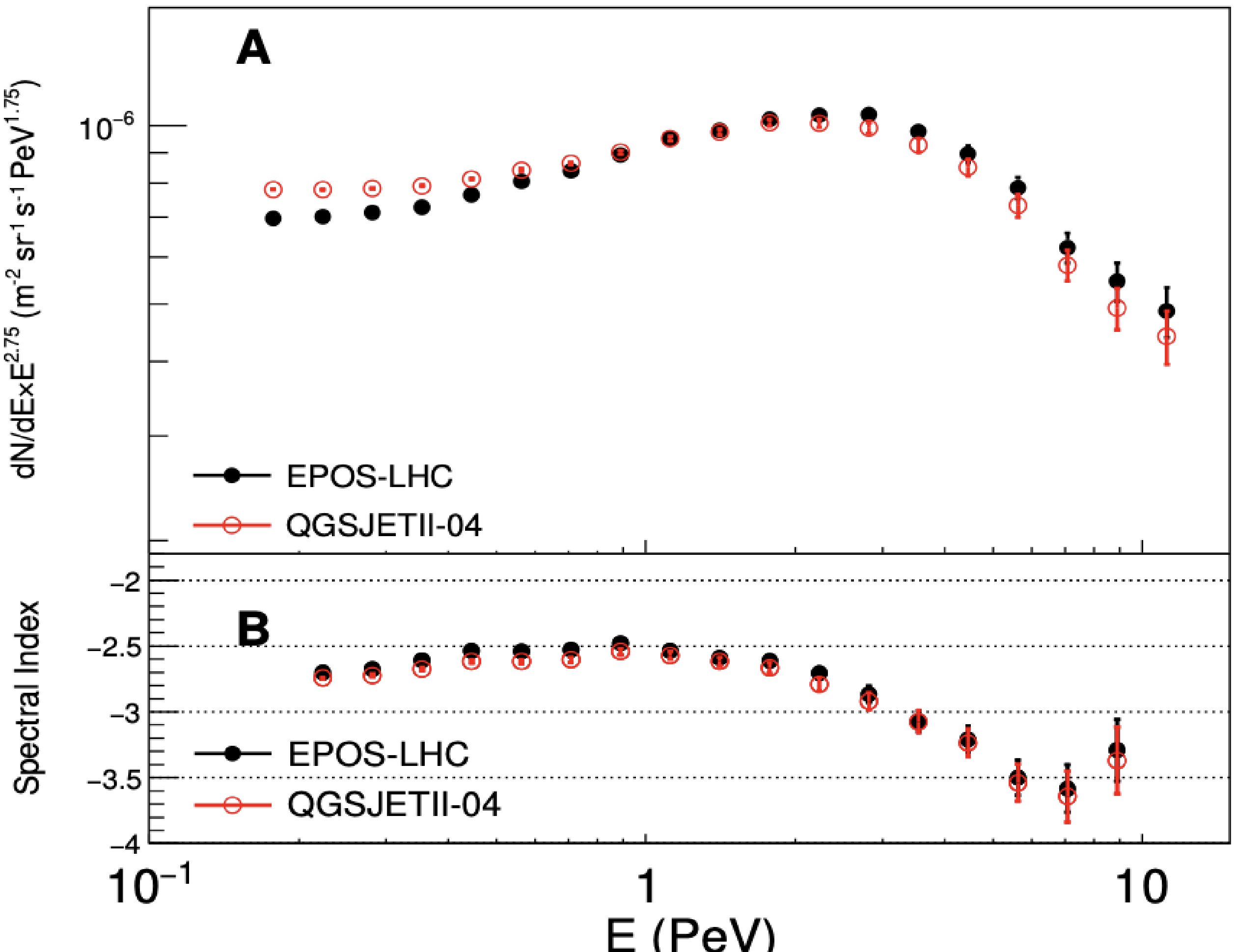

Proton spectrum measurement

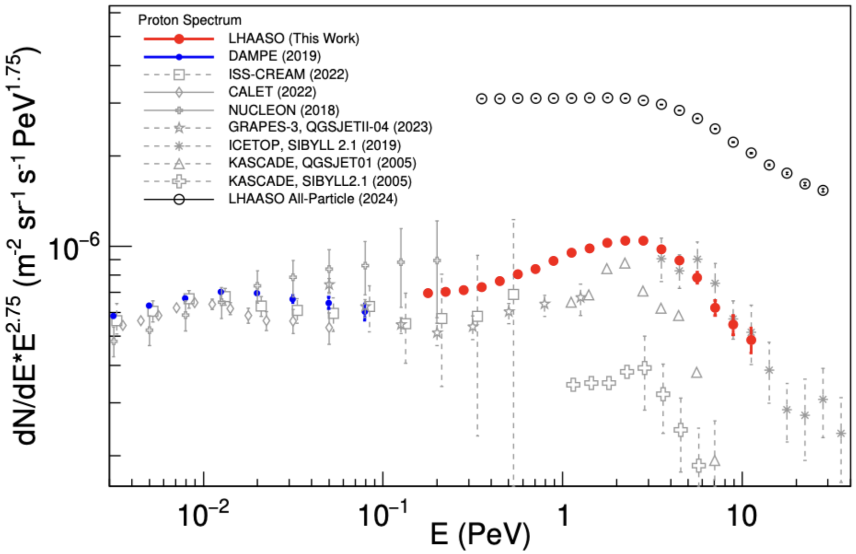

LHAASO collaboration, 2505.14447

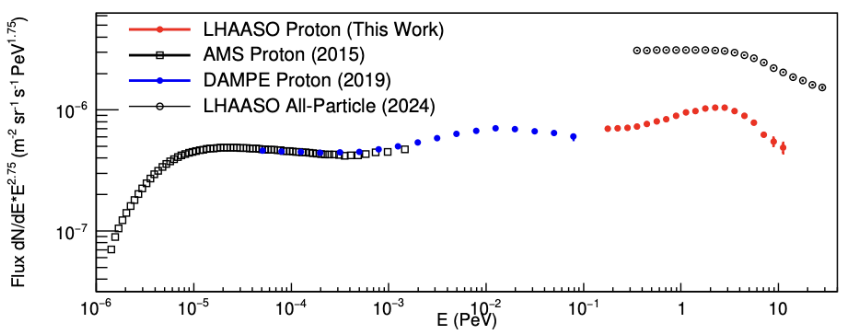

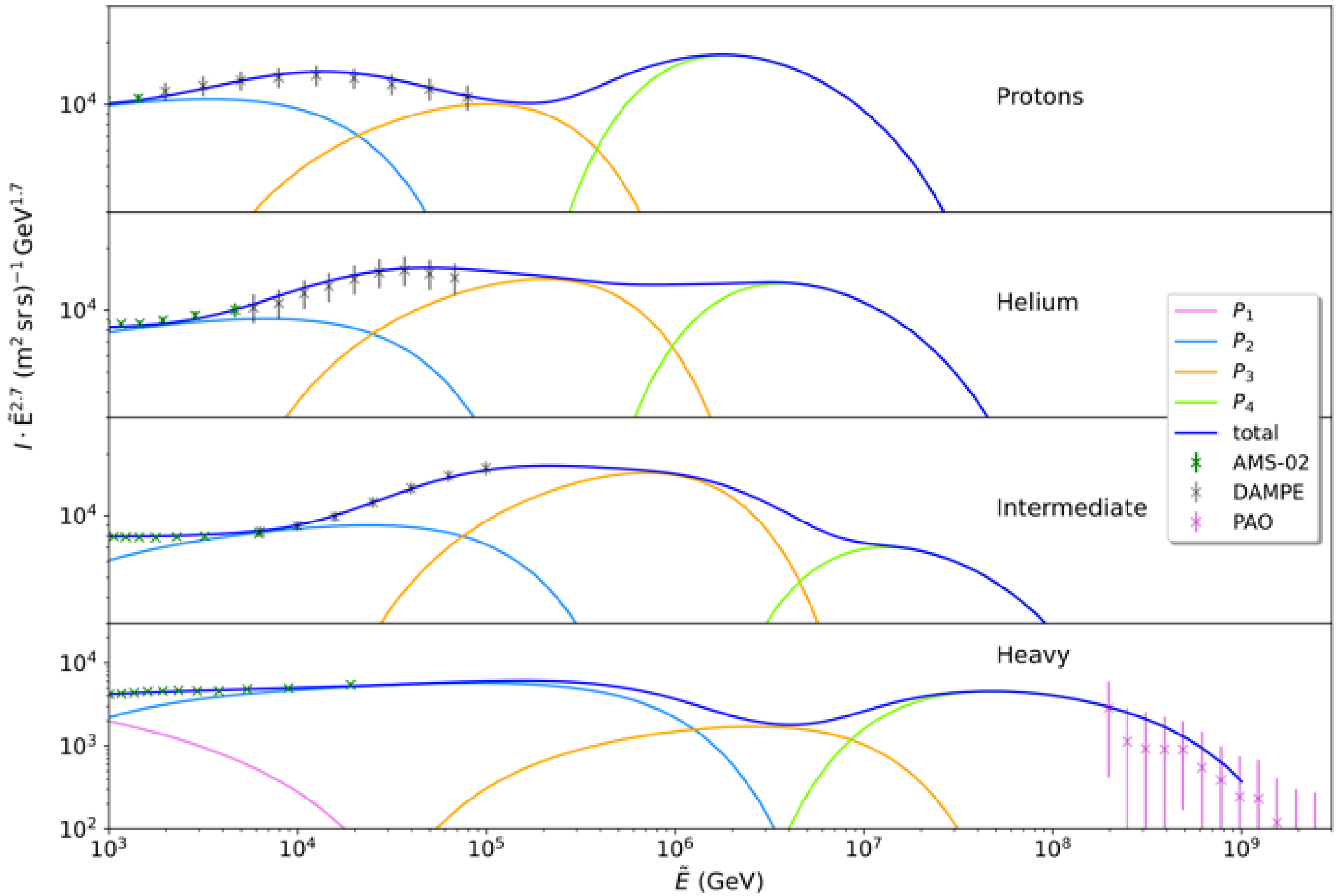

C. Prevotat et al, 2407.11911

Knee in Galaxy vs local Cosmic Rays

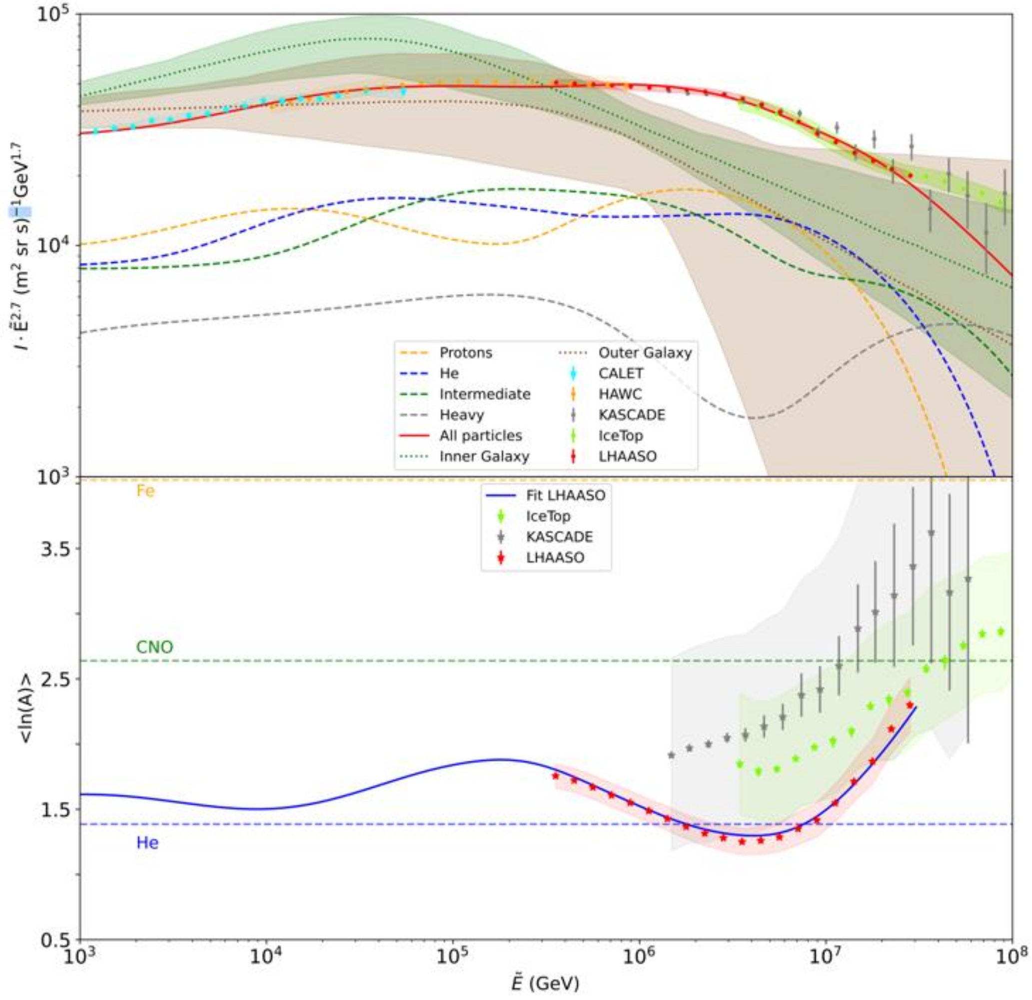

C. Prevotat et al, 2407.11911

Introduction: Gamma-ray astronomy

Gamma-ray detectors

Space-based
EGRET, AGILE, Fermi

HE: >0.1 GeV
Large FOV
80% duty cycle
0.1° ~ 5° resolution
1 m^2 area

IACTs:
H.E.S.S., MAGIC, VERITAS, CTA

VHE:>0.1 TeV
3°~5° FOV
15% duty cycle
0.06°~ 0.17° resolution
10^5 m^2 area

EAS arrays:
Milagro, ARGO-YBJ
Tibet Asγ, HAWC, LHAASO, SWGO

VHE: >0.1 TeV
UHE: >0.1 PeV
Large FOV
100% duty cycle
0.1° ~ 1° resolution
10^{3-6} m^2 area

Impressive Gamma-ray Source Catalogs

Fermi-LAT
12ys data
6658 sources
50 MeV to 1 TeV

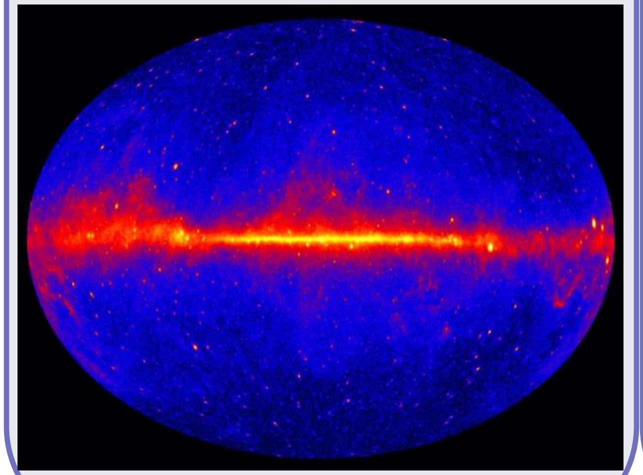

H.E.S.S.
10ys data
78 sources
0.2-100 TeV

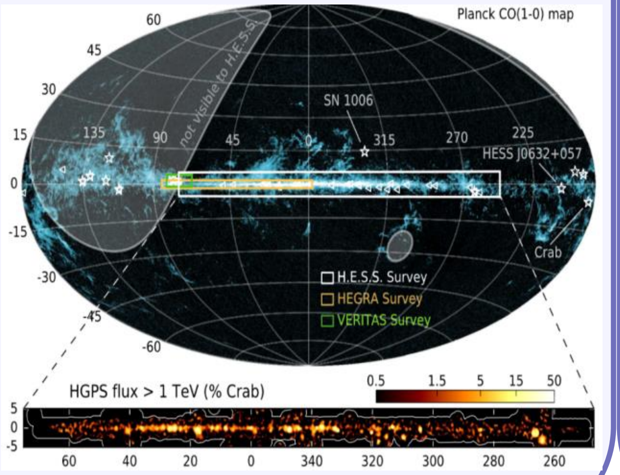

HAWC
5ys data
65 sources
1~100 TeV

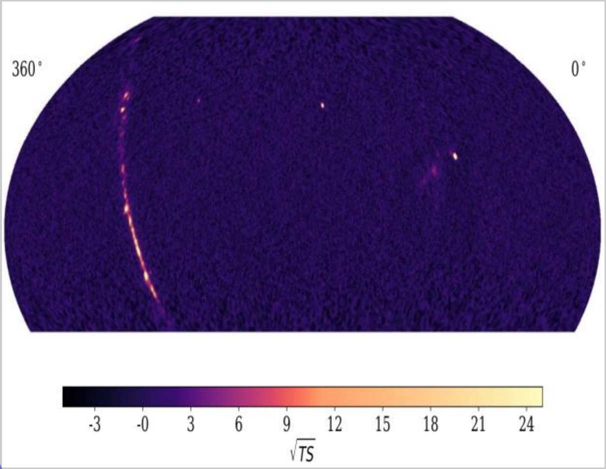

Gamma-Ray Attenuation

$$\left.\frac{dN}{dE}\right|_{obs} = \left.\frac{dN}{dE}\right|_{int} \exp\left[-\tau(E,z)\right]$$

$$\tau(E,z) = \int_0^z \left(\frac{dl'}{dz'}\right) dz' \int_0^2 d\mu \frac{\mu}{2} \int_{\varepsilon_{min}}^{\infty} d\varepsilon' \, \sigma_{\gamma\gamma}(\beta') n(\varepsilon', z')$$

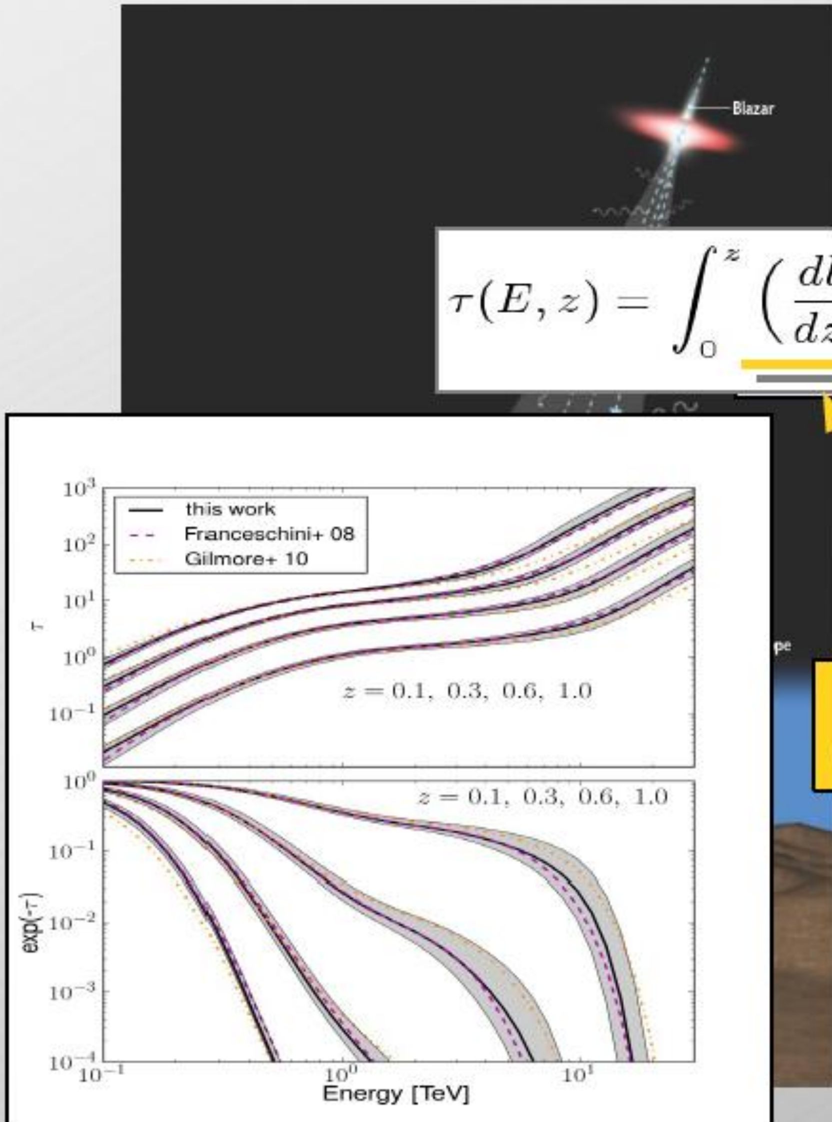

Distance (cosmology)

Interaction angle

Cross section

EBL photon density evolution (cosmology)

Status of VHE gamma-ray sources

Great progresses are achieved in ground-based VHE gamma-ray astronomy!

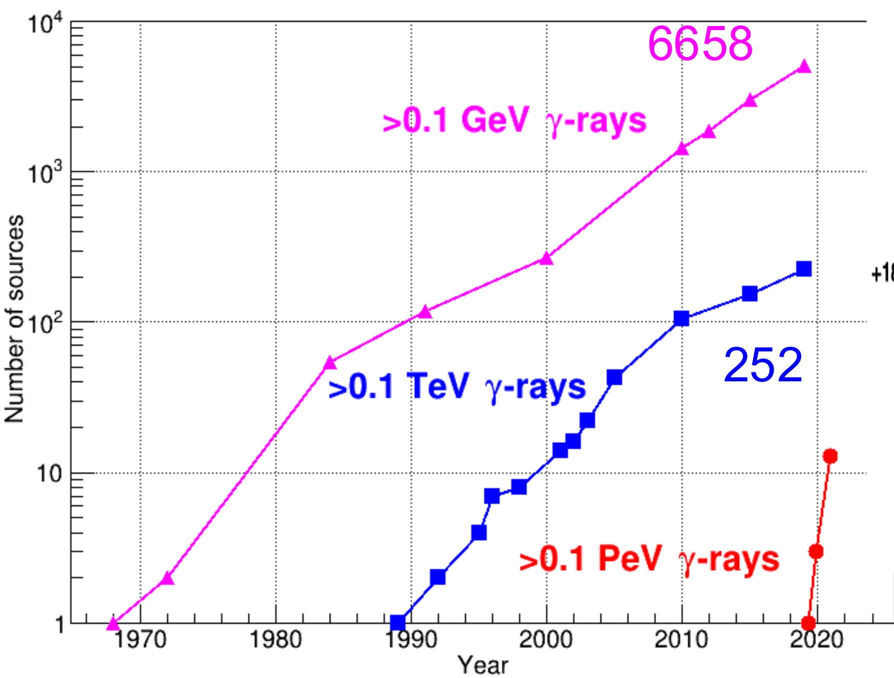

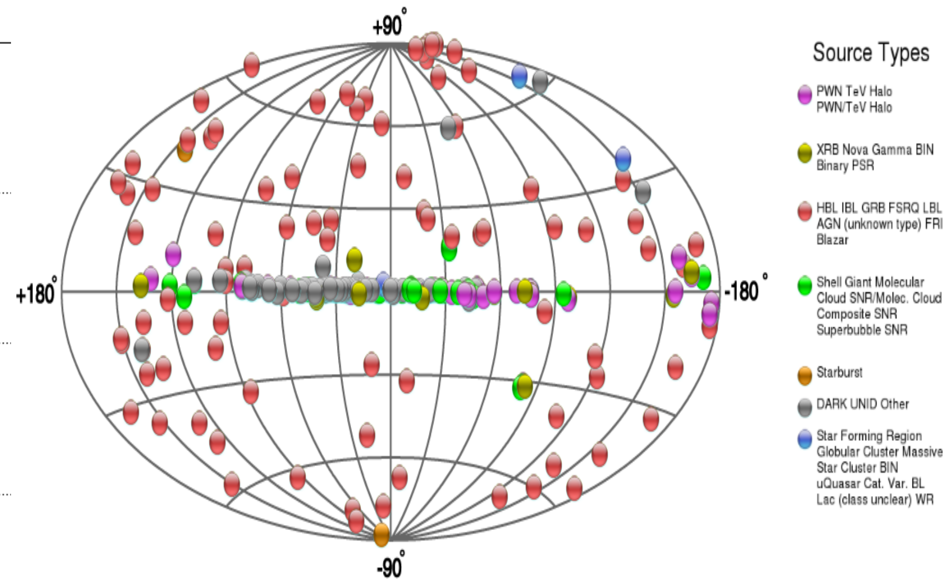

Field of view for GRB/TOO

1/7 of the sky at any time

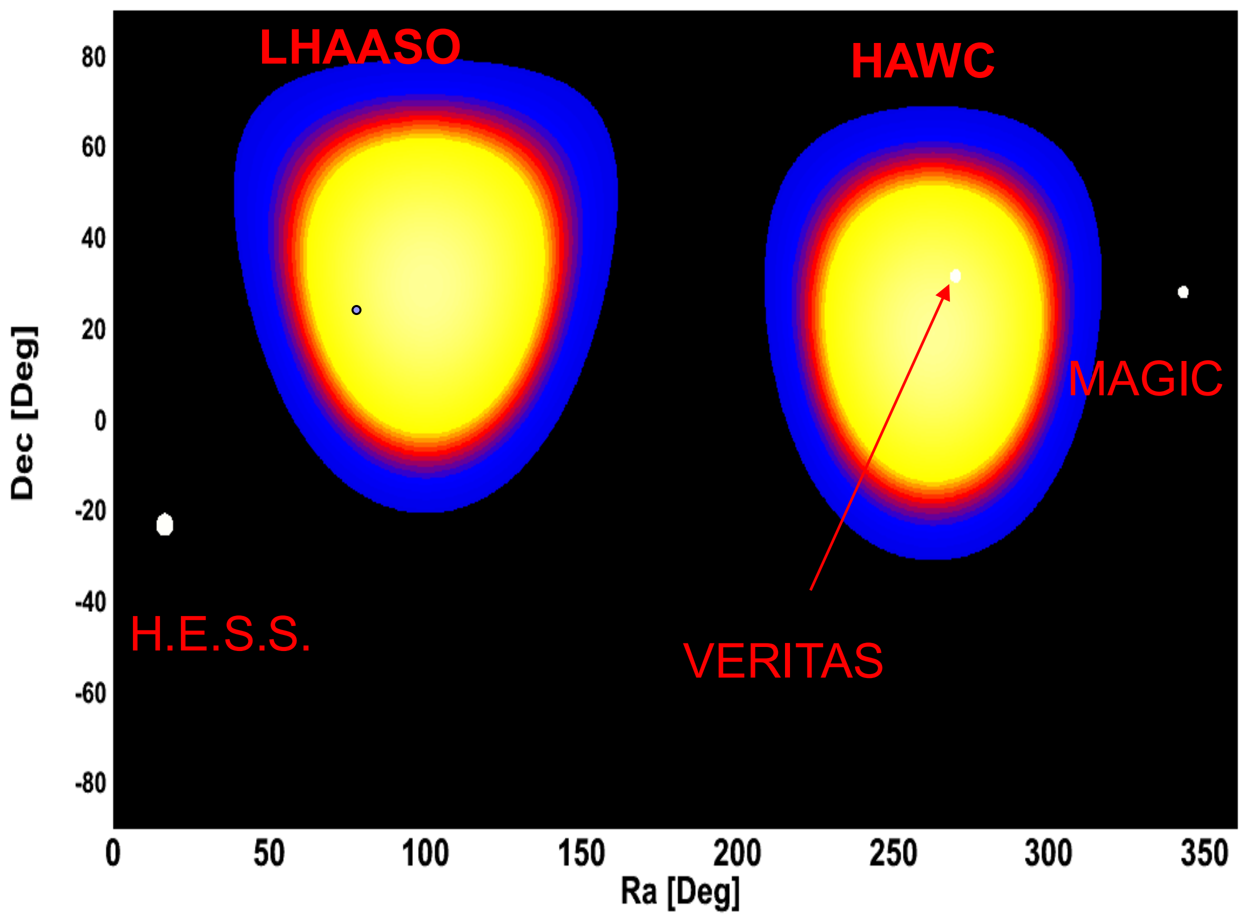

Cosmic ray energy spectrum

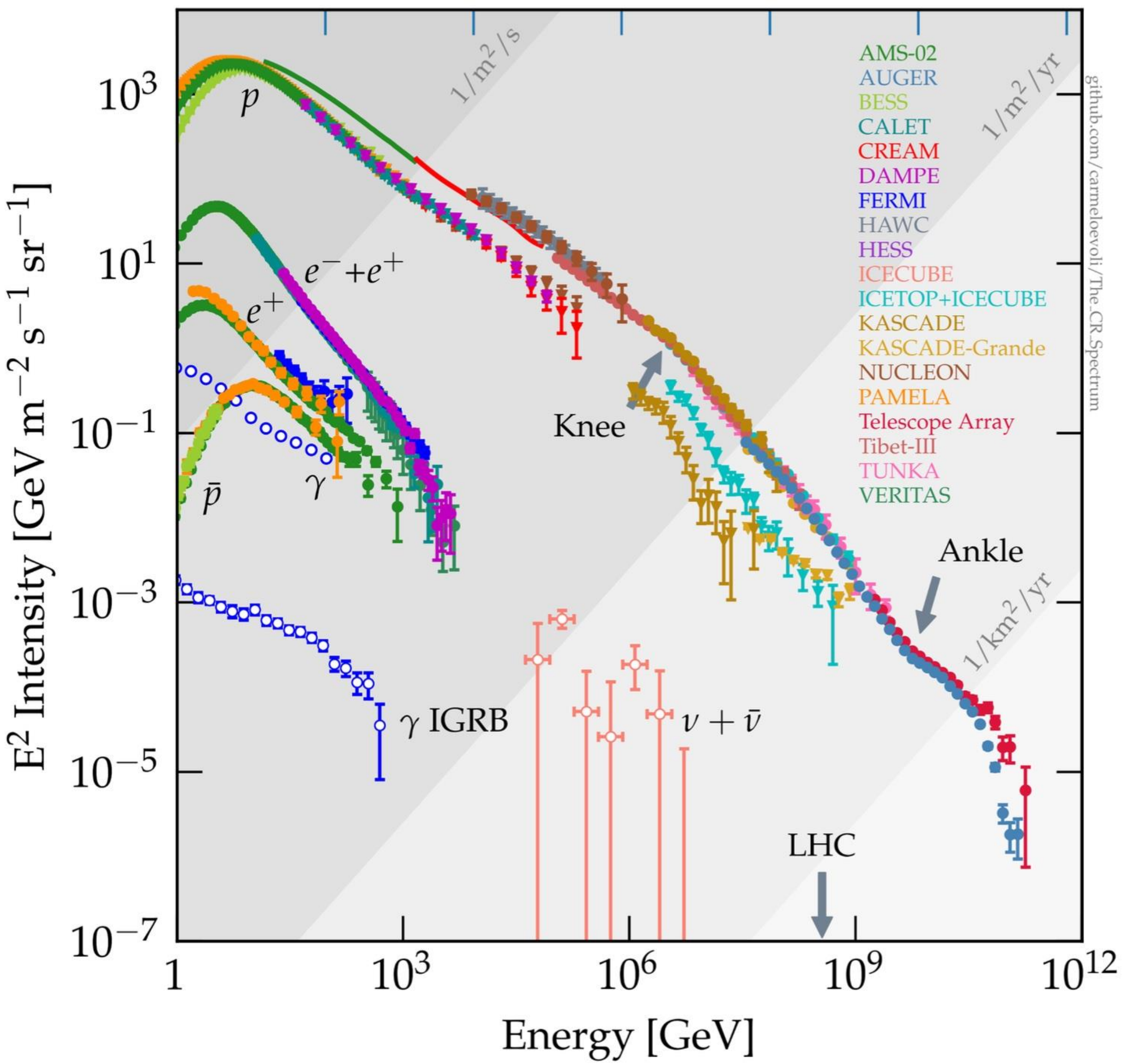

From C.Evoli

Gamma-ray telescopes sensitivity

With large FOV and high sensitivity, LHAASO is an ideal detector for sky survey to search VHE and UHE sources!

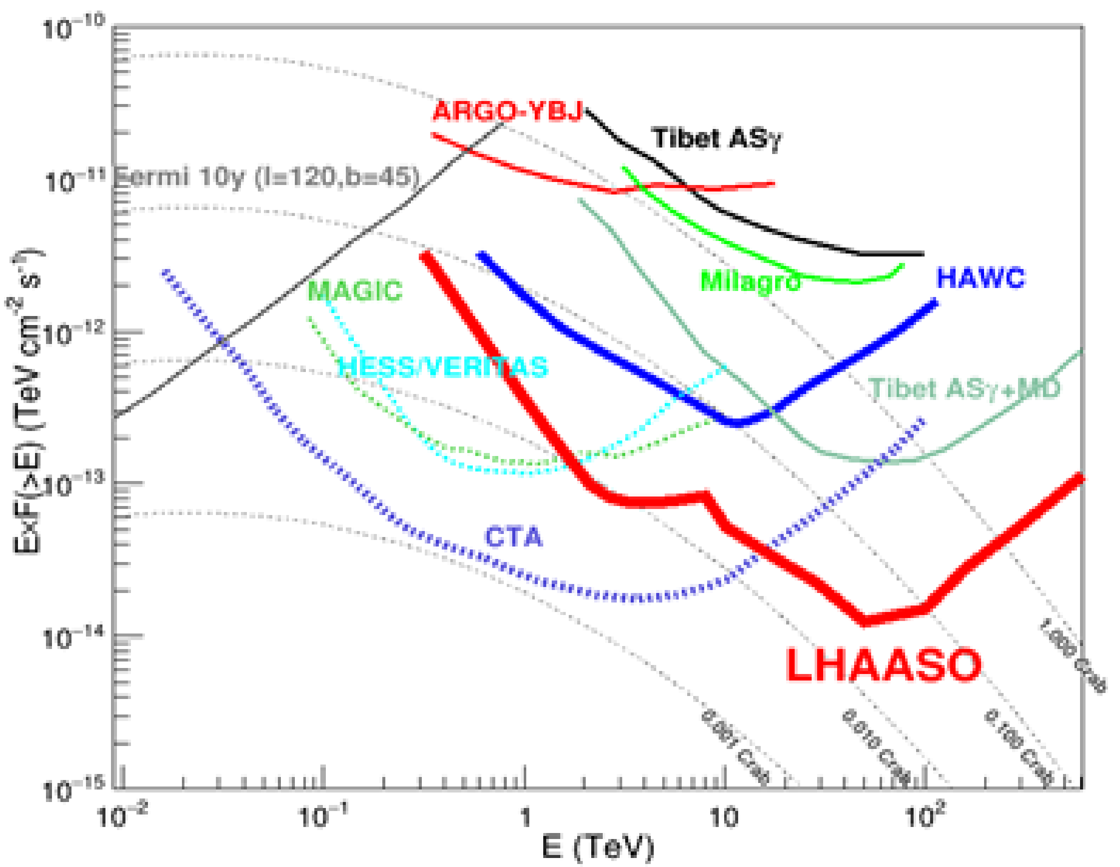

1 LHAASO catalog of gamma-ray sources

LHAASO data used for catalog analysis

KM2A

- 2019-12 to 2022-09
- 933 days (~730 days full array)
- 1.3×10^7 gamma-like events

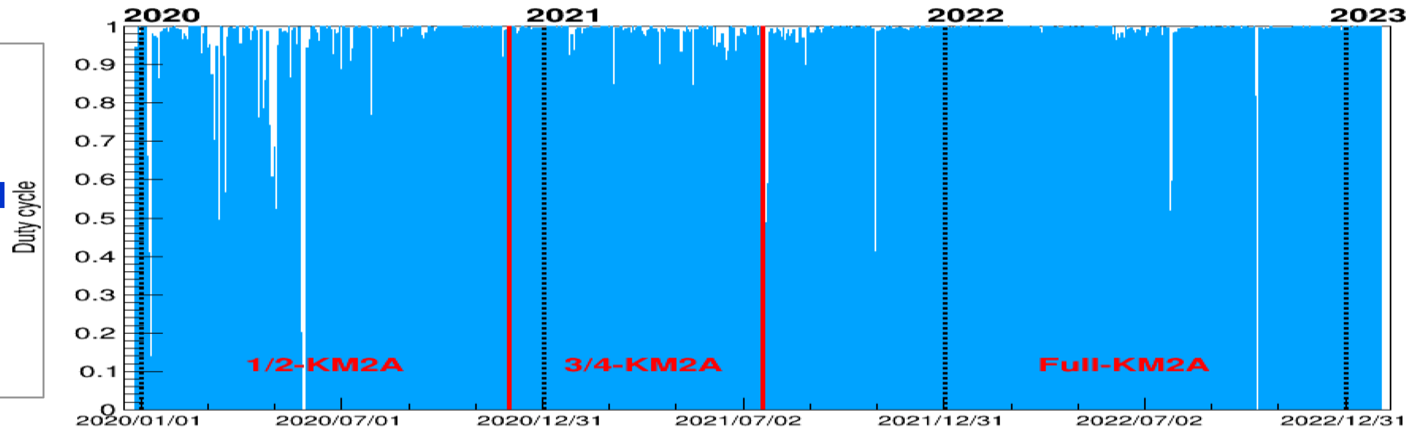

WCDA

- 2021-03 to 2022-09
- 508 days
- 1.3×10^9 gamma-like events

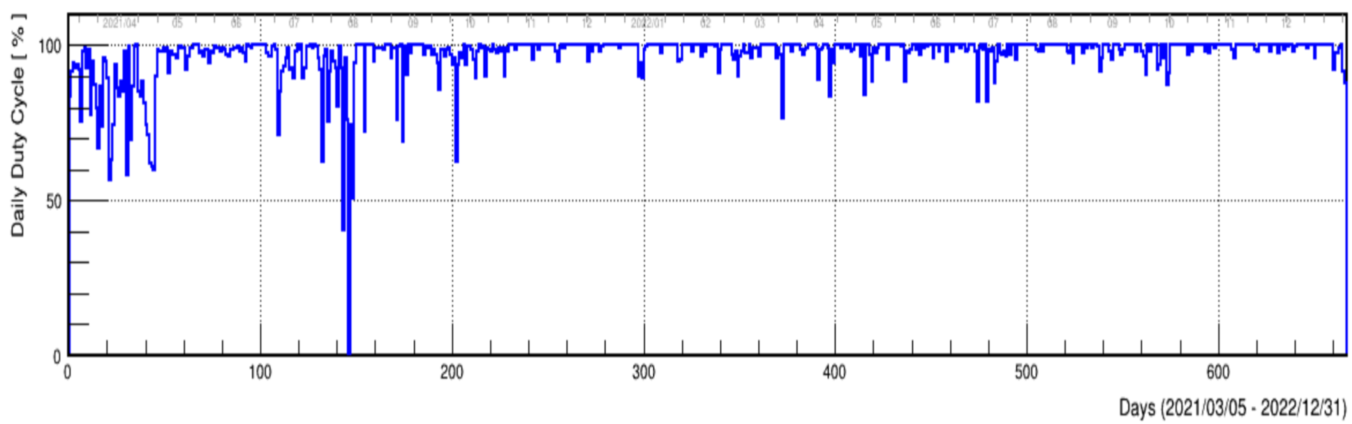

Point gamma-ray source searching

- **The candidates with significance >5σ are used to determine ROI and also as seeds for next fitting.**

WCDA SED: power-law with a index of

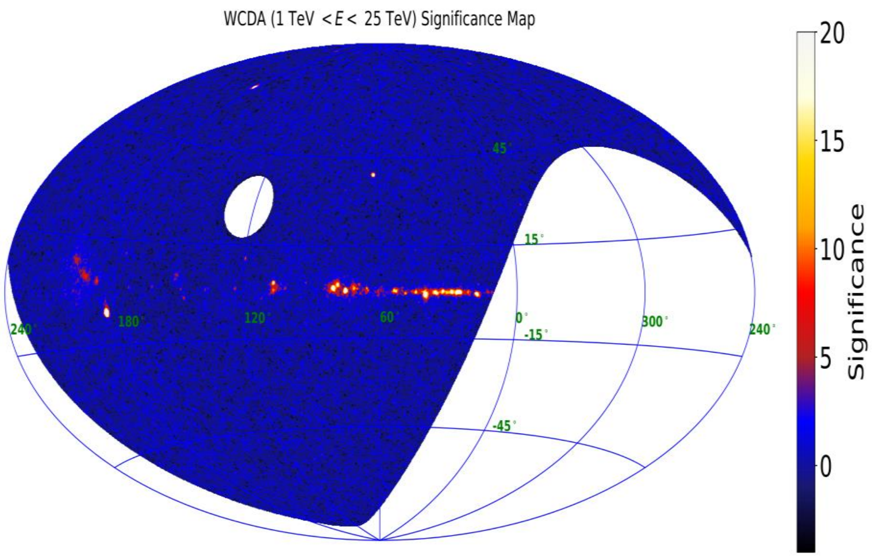

KM2A SED: power-law with a index of -3.0

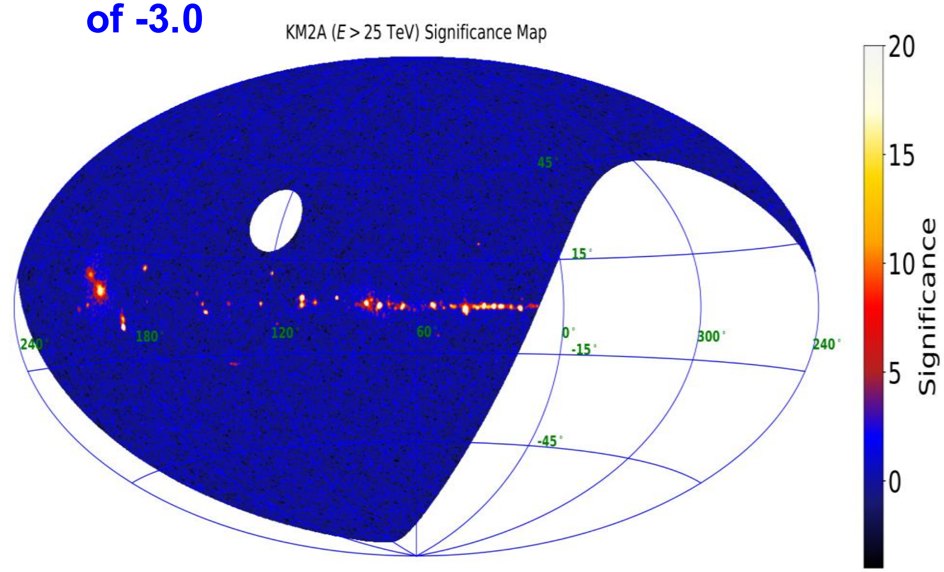

Construction of the 1st LHAASO sources

WCDA&KM2A

- Space Angle
- Position error
- Source extension

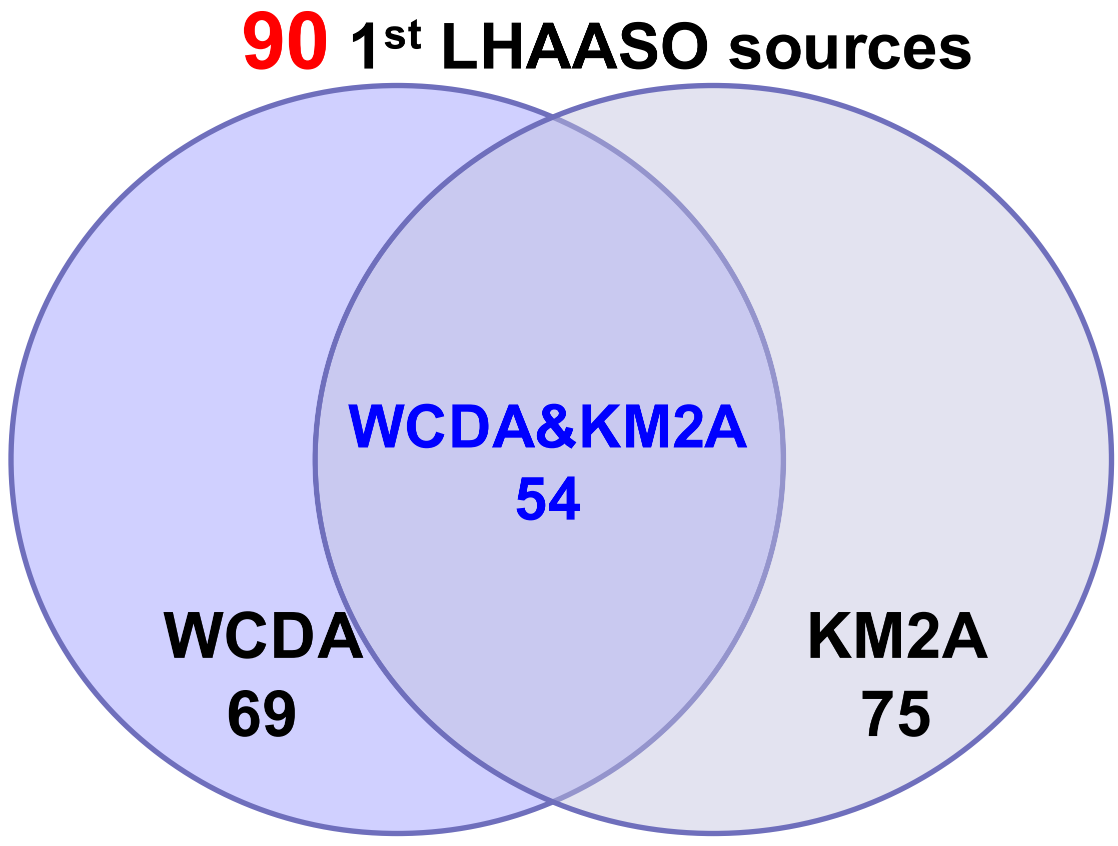

UHE gamma-ray sources

- The position and extension achieved by KM2A at >25 TeV are used.
- Sources with significance >4σ at >100 TeV are labeled as UHE sources
- LHAASO: 4 -> 43

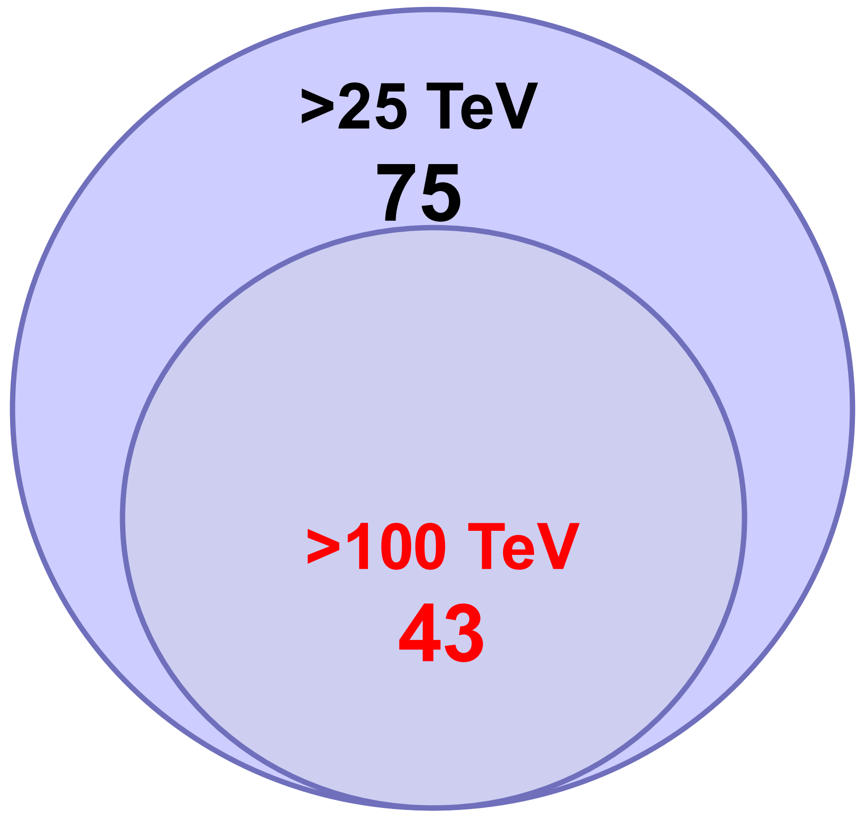

1st LHAASO source catalog

Source name	Components	α_{2000}	δ_{2000}	$\sigma_{p,95,stat}$	r_{39}	TS	N_0	Γ	TS_{100}	Asso.(Sep.[°])
1LHAASO J0007+5659u	KM2A	1.86	57.00	0.12	<0.18	86.5	0.33±0.05	3.10±0.20	43.6	
	WCDA						<0.27			
1LHAASO J0007+7303u	KM2A	1.91	73.07	0.07	0.17±0.03	361.0	3.41±0.27	3.40±0.12	171.6	CTA 1 (0.12)
	WCDA	1.48	73.15	0.10	<0.22	141.6	5.01±1.11	2.74±0.11		
1LHAASO J0056+6346u	KM2A	14.10	63.77	0.08	0.24±0.03	380.2	1.47±0.10	3.33±0.10	94.1	
	WCDA	13.78	63.96	0.15	0.33±0.07	106.1	1.45±0.41	2.35±0.13		
1LHAASO J0206+4302u	KM2A	31.70	43.05	0.13	<0.27	96.0	0.24±0.03	2.62±0.16	82.8	
	WCDA						<0.09			
1LHAASO J0212+4254u	KM2A	33.01	42.91	0.20	<0.31	38.4	0.12±0.03	2.45±0.23	30.2	
	WCDA						<0.07			
1LHAASO J0216+4237u	KM2A	34.10	42.63	0.10	<0.13	102.0	0.18±0.03	2.58±0.17	65.6	
	WCDA						<0.20			
1LHAASO J0249+6022	KM2A	42.39	60.37	0.16	0.38±0.08	148.8	0.93±0.09	3.82±0.18		
	WCDA	41.52	60.49	0.40	0.71±0.10	53.3	1.96±0.51	2.52±0.16		
1LHAASO J0339+5307	KM2A	54.79	53.13	0.11	<0.22	144.0	0.58±0.06	3.64±0.16		LHAASO J0341+5258 (0.37)
	WCDA						<0.21			
1LHAASO J0343+5254u*	KM2A	55.79	52.91	0.08	0.20±0.02	388.1	1.07±0.07	3.53±0.10	20.2	LHAASO J0341+5258 (0.28)
	WCDA	55.34	53.05	0.18	0.33±0.05	94.1	0.29±0.13	1.70±0.19		

82 sources with the Galactic latitude |b|<12º

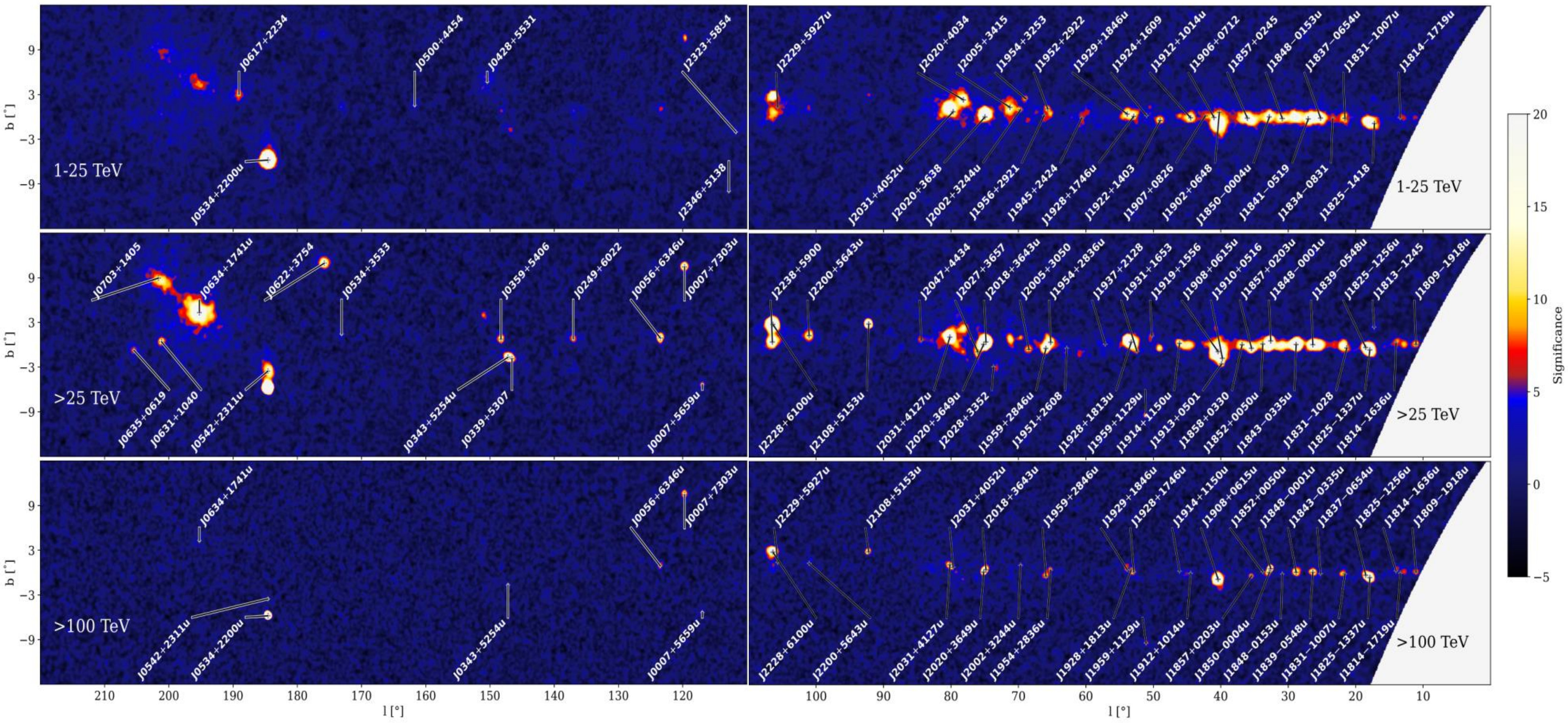

8 sources with the Galactic latitude |b|>12°

Mrk 421 z=0.031 | 1ES 1727+502 z=0.055 | 4 AGNs | Mrk 501 z=0.034 | NGC 4278 z=0.002

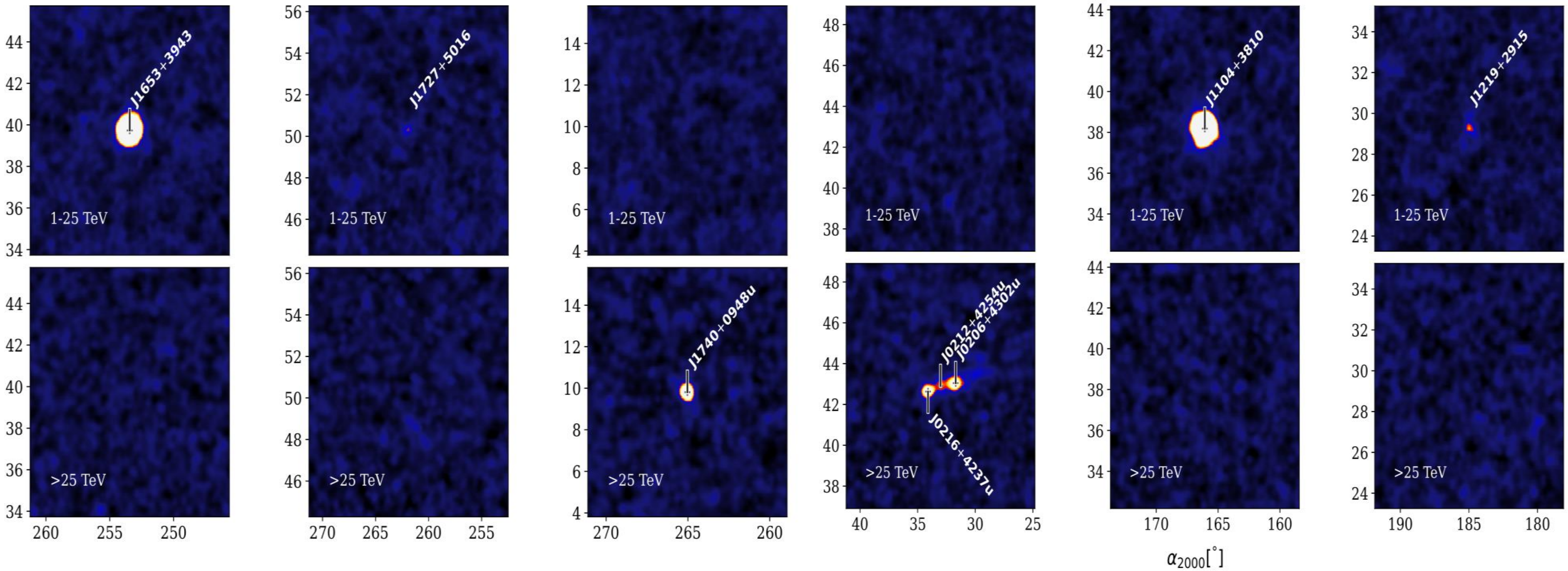

Association with known TeV Sources

- 58 sources with TeVCat+3HAWC association
- 32 new sources (25+7)

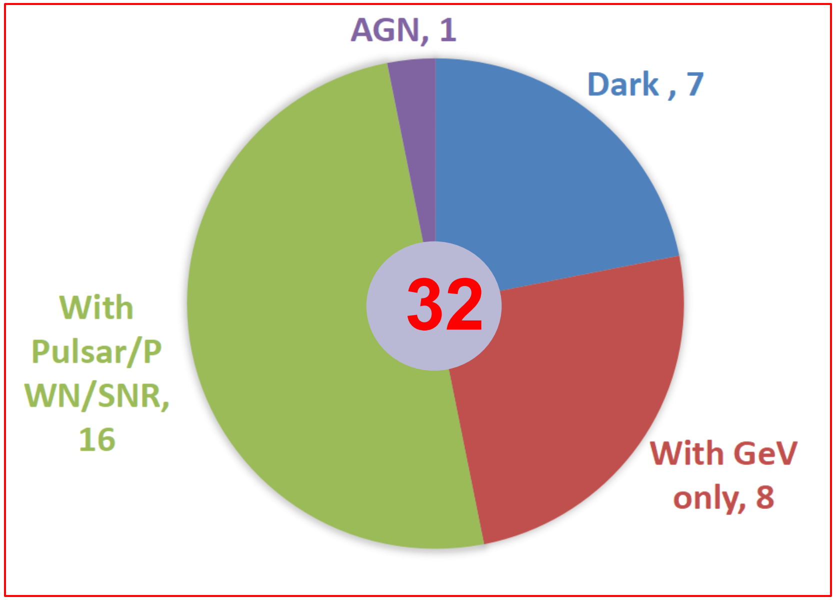

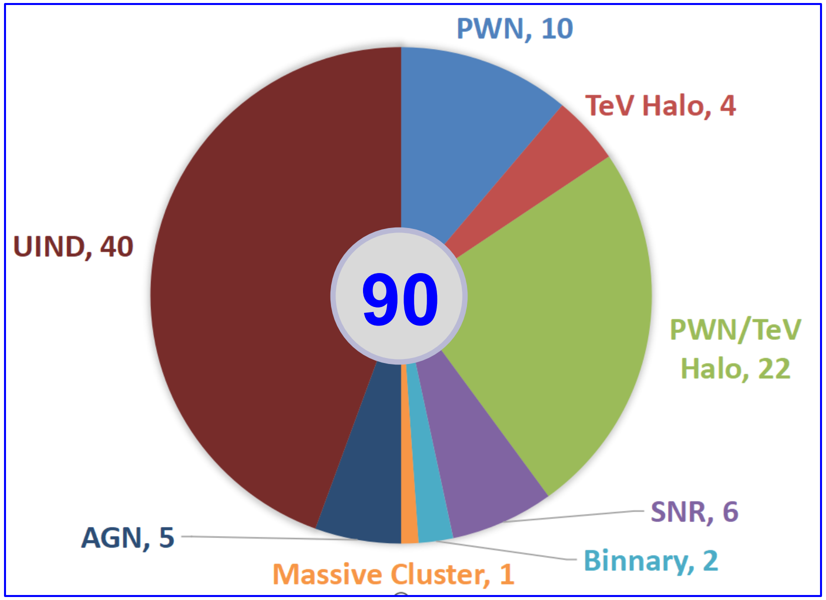

PeVatrons

- 51% (35/69) 1-25TeV sources are UHE sources.
- 57% (43/75) >25TeV sources are UHE sources.
- 19% (8/43) UHE sources are not detected at 1-25TeV (new class?).

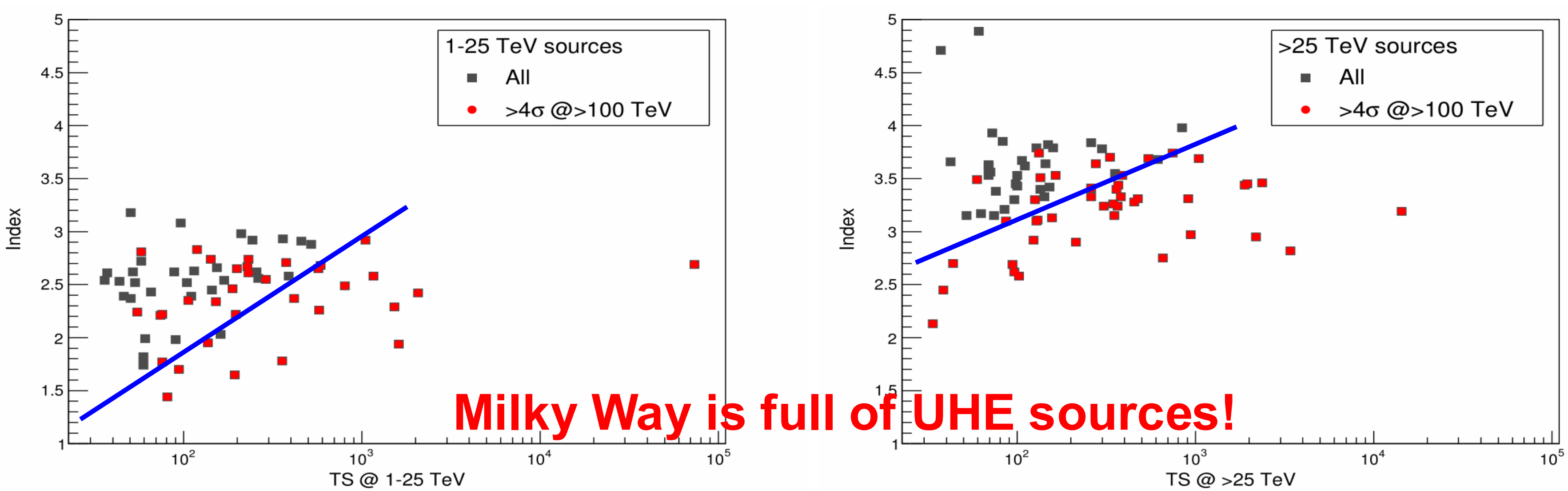

Milky Way is full of UHE sources!

1 LHAASO catalog

- 90 in 1st LHAASO sources.
- 32 new discoveries
- 43 UHE

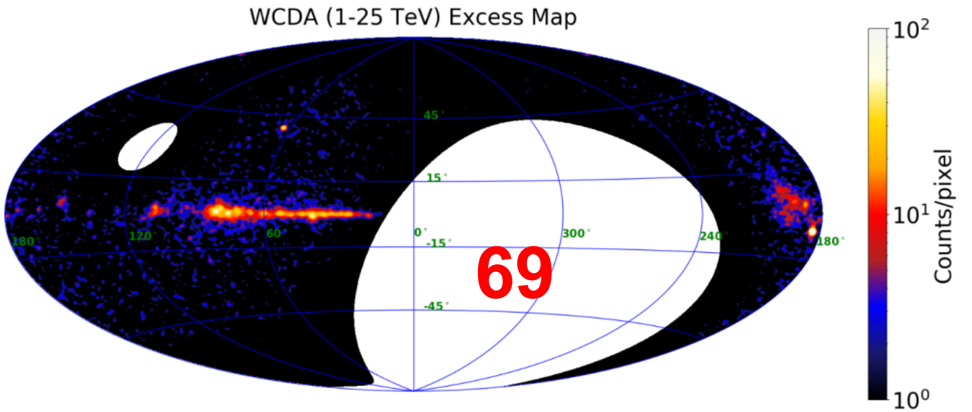

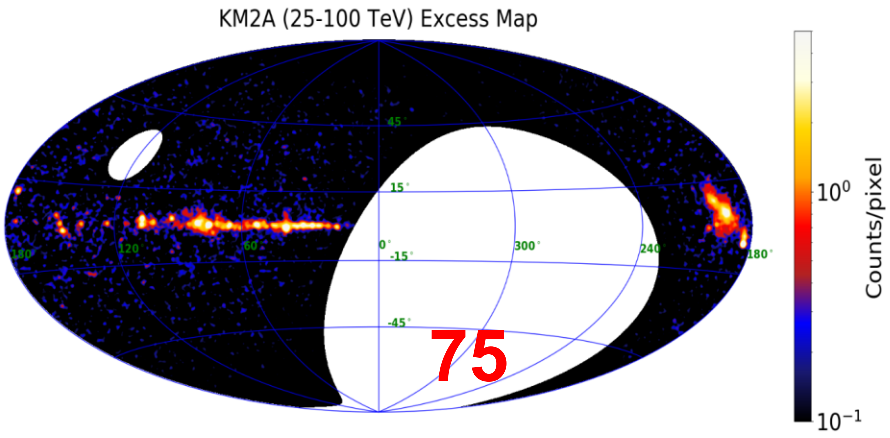

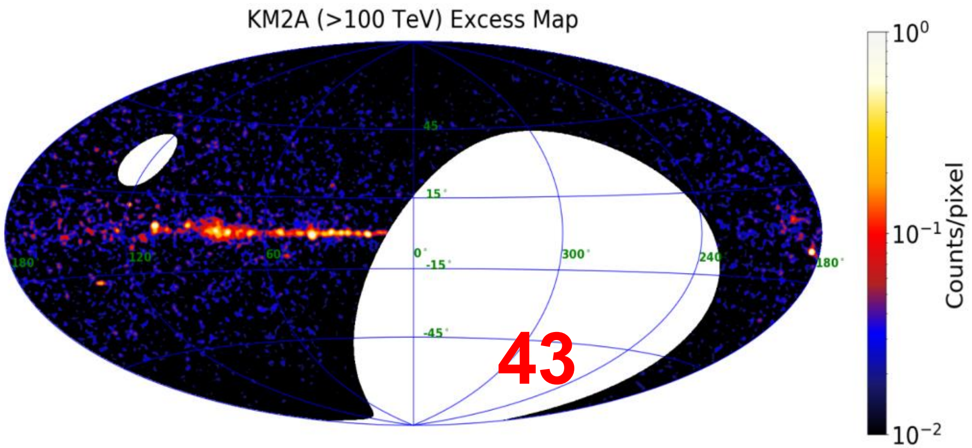

AGN's

M87

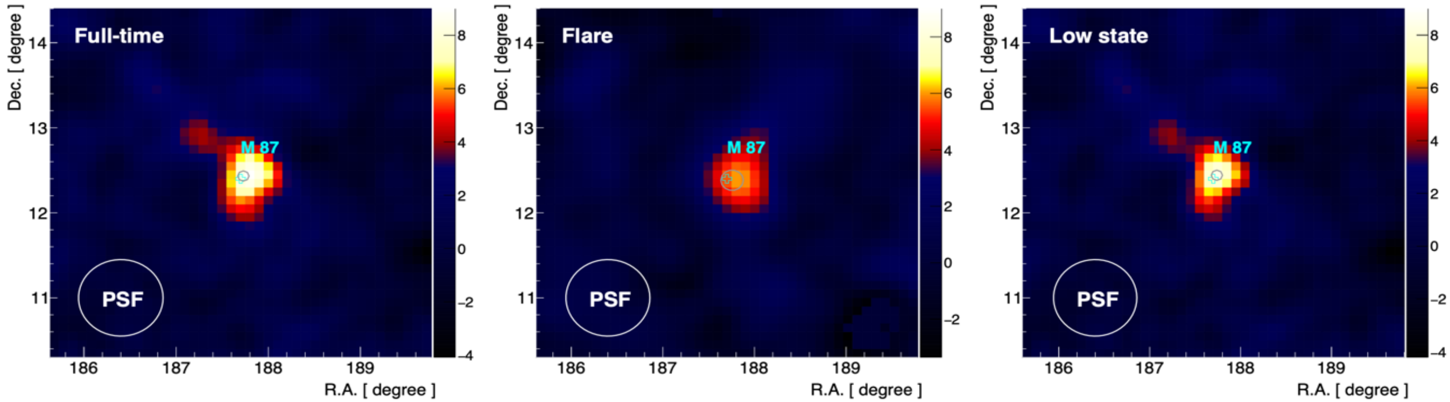

Figure 1. Significance maps of 2° × 2° region around M87 by LHAASO-WCDA for full-time period (left panel), flare state (middle panel) and low state (right panel), respectively. M87 is marked by cyan open cross. The gray circle indicates the 95%

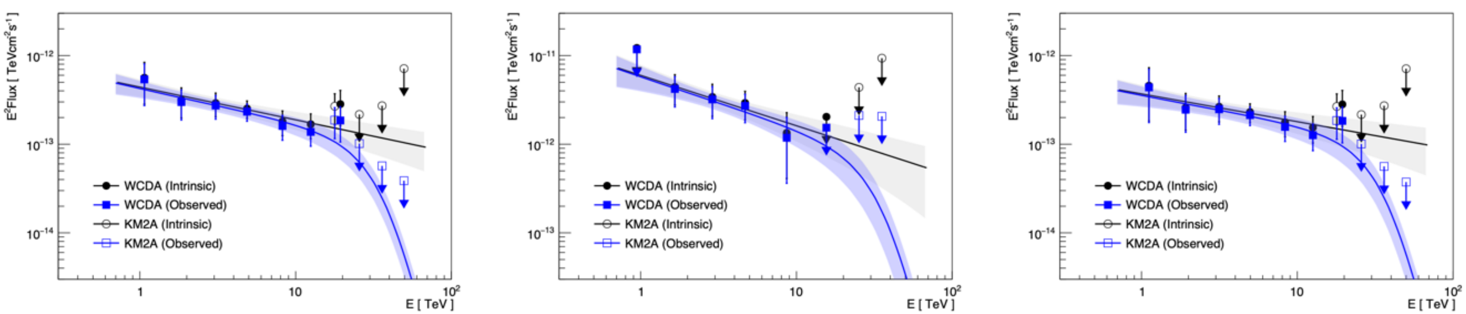

Figure 3. VHE spectra of M87 during the full-time period (left panel), the flare state (middle panel) and the low state (right panel), assuming a single power-law model for the intrinsic spectra and a EBL absorption model of Franceschini et al. (2008). The gray and blue shaded regions indicate 1σ statistical error for the intrinsic spectra and PLxEBL spectra, respectively.

LHAASO Collaboration, 2410.15353

M87

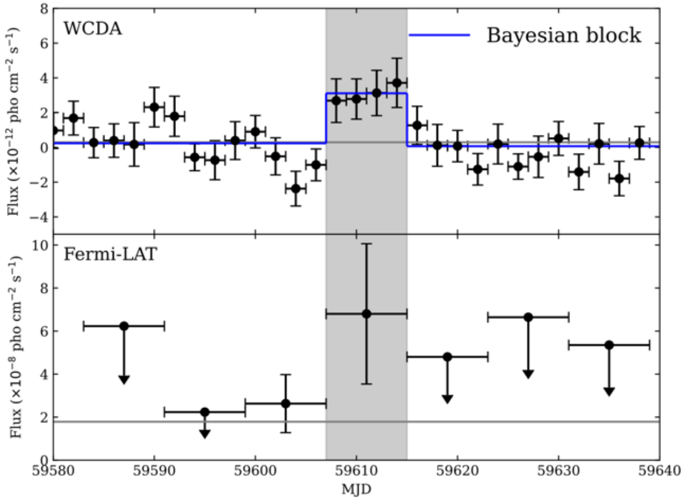

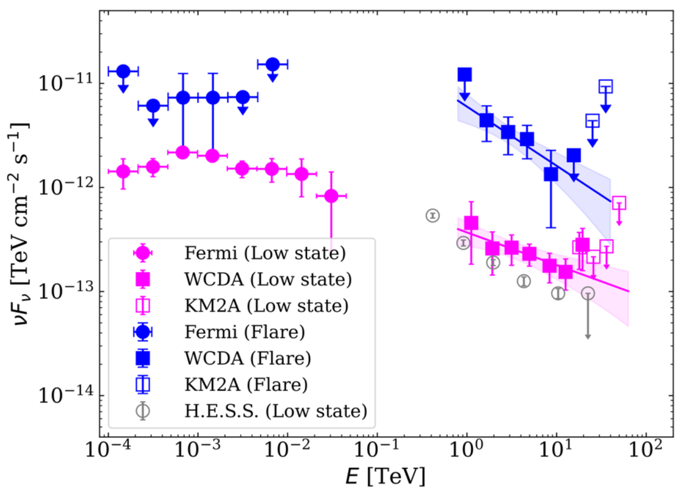

LHAASO Collaboration, 2410.15353

Pulsar Wind Nebulas

Pulsars as Counterparts of VHE gamma-ray sources

Pulsars – the most commonly potential counterparts of detected VHE gamma-ray emitter

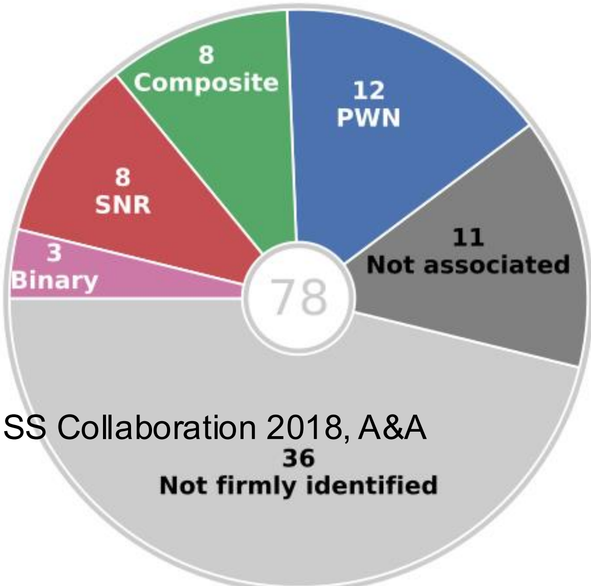

HESS Collaboration 2018, A&A

14 firmly identified PWN by HESS

HGPS name	ATNF name	Canonical name	lg $\dot{E}$	τ_c (kyr)	d (kpc)	PSR offset (pc)	Γ	R_{PWN} (pc)	$L_{1-10\,TeV}$ (10^{33} erg s^{-1})
J1813−178[1]	J1813−1749		37.75	5.60	4.70	<2	2.07 ± 0.05	4.0 ± 0.3	19.0 ± 1.5
J1833−105	J1833−1034	G21.5−0.9[2]	37.53	4.85	4.10	<2	2.42 ± 0.19	<4	2.6 ± 0.5
J1514−591	B1509−58	MSH 15−52[3]	37.23	1.56	4.40	<4	2.26 ± 0.03	11.1 ± 2.0	52.1 ± 1.8
J1930+188	J1930+1852	G54.1+0.3[4]	37.08	2.89	7.00	<10	2.6 ± 0.3	<9	5.5 ± 1.8
J1420−607	J1420−6048	Kookaburra (K2)[5]	37.00	13.0	5.61	5.1 ± 1.2	2.20 ± 0.05	7.9 ± 0.6	44 ± 3
J1849−000	J1849−0001	IGR J18490−0000[6]	36.99	42.9	7.00	<10	1.97 ± 0.09	11.0 ± 1.9	12 ± 2
J1846−029	J1846−0258	Kes 75[2]	36.91	0.728	5.80	<2	2.41 ± 0.09	<3	6.0 ± 0.7
J0835−455	B0833−45	Vela X[7]	36.84	11.3	0.280	2.37 ± 0.18	1.89 ± 0.03	2.9 ± 0.3	0.83 ± 0.11*
J1837−069[8]	J1838−0655		36.74	22.7	6.60	17 ± 3	2.54 ± 0.04	41 ± 4	204 ± 8
J1418−609	J1418−6058	Kookaburra (Rabbit)[5]	36.69	10.3	5.00	7.3 ± 1.5	2.26 ± 0.05	9.4 ± 0.9	31 ± 3
J1356−645[9]	J1357−6429		36.49	7.31	2.50	5.5 ± 1.4	2.20 ± 0.08	10.1 ± 0.9	14.7 ± 1.4
J1825−137[10]	B1823−13		36.45	21.4	3.93	33 ± 6	2.38 ± 0.03	32 ± 2	116 ± 4
J1119−614	J1119−6127	G292.2−0.5[11]	36.36	1.61	8.40	<11	2.64 ± 0.12	14 ± 2	23 ± 4
J1303−631[12]	J1301−6305		36.23	11.0	6.65	20.5 ± 1.8	2.33 ± 0.02	20.6 ± 1.7	96 ± 5

Among the 47 sources not yet identified, most of them (36) have possible associations with cataloged objects, notably PWNe and energetic pulsars that could power VHE PWN. —— HGPS

We have presented the third catalog of steady gamma-ray emitters detected by HAWC using 1523 days of data. The catalog consists of 65 sources, including two blazars. The most abundant source class among the potential counterpart of HAWC sources in the Galactic plane is pulsars (56). —— 3HWC (HAWC Collaboration 2020, ApJ)

Three Evolution Stages

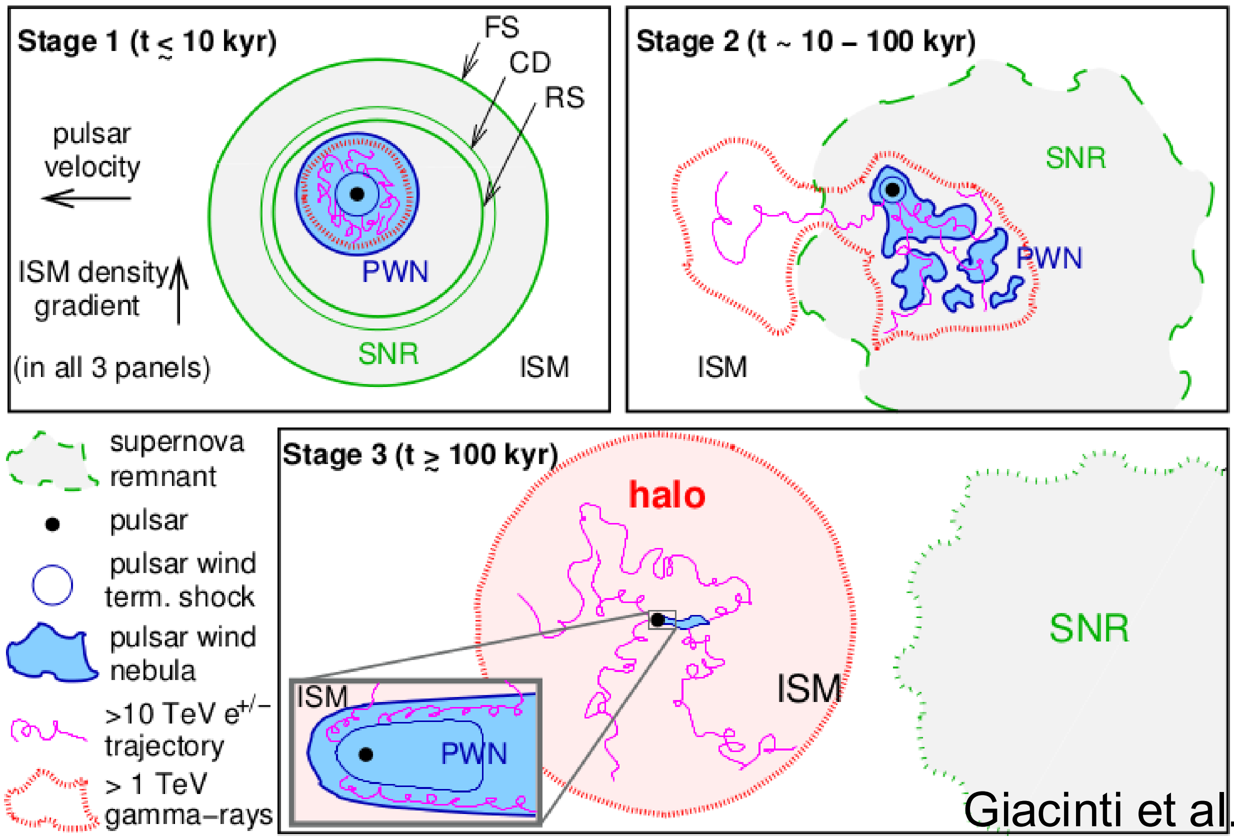

Giacinti et al. 2020

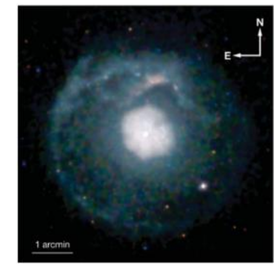

SNR G21.5-0.9
PSR J1833-1034

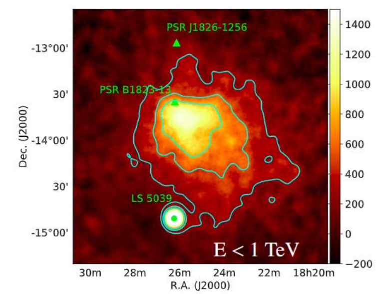

HESS J1825-137
PSR J1826-1334

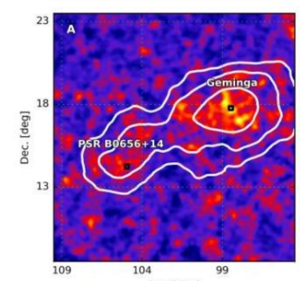

Geminga
Monogem

1LHAASO Catalogue

35 sources associated with pulsars with $\dot{E} > 10^{34}\mathrm{erg/s}$ at a chance probablity <1%
(65 have ≥1 pulsar within 0.5 deg)

Source name	PSR name	dist.(°)	Distance (kpc)	τ_c (kyr)	$\dot{E}$ (ergs/s)	P_c	Identified type in TeVCat
1LHAASO J0007+7303u	PSR J0007+7303	0.05	1.40	14	4.5e+35	7.3e-05	PWN
1LHAASO J0216+4237u	PSR J0218+4232	0.33	3.15	476000	2.4e+35	3.6e-03	
1LHAASO J0249+6022	PSR J0248+6021	0.16	2.00	62	2.1e+35	1.5e-03	
1LHAASO J0359+5406	PSR J0359+5414	0.15	-	75	1.3e+36	7.2e-04	
1LHAASO J0534+2200u	PSR J0534+2200	0.01	2.00	1	4.5e+38	3.2e-06	PWN
1LHAASO J0542+2311u	PSR J0543+2329	0.30	1.56	253	4.1e+34	8.3e-03	
1LHAASO J0622+3754	PSR J0622+3749	0.09	-	208	2.7e+34	2.5e-04	PWN/TeV Halo
1LHAASO J0631+1040	PSR J0631+1037	0.11	2.10	44	1.7e+35	3.5e-04	PWN
1LHAASO J0634+1741u	PSR J0633+1746	0.12	0.19	342	3.3e+34	1.3e-03	PWN/TeV Haloa
1LHAASO J0635+0619	PSR J0633+0632	0.39	1.35	59	1.2e+35	9.4e-03	
1LHAASO J1740+0948u	PSR J1740+1000	0.21	1.23	114	2.3e+35	1.4e-03	
1LHAASO J1809-1918u	PSR J1809-1917	0.05	3.27	51	1.8e+36	6.2e-04	
1LHAASO J1813-1245	PSR J1813-1245	0.01	2.63	43	6.2e+36	6.3e-06	
1LHAASO J1825-1256u	PSR J1826-1256	0.09	1.55	14	3.6e+36	1.6e-03	
1LHAASO J1825-1337u	PSR J1826-1334	0.11	3.61	21	2.8e+36	2.8e-03	PWN/TeV Halo
1LHAASO J1837-0654u	PSR J1838-0655	0.12	6.60	23	5.6e+36	2.2e-03	PWN
1LHAASO J1839-0548u	PSR J1838-0537	0.20	-	5	6.0e+36	6.1e-03	
1LHAASO J1848-0001u	PSR J1849-0001	0.06	-	43	9.8e+36	1.2e-04	PWN
1LHAASO J1857+0245	PSR J1856+0245	0.16	6.32	21	4.6e+36	3.1e-03	PWN
1LHAASO J1906+0712	PSR J1906+0722	0.19	-	49	1.0e+36	5.9e-03	
1LHAASO J1908+0615u	PSR J1907+0602	0.23	2.37	20	2.8e+36	6.8e-03	
1LHAASO J1912+1014u	PSR J1913+1011	0.13	4.61	169	2.9e+36	1.5e-03	
1LHAASO J1914+1150u	PSR J1915+1150	0.09	14.01	116	5.4e+35	1.8e-03	
1LHAASO J1928+1746u	PSR J1928+1746	0.04	4.34	83	1.6e+36	1.6e-04	
1LHAASO J1929+1846u	PSR J1930+1852	0.29	7.00	3	1.2e+37	2.6e-03	PWN
1LHAASO J1954+2836u	PSR J1954+2836	0.01	1.96	69	1.1e+36	1.6e-05	PWN
1LHAASO J1954+3253	PSR J1952+3252	0.33	3.00	107	3.7e+36	6.7e-03	
1LHAASO J1959+2846u	PSR J1958+2845	0.10	1.95	22	3.4e+35	2.8e-03	PWN
1LHAASO J2005+3415	PSR J2004+3429	0.25	10.78	18	5.8e+35	9.9e-03	
1LHAASO J2005+3050	PSR J2006+3102	0.20	6.04	104	2.2e+35	9.2e-03	
1LHAASO J2020+3649u	PSR J2021+3651	0.05	1.80	17	3.4e+36	1.5e-04	PWN
1LHAASO J2028+3352	PSR J2028+3332	0.36	-	576	3.5e+34	8.0e-03	
1LHAASO J2031+4127u	PSR J2032+4127	0.08	1.33	201	1.5e+35	1.0e-03	PWN
1LHAASO J2228+6100u	PSR J2229+6114	0.27	3.00	10	2.2e+37	2.2e-03	PWN
1LHAASO J2238+5900	PSR J2238+5903	0.07	2.83	27	8.9e+35	3.0e-04	

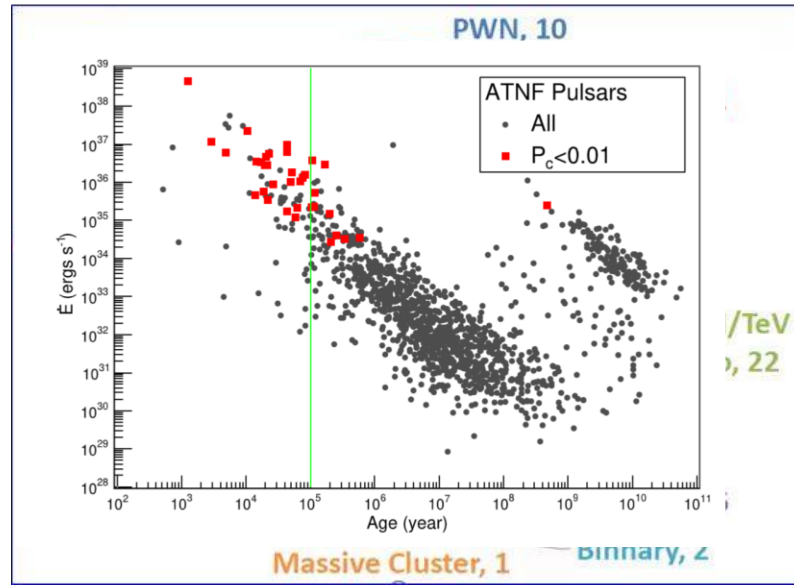

$$P_c = 1 - e^{r^2/r_0^2} \qquad r_0 = [\pi\rho(\dot{E})]^{-1/2}$$

$$|b - b_c| < 2.5^\circ \;\&\; |l - l_c| < 10^\circ$$

LHAASO J0621+3755

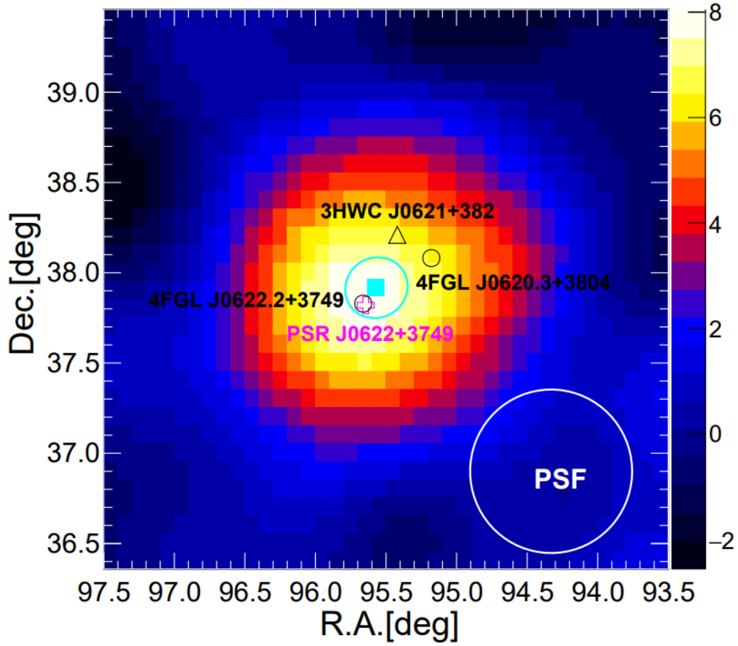

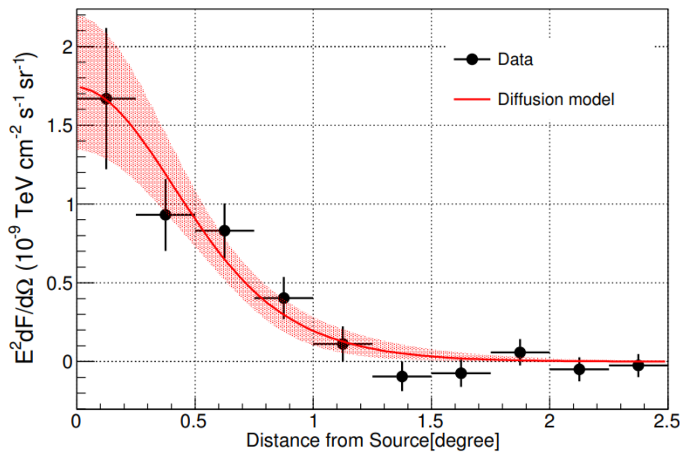

$D \approx (8.9\,^{+4.5}_{-3.9}) \times 10^{27} (d/1.6\ \mathrm{kpc})^2\ \mathrm{cm^2 s^{-1}}$ for $E_e \sim 160$ TeV

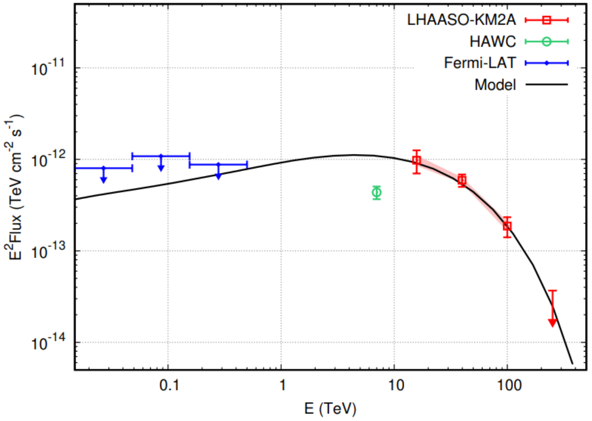

LHAASO Collaboration 2021, PRL

PWN/Pulsar Halos by LHAASO

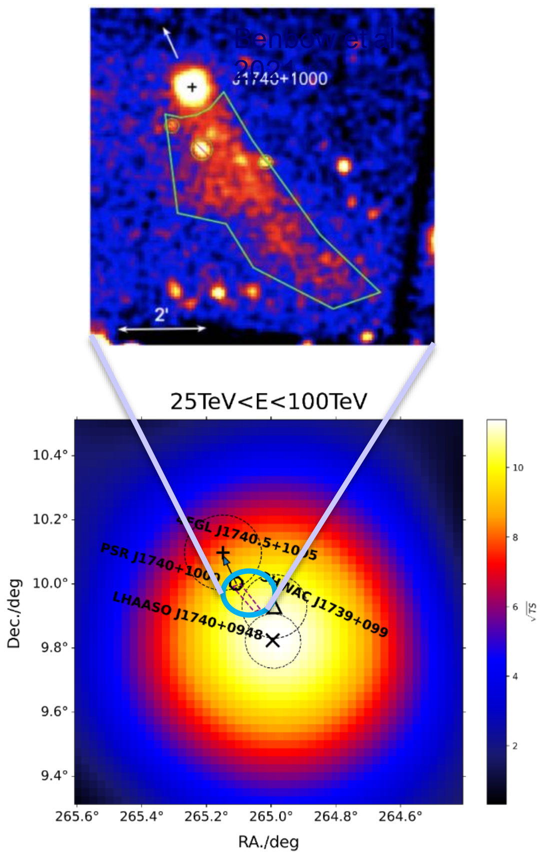

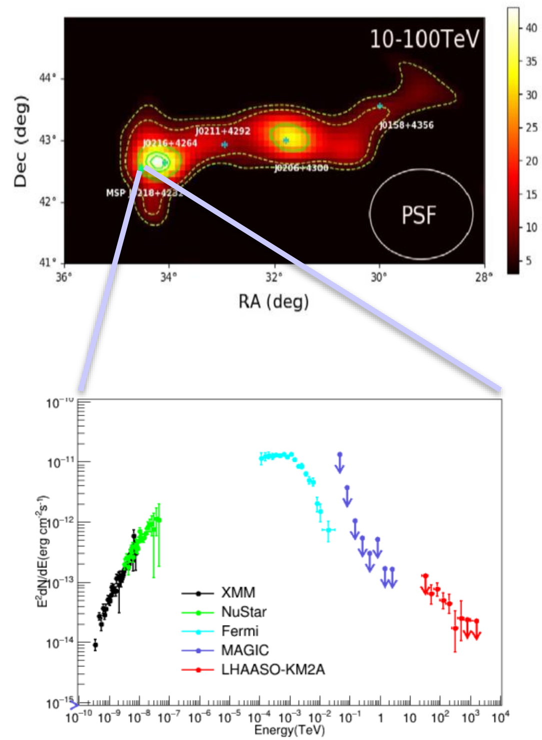

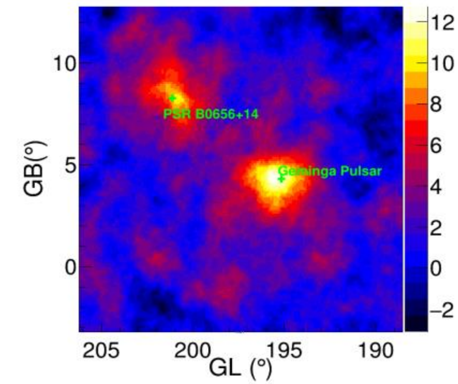

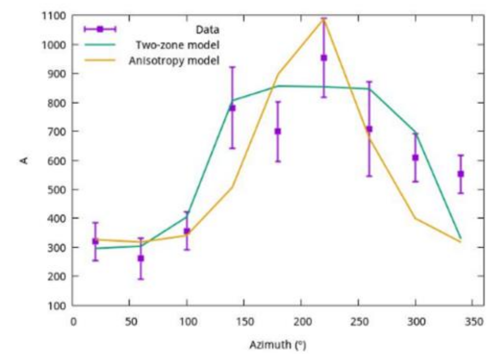

Super Nova Remnants

Origin of Cosmic Rays

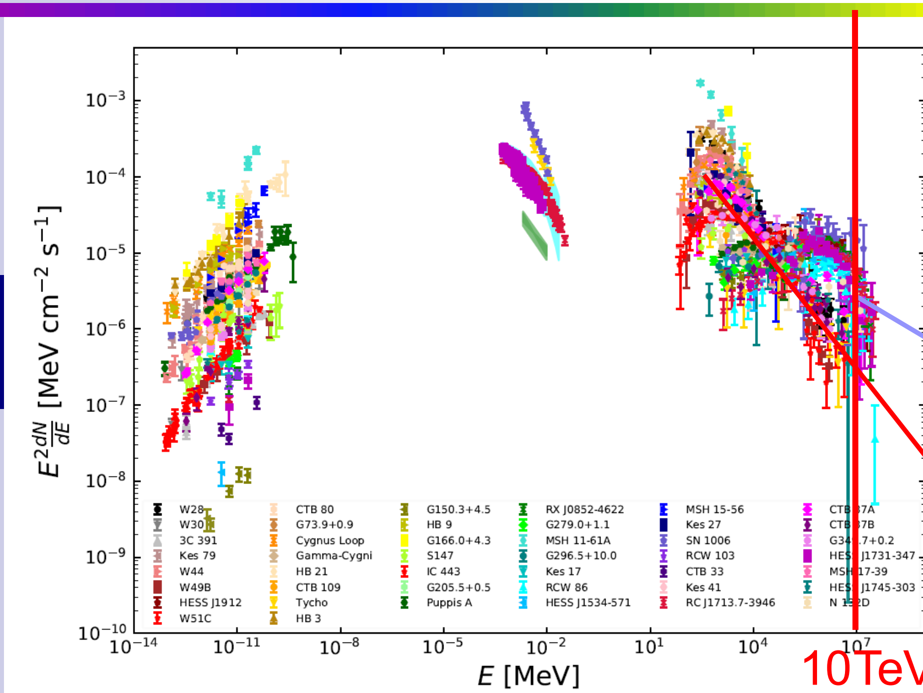

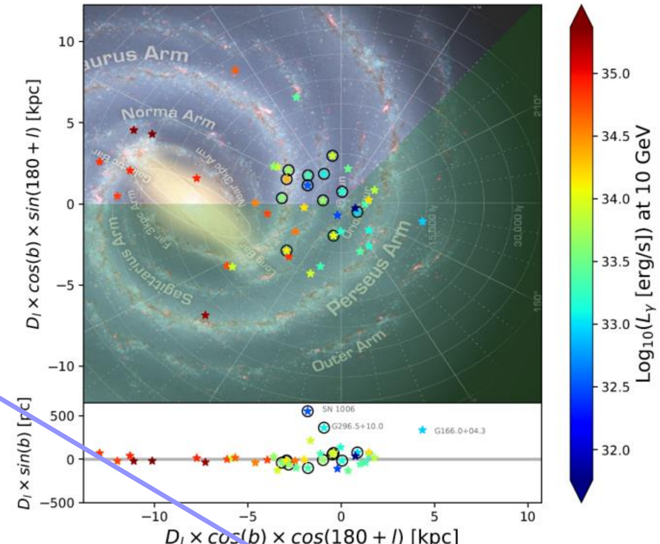

Multiwavelength spectra of 44 SNRs normalized at 100 GeV and their distribution in the

Spectra of Proton and Helium

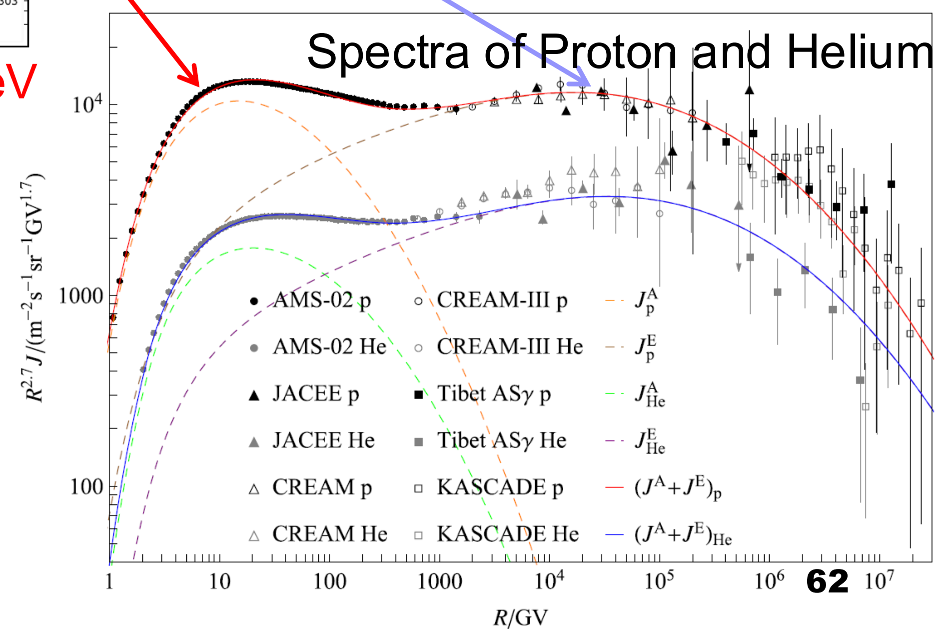

Reviews of Modern Plasma Physics (2022) 6:19
https://doi.org/10.1007/s41614-022-00080-6

REVIEW PAPER

The origin of galactic cosmic rays

Siming Liu[1] · Houdun Zeng[2,4] · Yuliang Xin[1] · Yiran Zhang[3]

LHAASO

7 SNRs Detected by LHAASO

Cas A; IC 443; W51C; Gamma-Cygni; G106.3+2.7; G69.7+1.0; G150.3+4.5

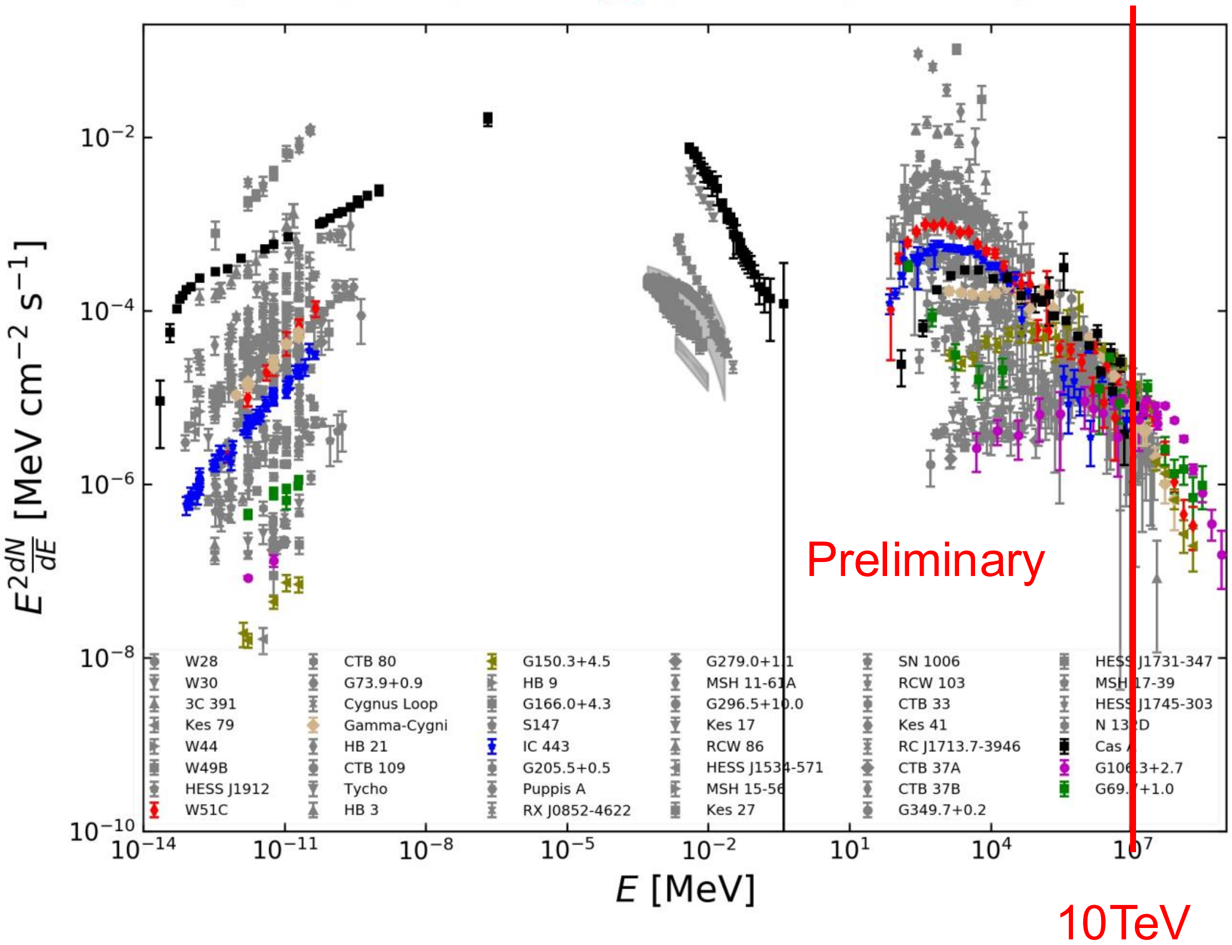

The higher energy spectra are softer (but harder than an exponential cutoff)

γ Cygni SNR

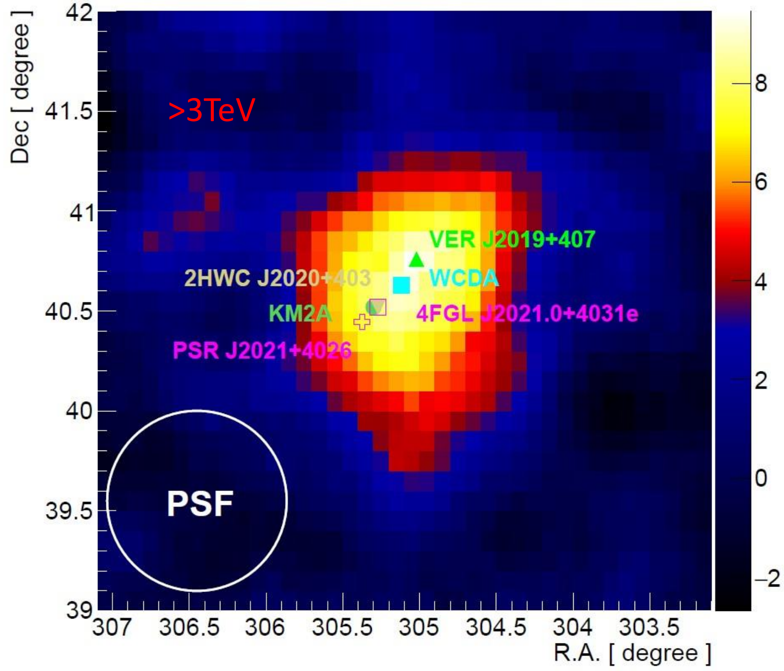

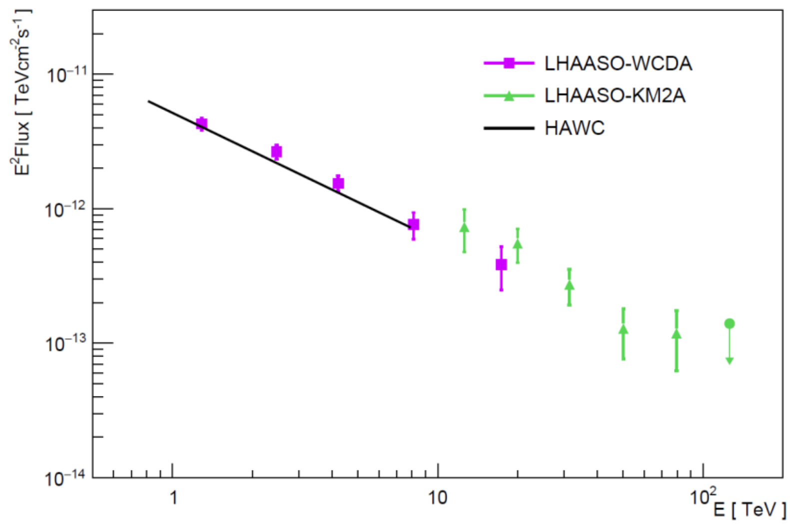

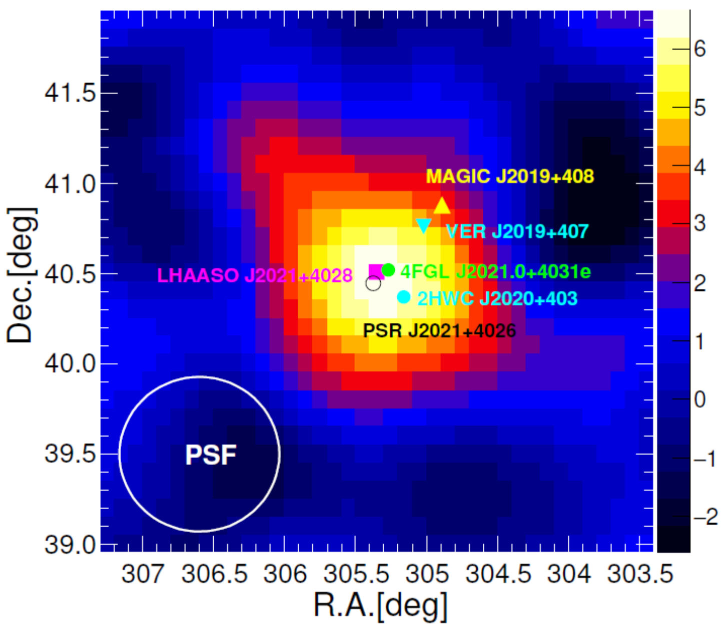

- gaussian： sigma = 0.374 +/- 0.040
- disk： radius = 0.592 +/- 0.056

PaVarton at HII Region G35.6−−0.5

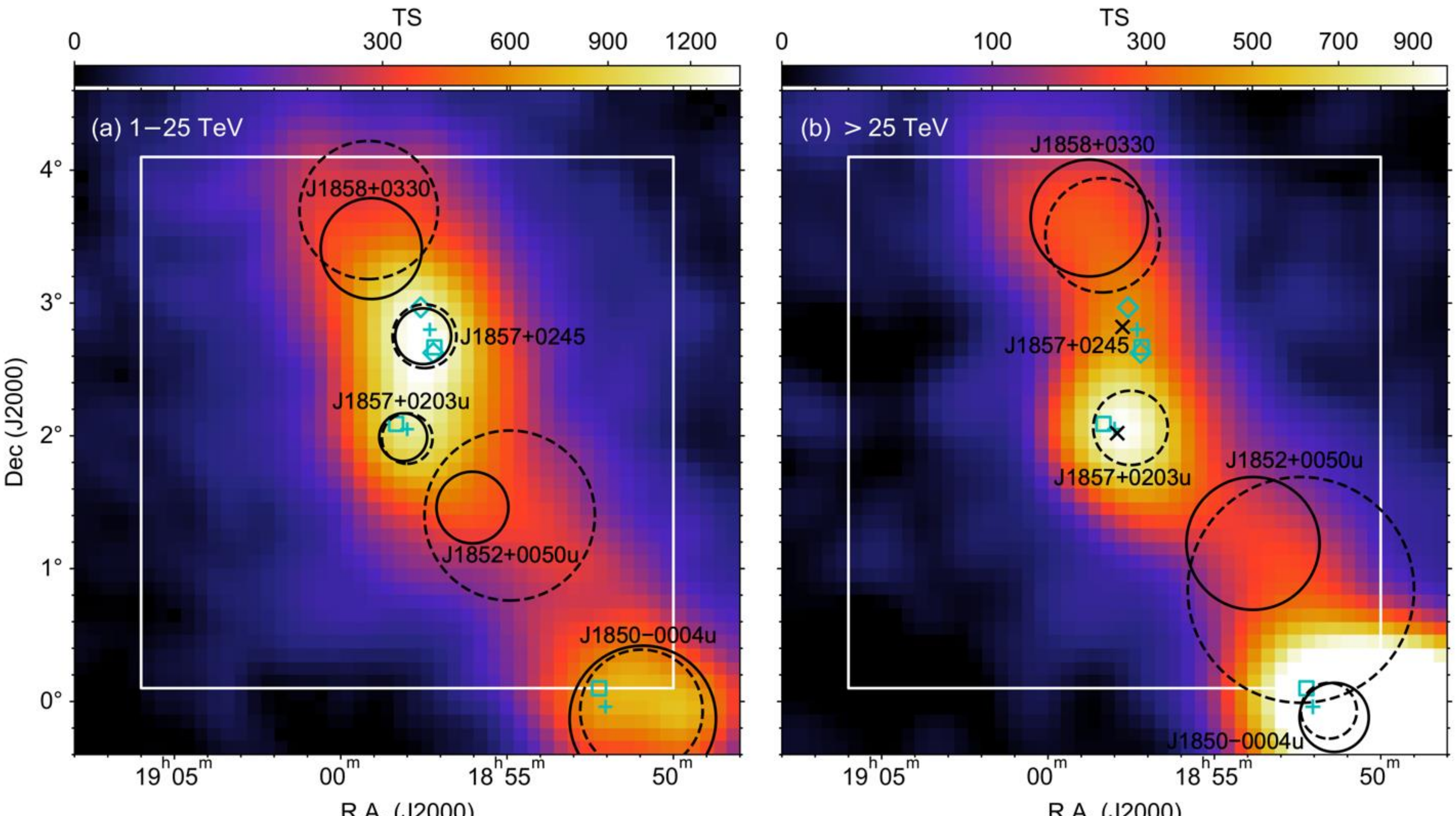

LHAASO Collaboration 2412.00379

PaVarton at HII Region G35.6−−0.5

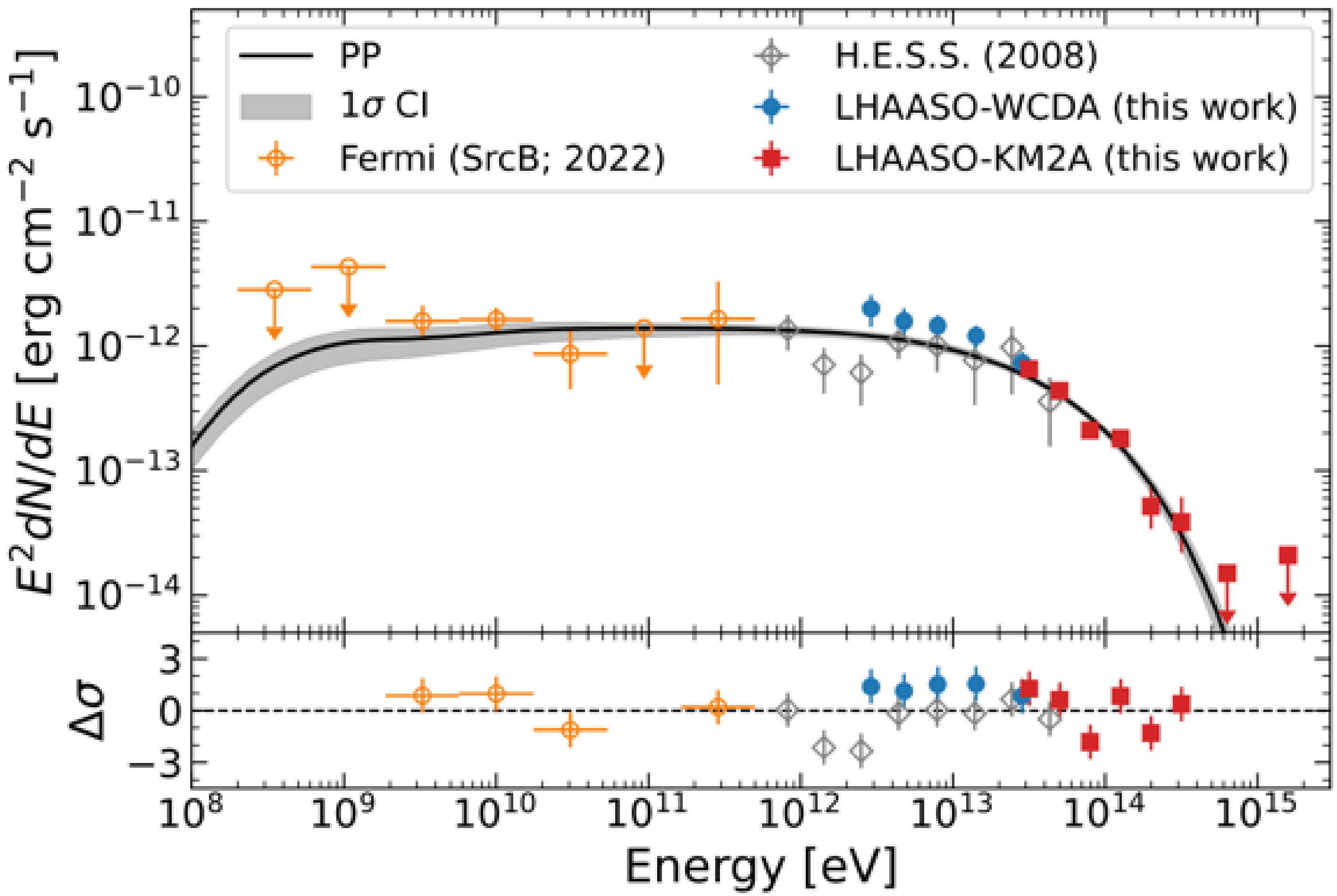

LHAASO Collaboration 2412.00379

Star Clusters

YMSC IN OUR GALAXY

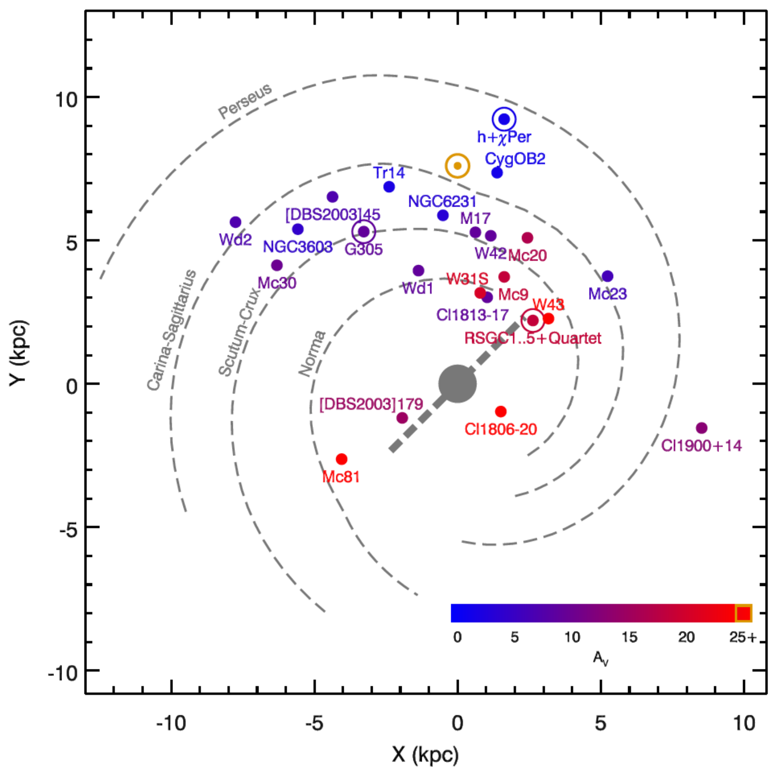

Davies et.al 2011

- ~20 in our Galaxy
- More to be discovered (high extinction in Galactic plane)

Stellar type	log[$\dot{M}$] $M_\odot$ yr^{-1}	V_∞ [km s^{-1}]
WNL	-4.2	1650
WNE	-4.5	1900
WC6-9	-4.4	1800
WC4-5	-4.7	2800
WO	-5.0	3500
O3	-5.2	3190
O4	-5.4	2950
O4.5	-5.5	2900
O5	-5.6	2875

- The wind power of a single young star can be as high as 1e37 erg/s

Gamma-ray emitting YMSC

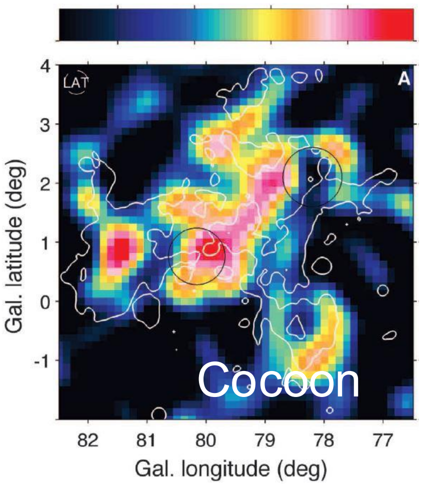

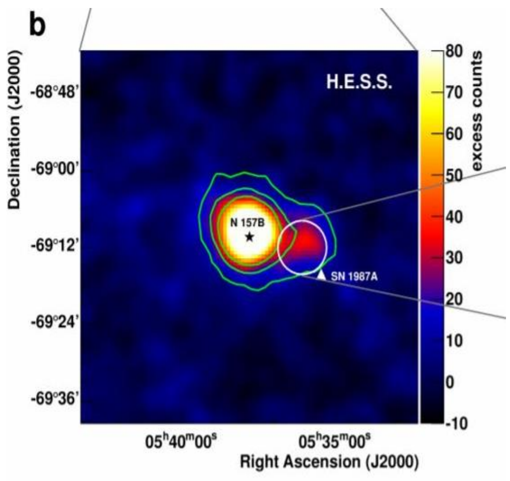

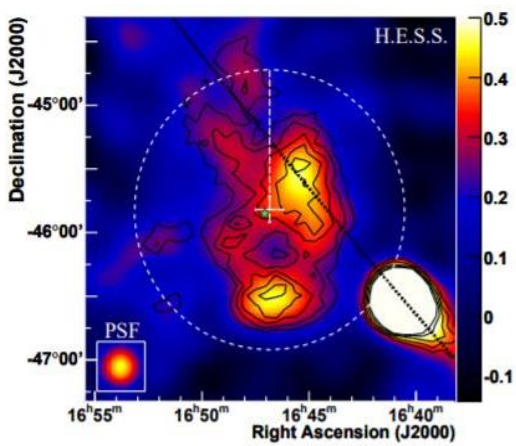

New GAMMA-RAY Source population:

Cygnus Cocoon(GeV-TeV)[Fermi 2012, HAWC2022]
Westerlund 1 (TeV) [HESS collaboration 2012]
Westerlund 2 (GeV, TeV？)[Yang et.al 2018]
NGC 3603 (GeV, TeV)[Yang et.al 2017]
W43 (GeV, TeV?) [Yang et.al 2020]
W40 (GeV) [Sun et.al 2019]
G25/RSGC 1[Sun et.al 2020]
Carina nebular [Ge et.al 2022]
M17 [Liu et.al 2022]

LHAASO VIEW ON CYGNUS

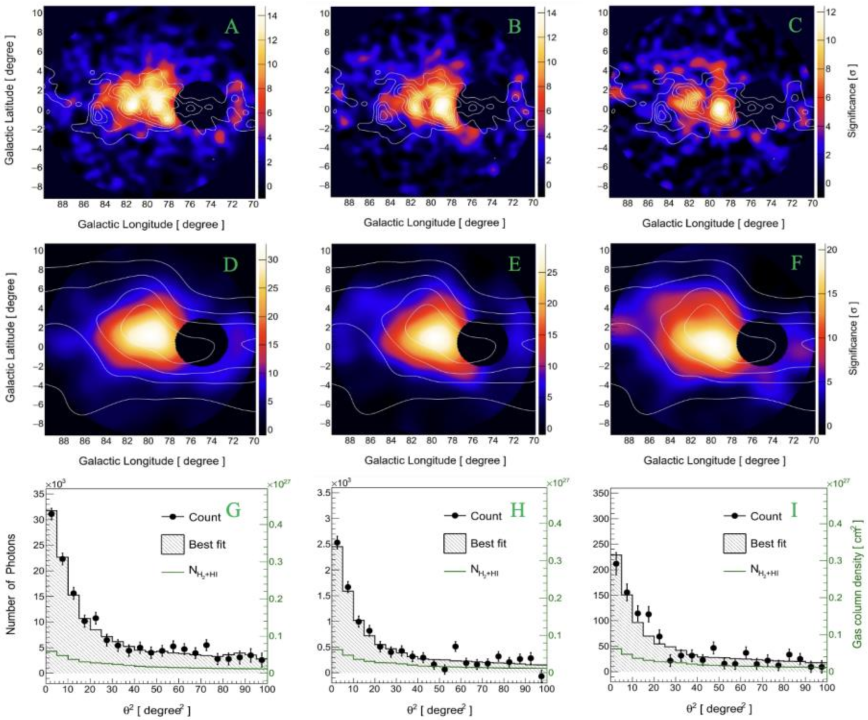

Huge bubble beyond ~10 degrees (200 pc)

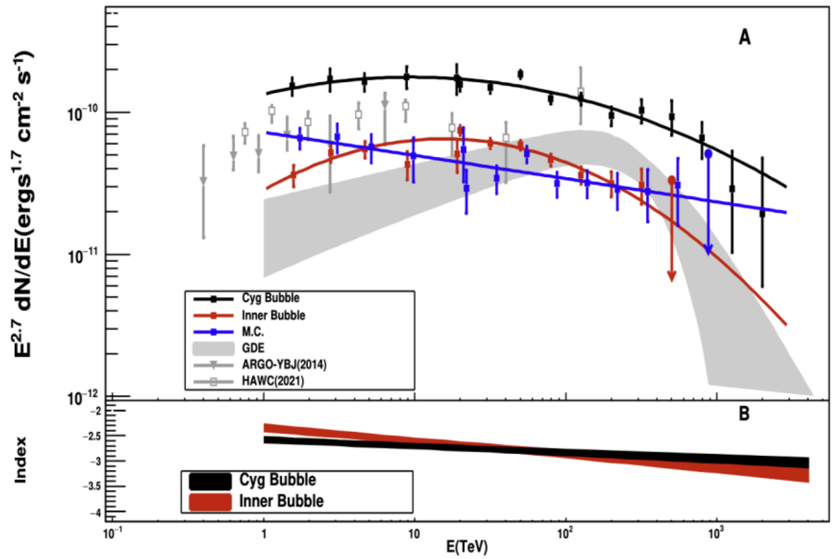

Curved and uniform spectral shape

inner bubble: r~3 degrees, similar to “cocoon”

cygnus bubble: r~10 degrees

LHAASO view on w43

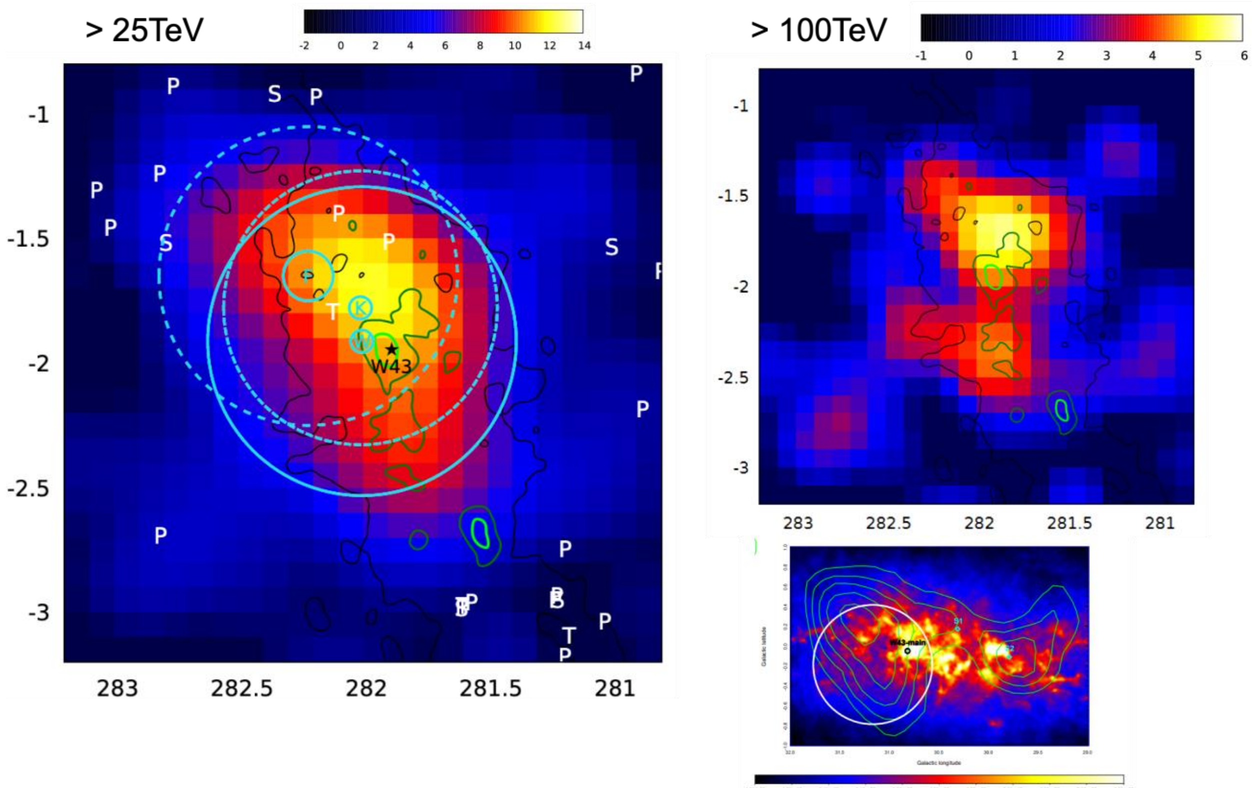

- UHE gamma-ray emission reveal good correlation with dense gas
- Spectrum up to PeV

Diffuse gamma-ray emission

Gamma/CR discrimination

$$R = \log\left(\frac{N_\mu + 0.0001}{N_e}\right)$$

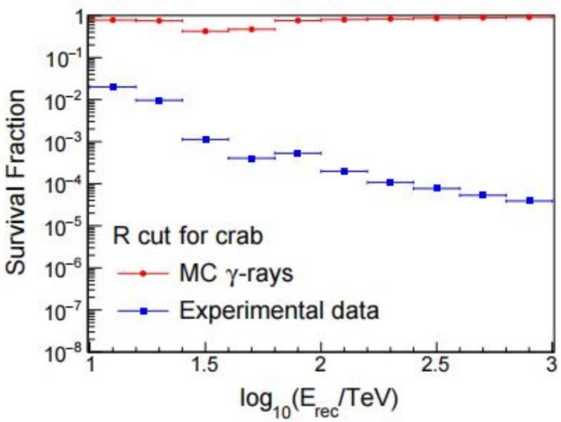

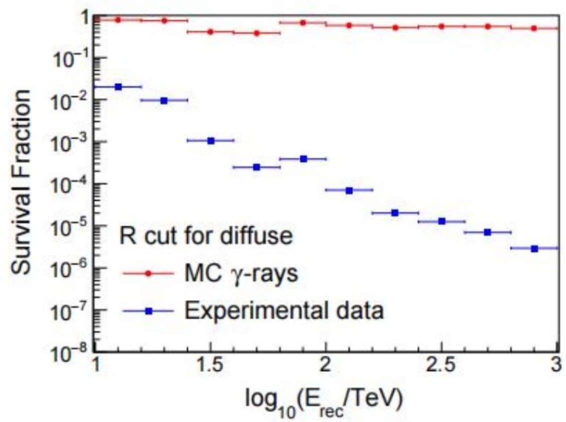

$\log(E_{\mathrm{rec}}/\mathrm{TeV})$	R for crab	R for diffuse
1.0 – 1.2	−5.11	−5.00
1.2 – 1.4	−5.24	−3.20
1.4 – 1.6	−5.95	−5.96
1.6 – 1.8	−6.08	−6.17
1.8 – 2.0	−2.34	−2.50
2.0 – 2.2	−2.35	−2.69
2.2 – 2.4	−2.36	−2.79
2.4 – 2.6	−2.36	−2.74
2.6 – 2.8	−2.36	−2.75
2.8 – 3.0	−2.36	−2.79

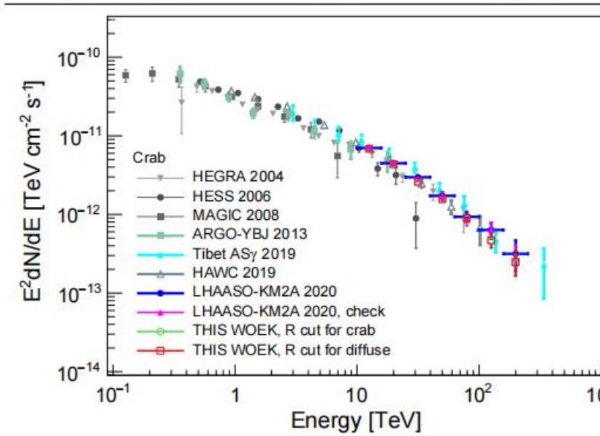

- ➢ R cuts adjusted from the Crab analysis to enable a higher $Q=S/B^{1/2}$ factor
- ➢ Efficiencies change from ~90% to ~60%

Mask LHAASO

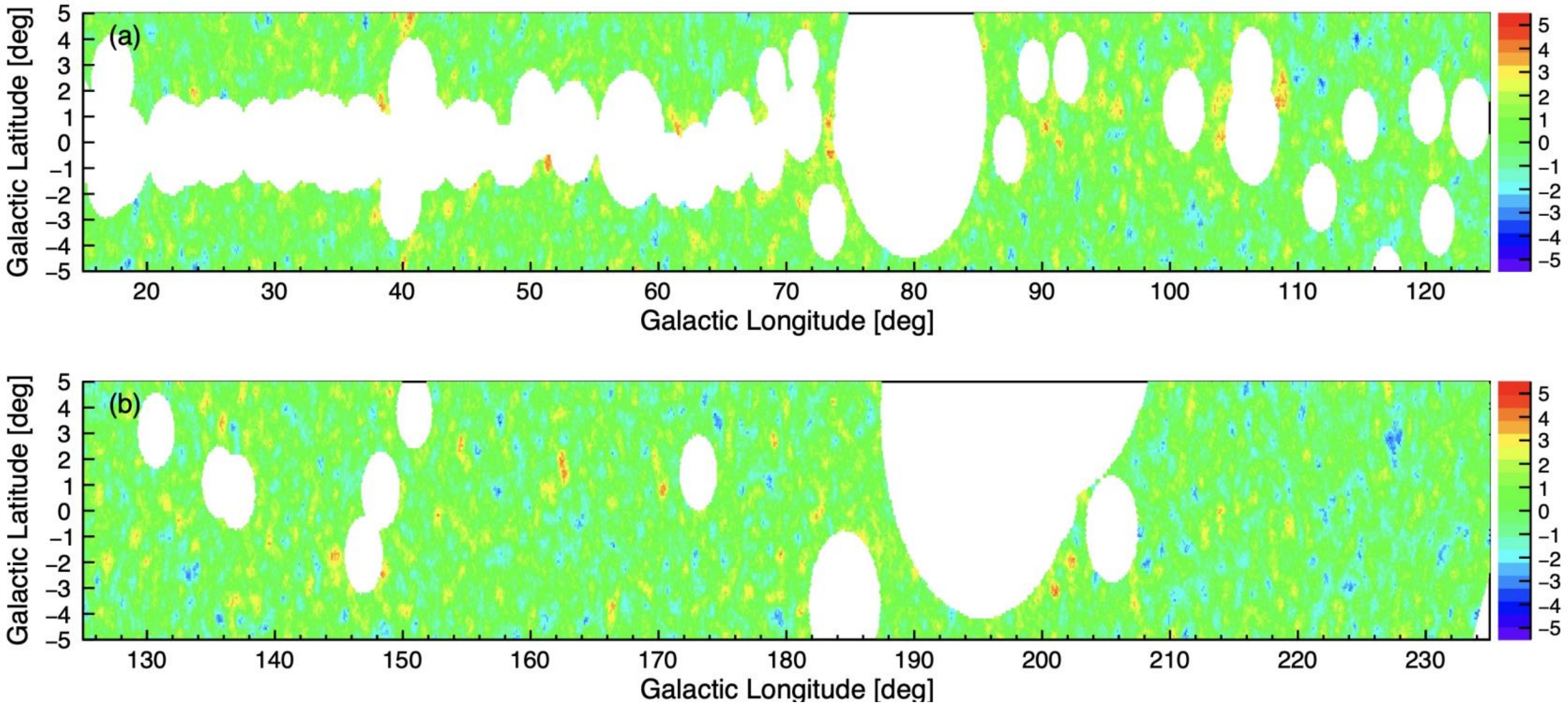

LHAASO collaboration arXiv: 2305.05372

LHAASO diffuse

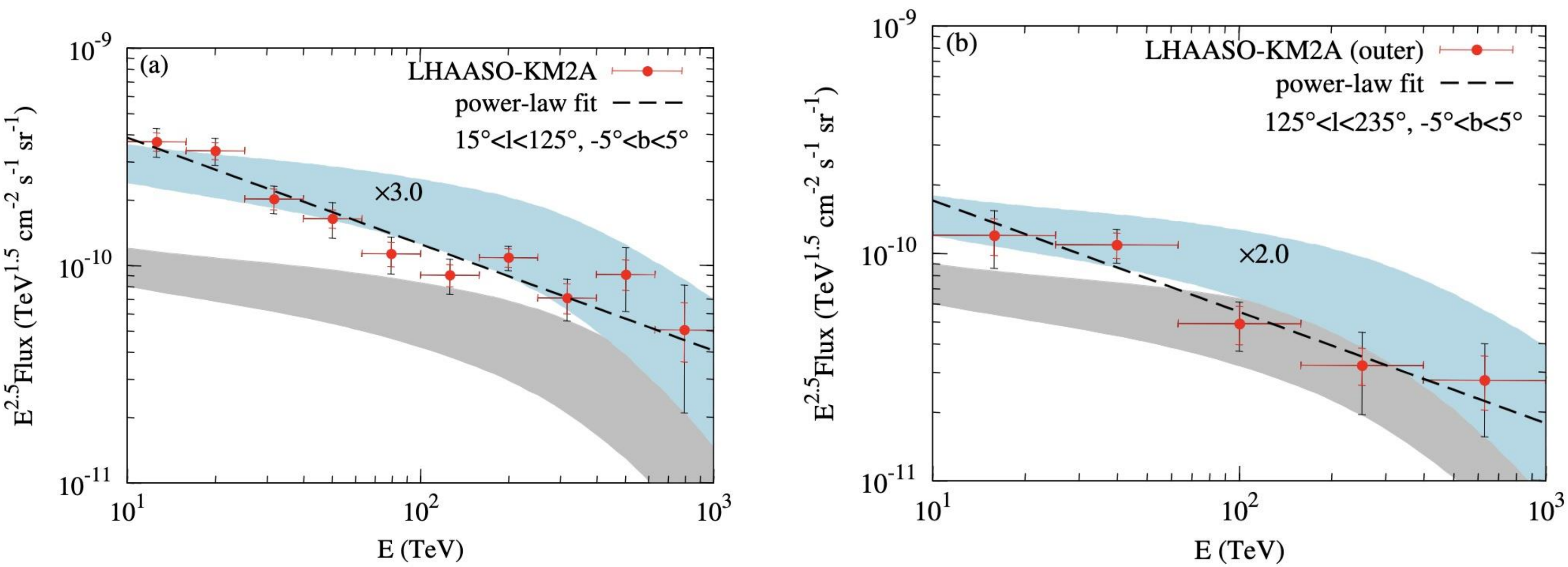

$$\Xi^{A,A'}(E,l,b) = \int_0^\infty \mathrm{d}s\, n_{\mathrm{gas}}^{A'}(\boldsymbol{x}) I_{\mathrm{CR}}^{A}(E,\boldsymbol{x}) \qquad I_\nu(E,l,b) = \sum_{A,A'} \int_E^\infty \mathrm{d}E'\, \Xi^{A,A'}(E',l,b) \frac{\mathrm{d}\sigma^{AA'\to\nu}(E',E)}{\mathrm{d}E}$$

arXiv: 2305.05372

1 PeV CR density in the Gal. plane

Lipari & Vernetto (2018)

G.Giacinti & D.S., 2305.10251

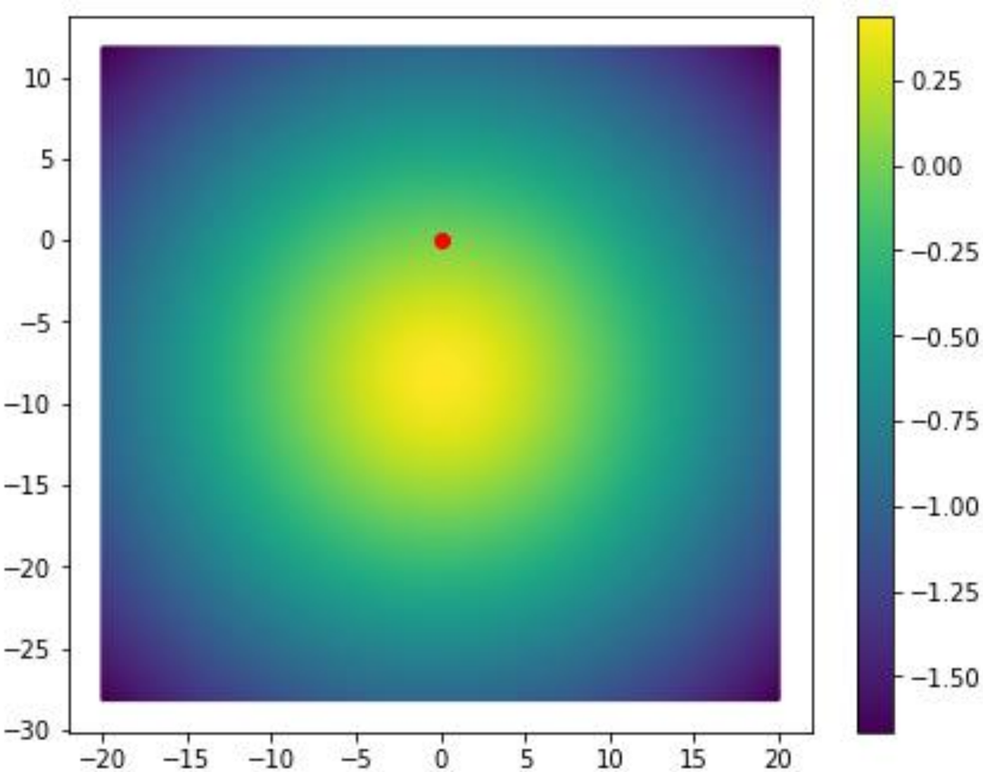

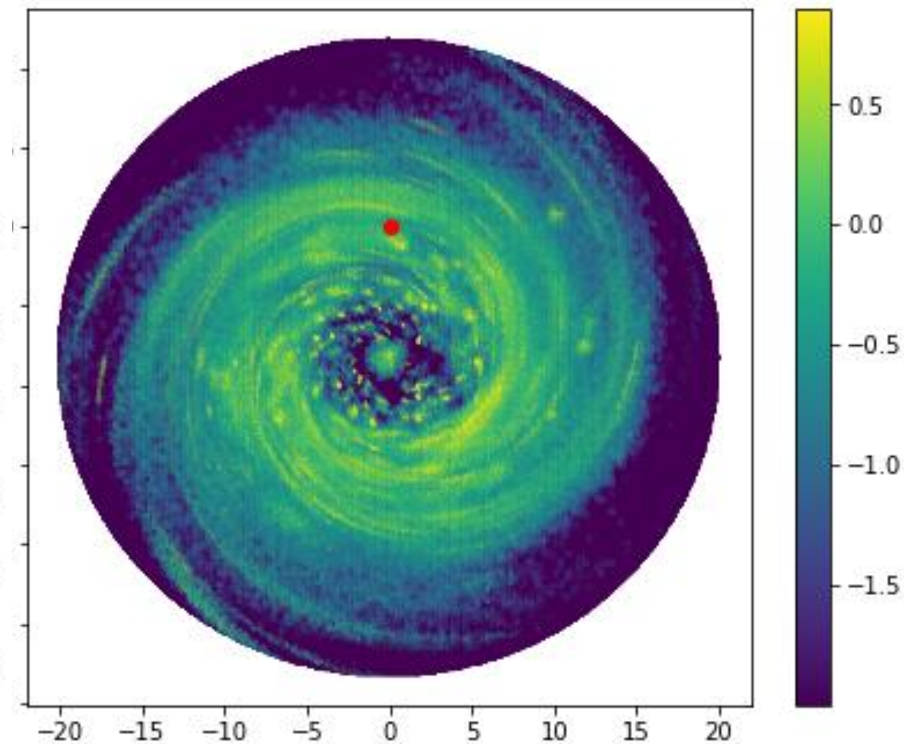

$$\Xi^{A,A'}(E,l,b) = \int_0^\infty \mathrm{d}s\, n_{\mathrm{gas}}^{A'}(\boldsymbol{x}) I_{\mathrm{CR}}^{A}(E,\boldsymbol{x})$$

$$I_\nu(E,l,b) = \sum_{A,A'} \int_E^\infty \mathrm{d}E'\, \Xi^{A,A'}(E',l,b) \frac{\mathrm{d}\sigma^{AA'\to\nu}(E',E)}{\mathrm{d}E}$$

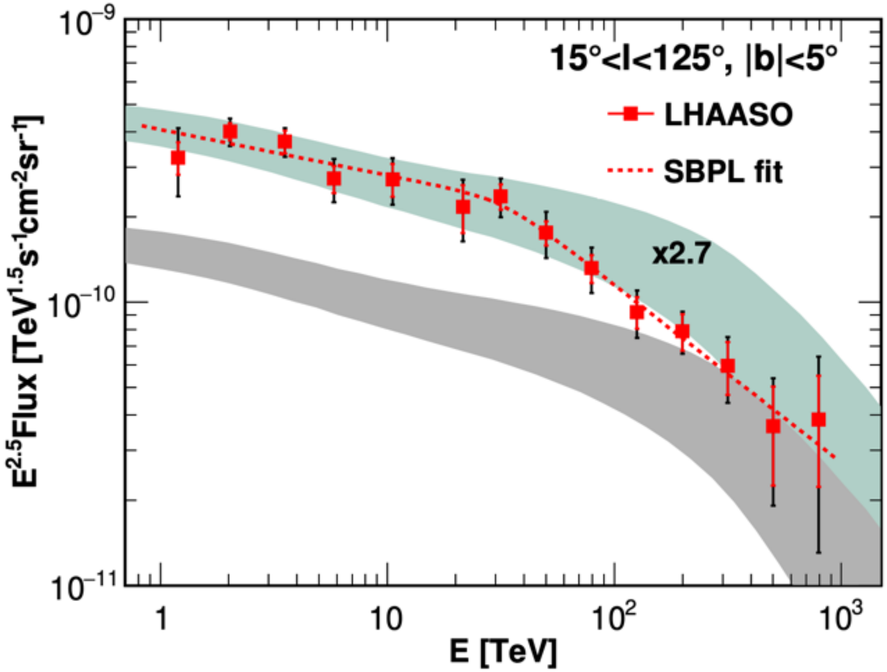

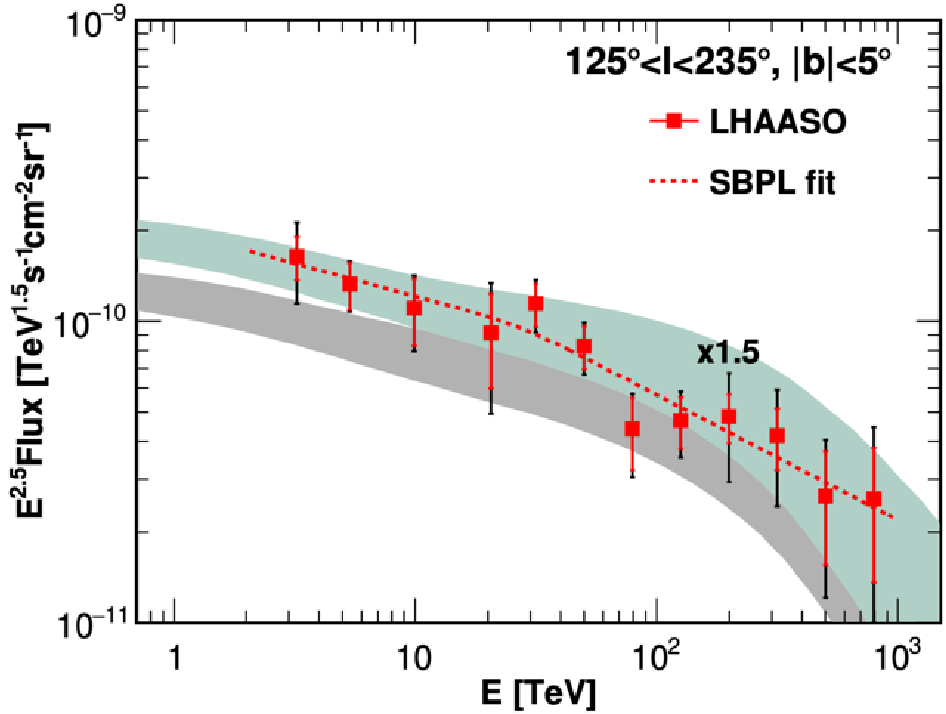

LHAASO Collaboration 2411.16021

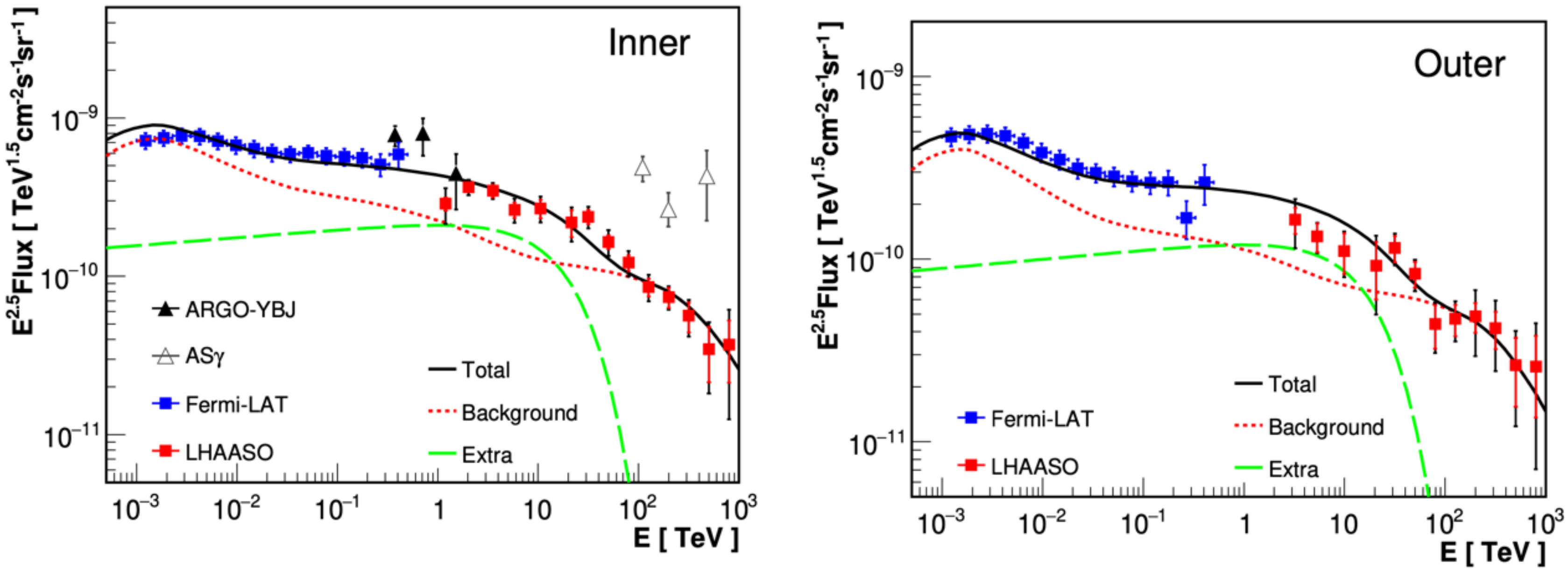

LHAASO Collaboration 2411.16021

Lower knee in Galaxy

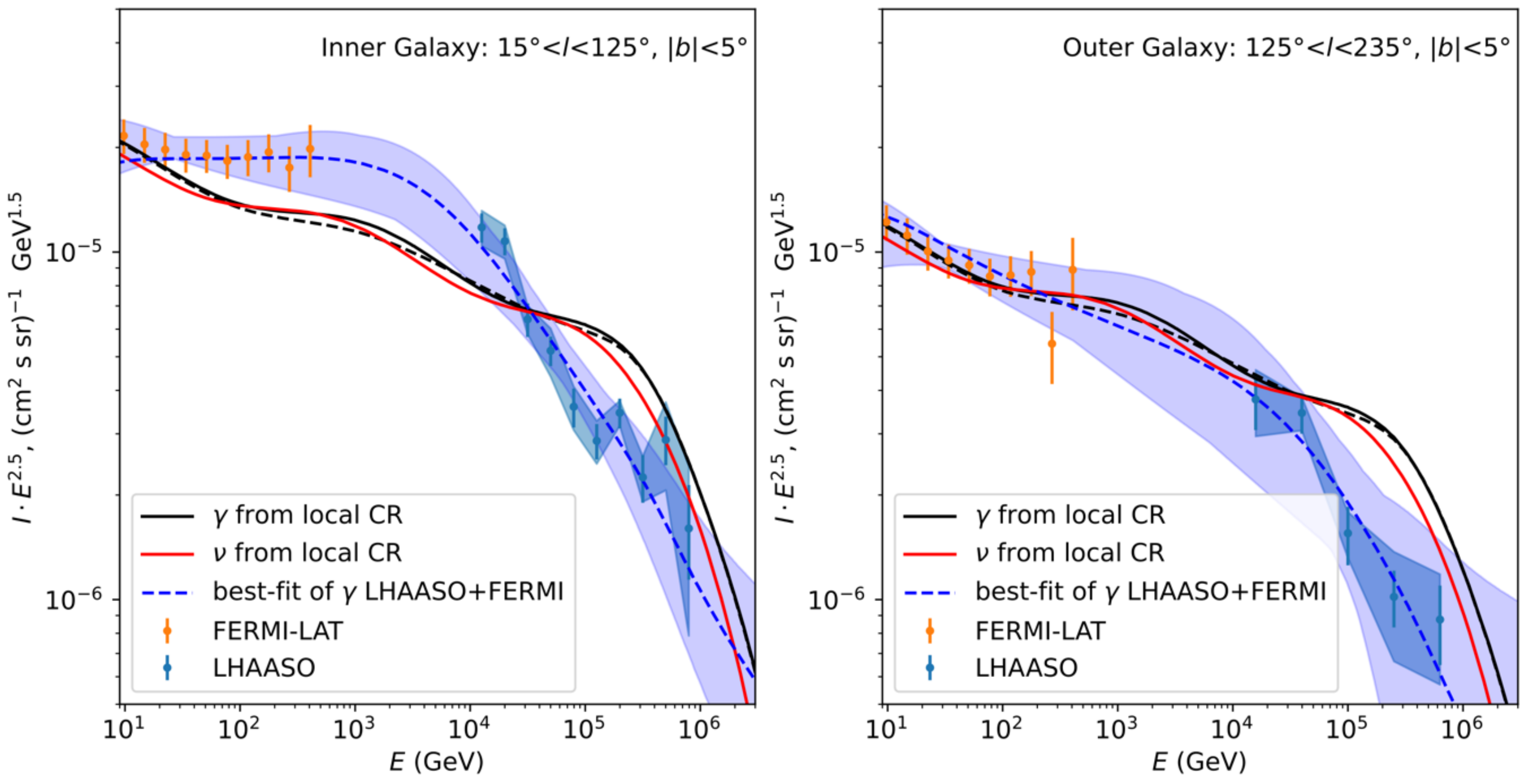

C. Prevotat et al, 2407.11911

Low energy knee in Galaxy

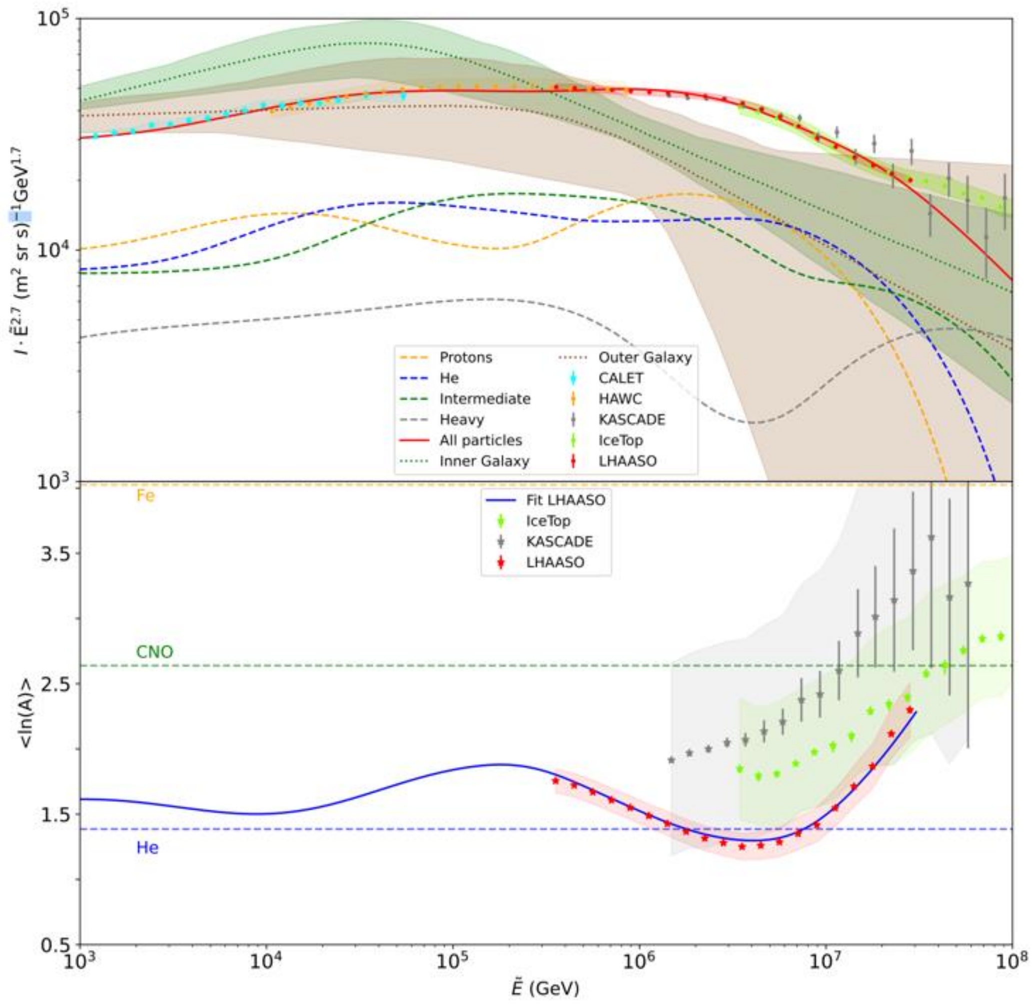

C. Prevotat et al, 2407.11911

Low energy knee in Galaxy

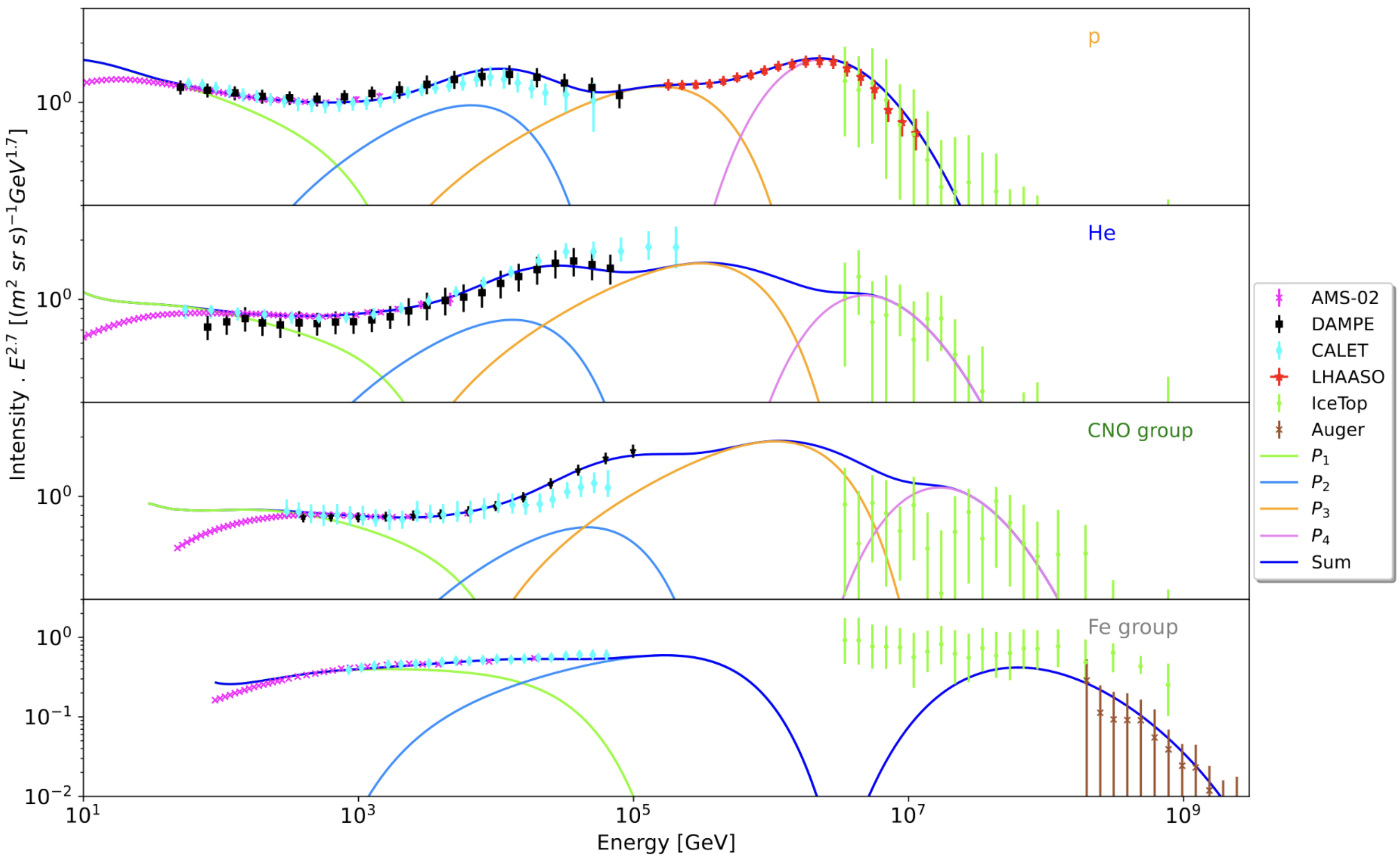

C. Prevotat et al, in preparation, 2507.xxxxx

Detection of GRB 221009A by LHAASO WCDA and km2a

Brightest over all time GRB in 57 years

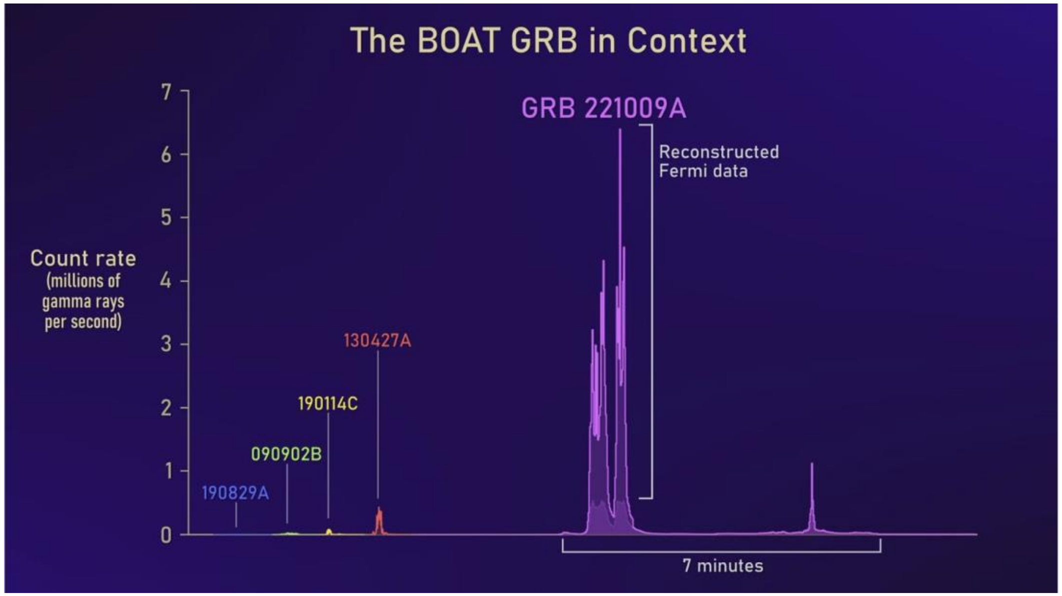

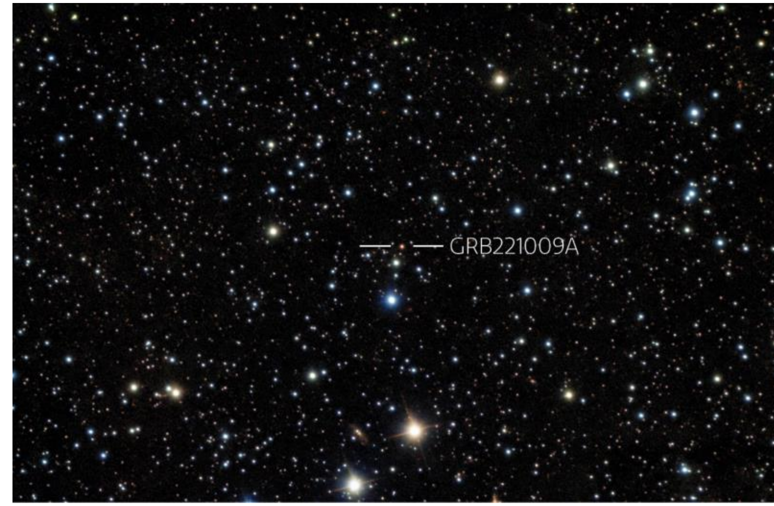

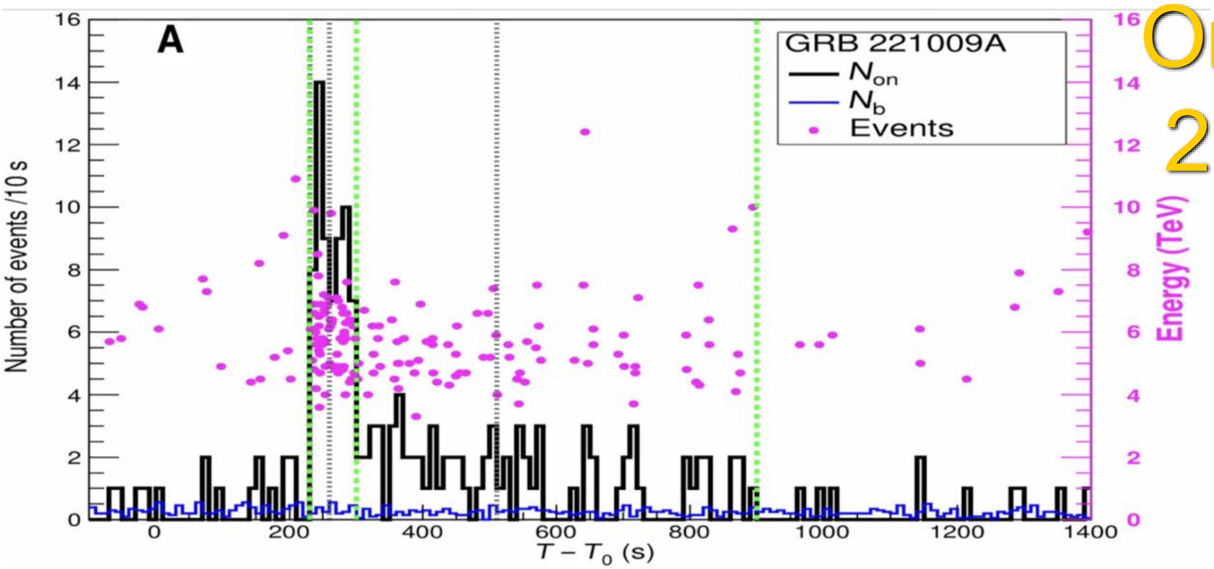

One time in 200-1000 years

GRB 221009A: A very rare event

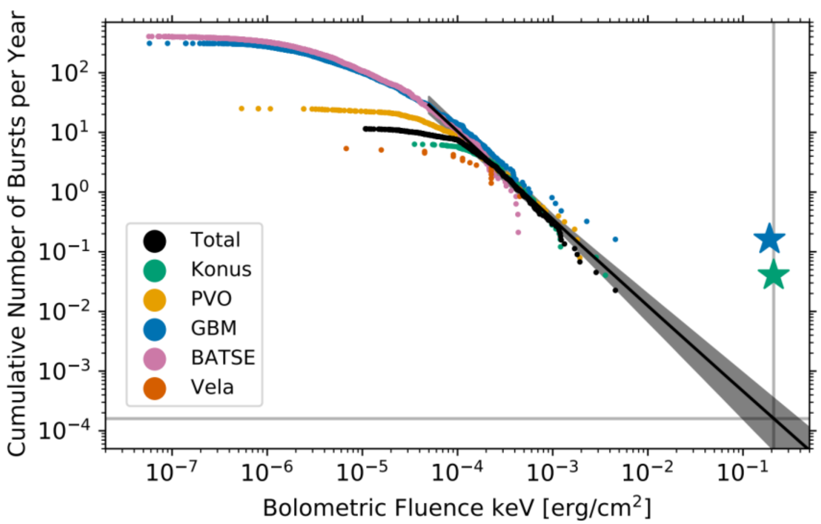

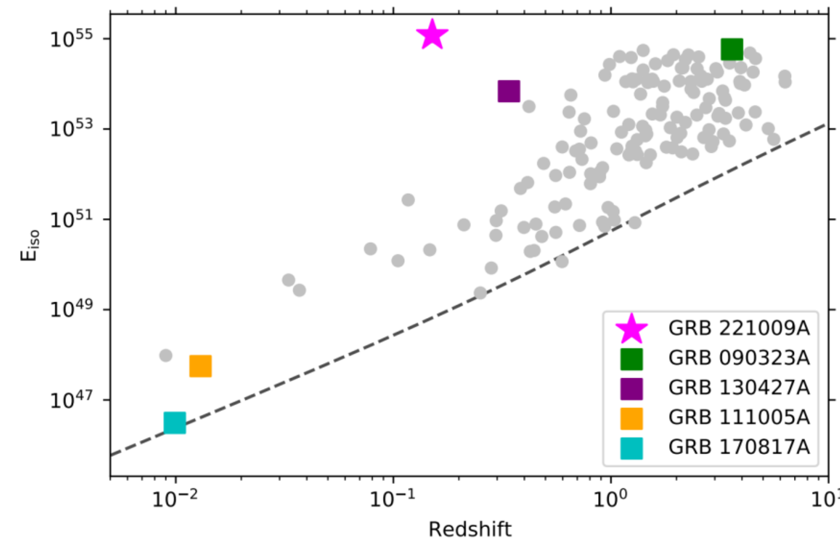

Fluence: >5 × 10 $^{-2}$ erg/cm^{2}

R_GRB≤ 6.1 × 10^{-4} Gpc^{-3} yr^{-1}

R<10^-3 yr

Buns et al. 2023

z=0.151 volume ~ 1 Gpc^3

LHAASO GRB221009A

- LHAASO detection of GRB 221009A: first GRB seen by a extensive air shower detector

- High statistics: >60,000 photons above 0.2TeV (LHAASO-WCDA)
- TeV count rate light curve: Smooth temporal profile – **external shock origin**

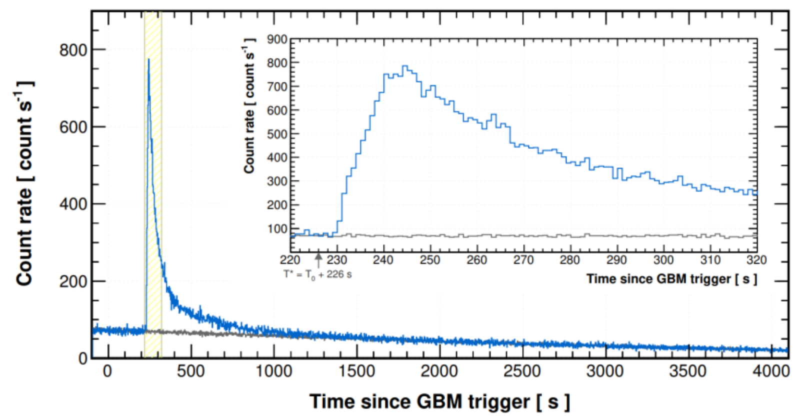

First time detection of the TeV afterglow onset !

What we've learnt from the GRB 221009A

Initial Lorentz Factor Γ_0

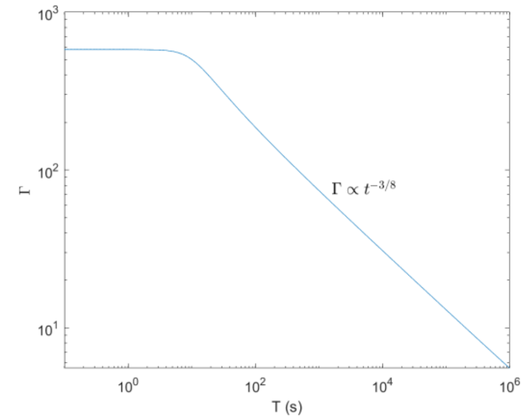

- From T* to the peak (energy-independent peak time), it takes

  ~18 s

- The bulk Lorentz factor is estimated as

$$\Gamma_0 = \left(\frac{3E_k}{32\pi n m_p c^5 t_{\rm peak}^3}\right)^{1/8} = 440 E_{k,55}^{1/8} n_0^{-1/8} \left(\frac{t_{\rm peak}}{18\,{\rm s}}\right)^{-3/8}$$

it is among the highest values for all GRBs

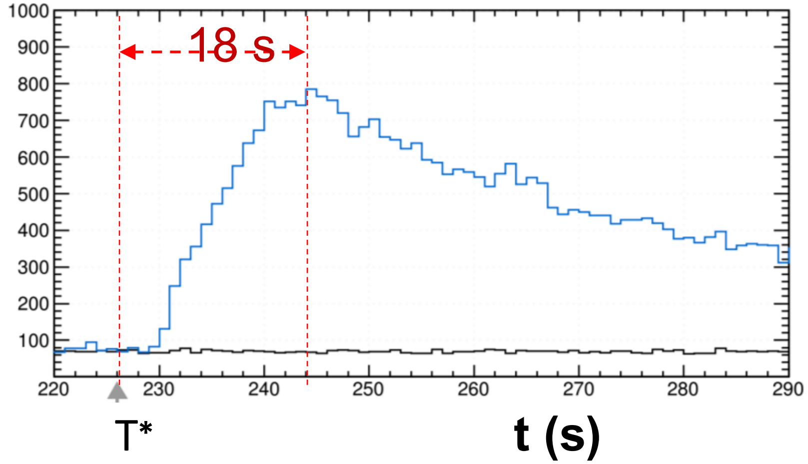

LHAASO, Science, June 8, 2023

A narrow GRB jet

- Jet breaks have been seen in optical/X-ray bands
- First time seeing a jet break at TeV band
- Helps to understand the total energy of the GRB

$$\theta_0 \sim 0.6^\circ E_{k,55}^{-1/8} n_0^{1/8} \left(\frac{t_{\rm b,2}}{670\,{\rm s}}\right)^{3/8}$$

➢ assuming jet angles derived from the break time of the optical afterglow light curve, the collimation-corrected radiated energy is clustered around ~10^{51} erg.

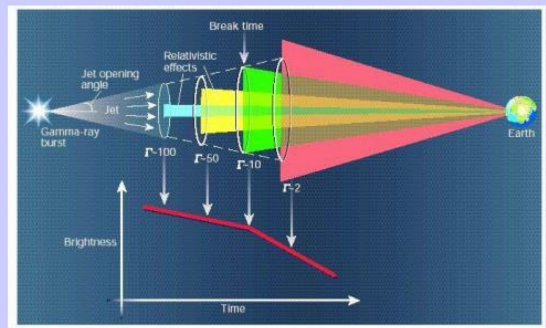

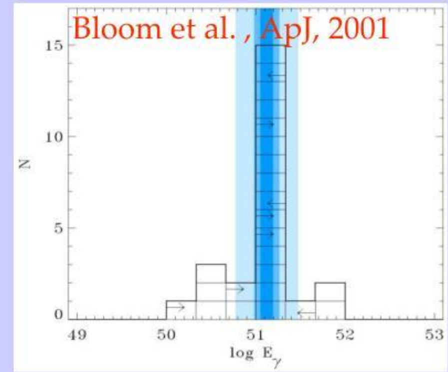

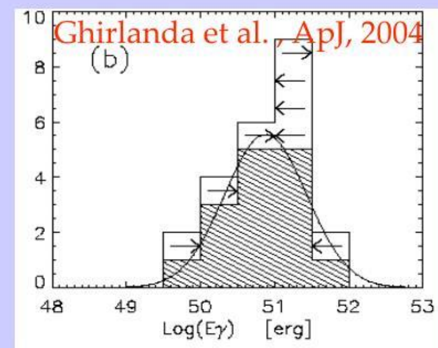

$$E_{\gamma,j} = E_{\gamma,\rm iso}\theta_0^2/2 \sim 7.5\times10^{50}\ {\rm erg}\, E_{\gamma,\rm iso,55}(\theta_0/0.7^\circ)^2$$

What we've learnt from GRB 221009A

Upper limit in prompt phase

- The most strict limit on the prompt TeV emission

$R = F_{TeV}/F_{MeV} < 2 \times 10^{-5}$

1. A large $\gamma\gamma$ absorption optical depth ?
2. Or a magnetized jet?

$$R_{\rm in} \sim 2\Gamma_0^2 c t_v = 10^{15}\,{\rm cm}\,(\Gamma_0/440)^2\,(t_v/0.082\,{\rm s})$$

$$\tau_{\gamma\gamma} \sim \sigma_{\gamma\gamma} n_t' \frac{R_{\rm in}}{\Gamma_0} \sim 190 \left(\frac{R_{\rm in}}{10^{15}\,{\rm cm}}\right)^{-1} \left(\frac{\Gamma_0}{440}\right)^{-2} \left(\frac{\varepsilon_t}{h\nu_m}\right)^{\beta_1+1}$$

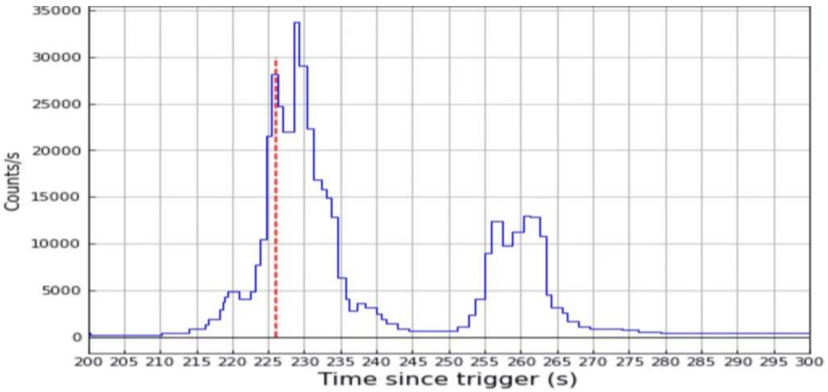

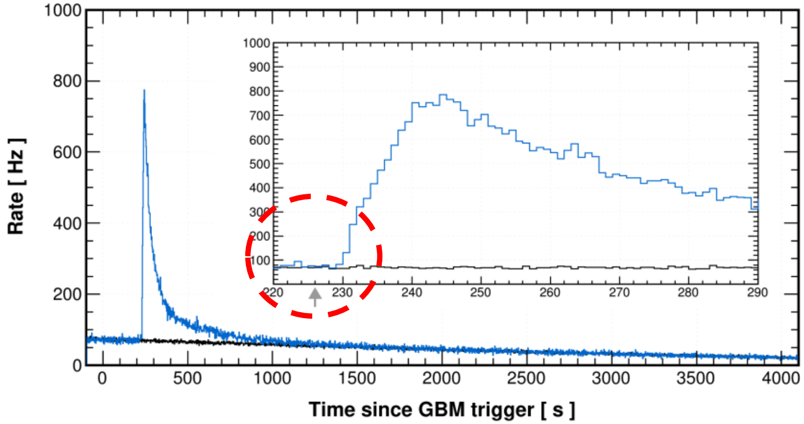

GRB 221009A км2а

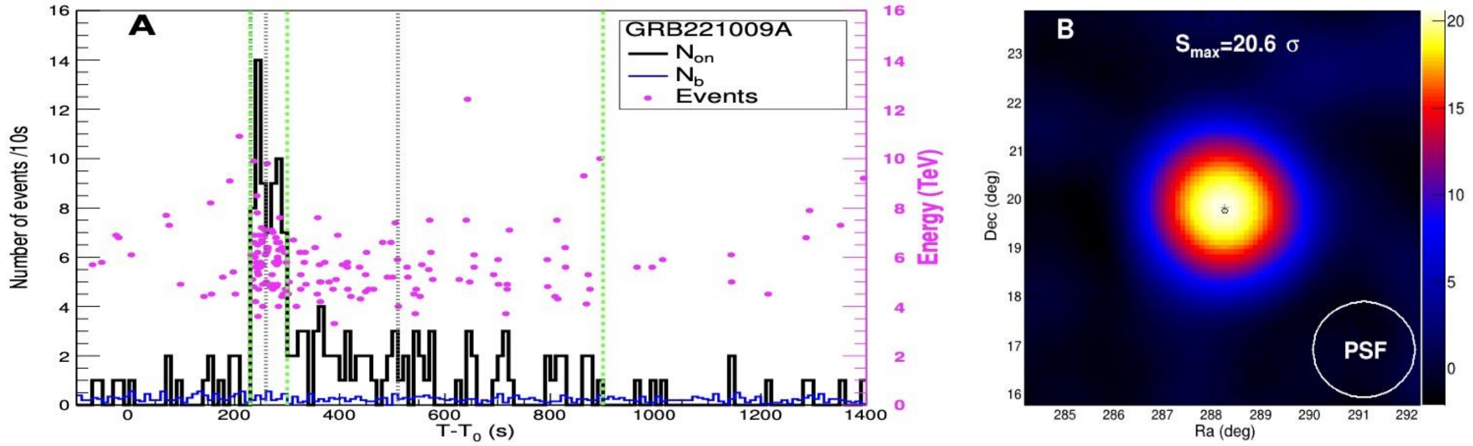

Figure 1: **The light curve and significance map of GRB 221009A obtained by KM2A.** (A) The gamma-ray-count light curve obtained by KM2A with each time-bin of 10s. The black curve indicates the events from the angular cone centered on the GRB, and the blue curve indicates the number of events due to cosmic ray background estimated from 20 similar angular cones at off-source directions with the same zenith angle. The gray dashed lines indicate the peak times of the multi-pulsed emission observed by GECAM-C (*10*) in the MeV band. The green dashed lines indicate the times of T_0+230s, T_0+300s, and T_0+900s. The pink points indicate the energy marked by the right label and the arrival time of each event. The energies of each event were reconstructed assuming the spectra shown in panel B of Figure 2. (B) The significance map around GRB 221009A as observed by KM2A. The plus sign and corresponding length denote the position and error determined by KM2A. The black circle denotes the position of the GRB reported by Fermi-LAT. The white circle shows the size of the PSF that contains 68% of the events.

LHAASO collab., Sci.Adv. 9 (2023) 46, adj2778 e-Print: 2310.08845

GRB 221009A км2а

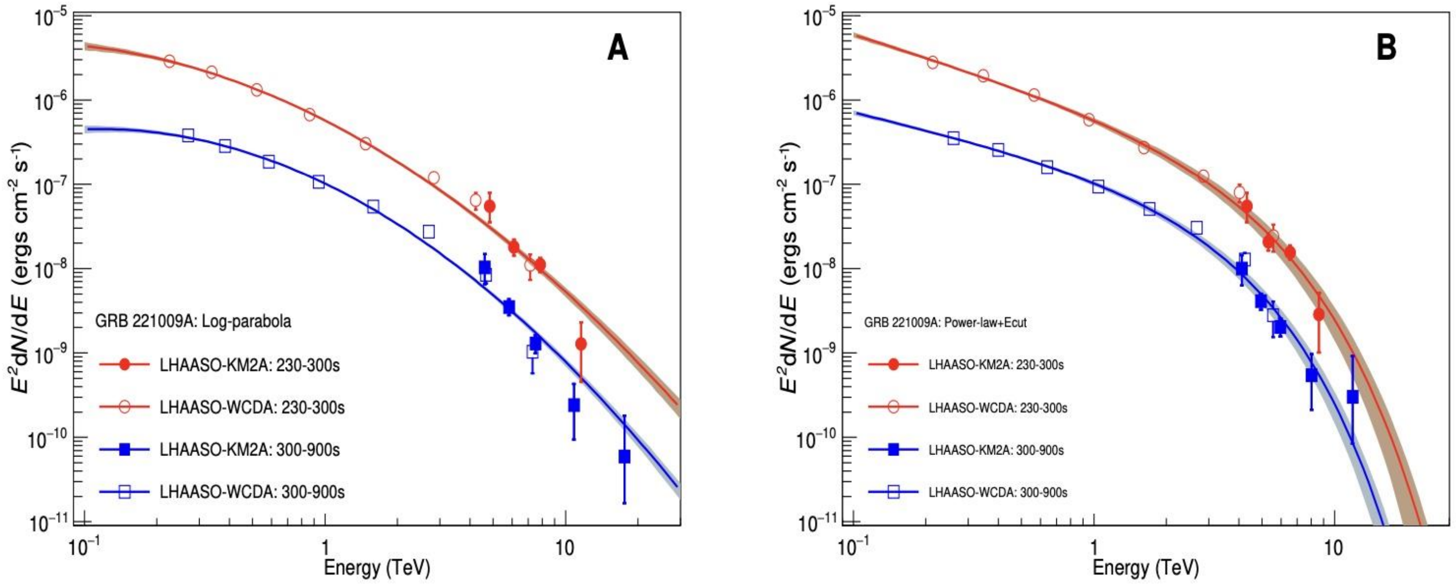

Figure 2: **Observed VHE spectra of GRB 221009A by LHAASO for the two intervals.** Interval 1 is from T_0+230s to T_0+300s (red points) and interval 2 is from T_0+300s to T_0+900s (blue points). The solid lines indicate the best-fitting results, and the shaded regions indicate the 1-sigma error region. (A) The log-parabola function is used to fit the observational data. (B) The power-law with exponential cutoff function is adopted to fit the observational data.

LHAASO collab., Sci.Adv. 9 (2023) 46, adj2778 e-Print: 2310.08845

GRB 221009A км2а

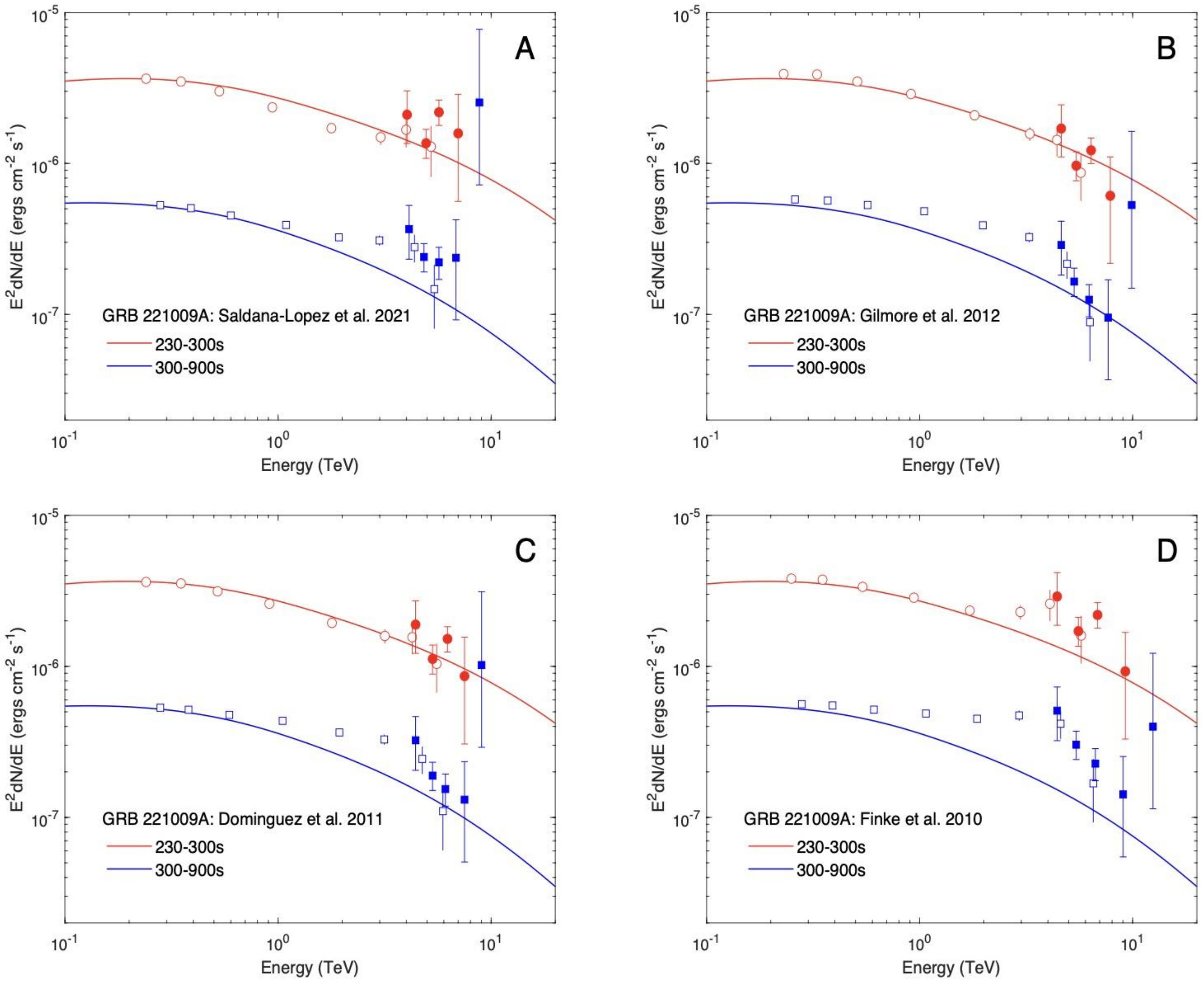

LHAASO collab., Sci.Adv. 9 (2023) 46, adj2778 e-Print: 2310.08845

Cygnus region with LHAASO

Cygnus region

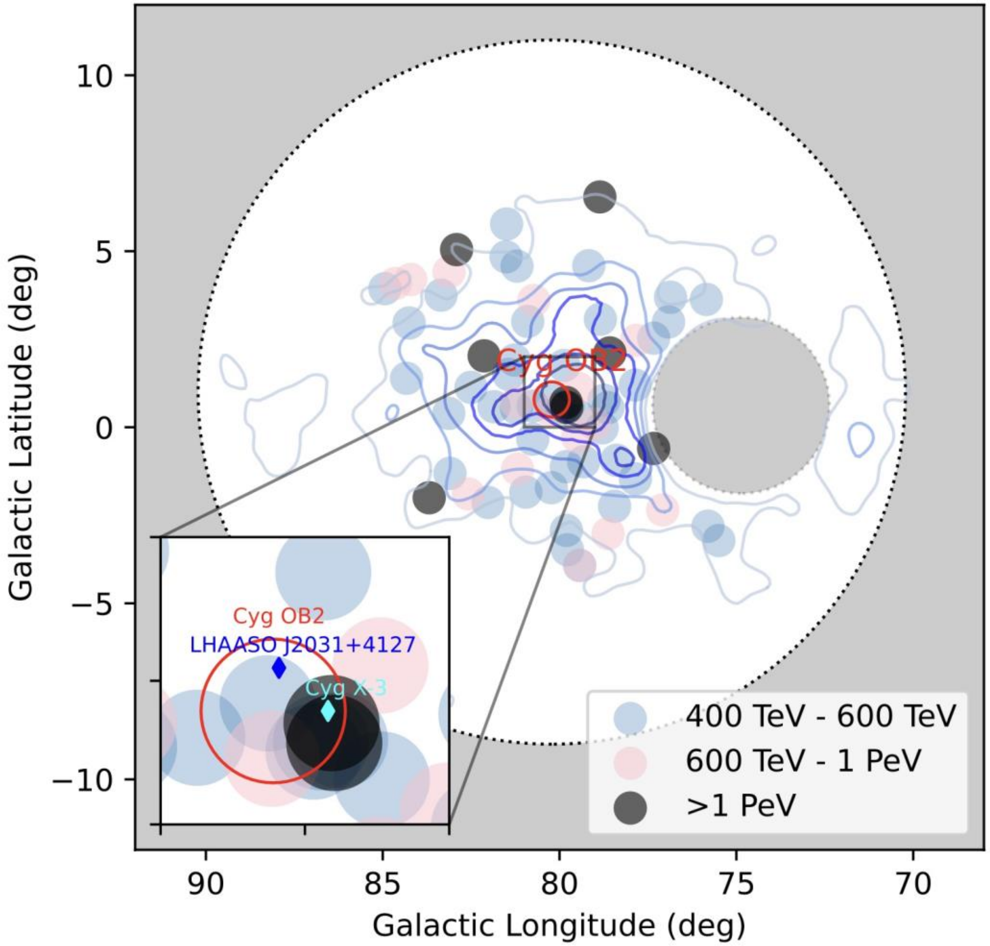

•*LHAASO collab.*, Zh.Cao et al, 2310.10100, *Sci.Bull.* 69 (2024) 4, 449

Cygnus region

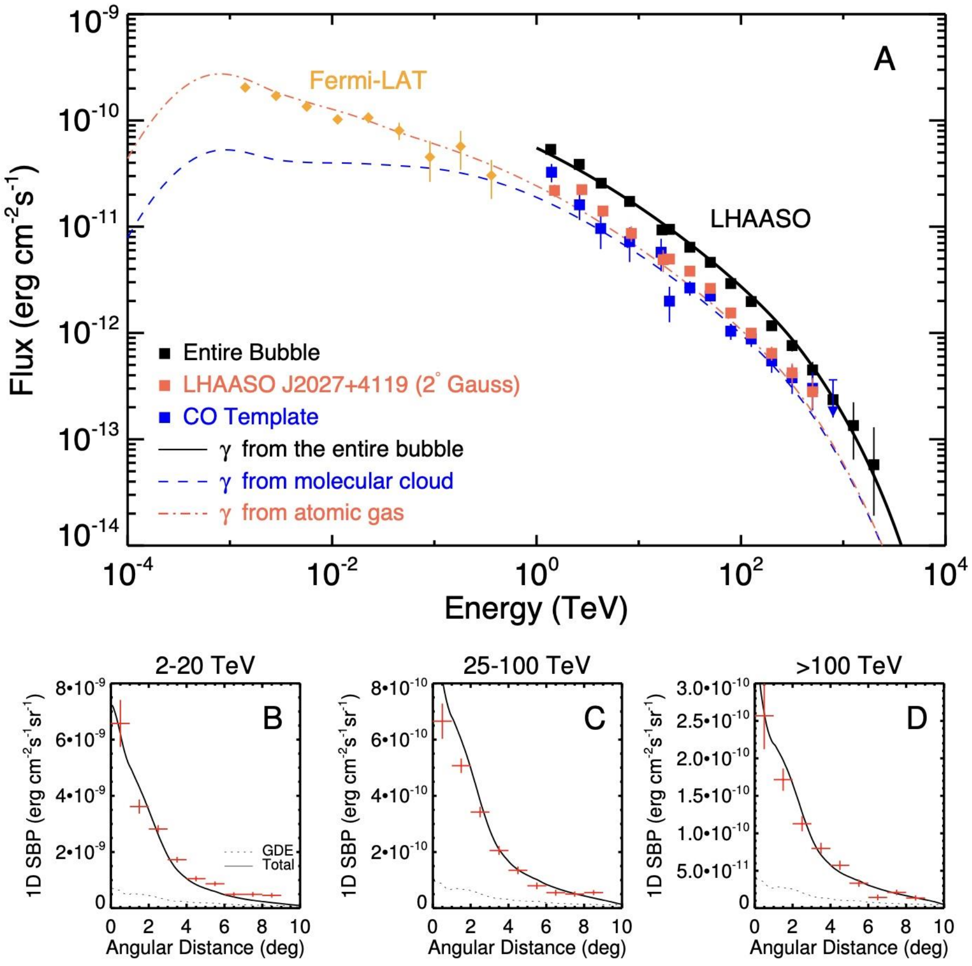

•*LHAASO collab.*, Zh.Cao et al, 2310.10100 , *Sci.Bull.* 69 (2024) 4, 449

Neutrinos from Cygnus region

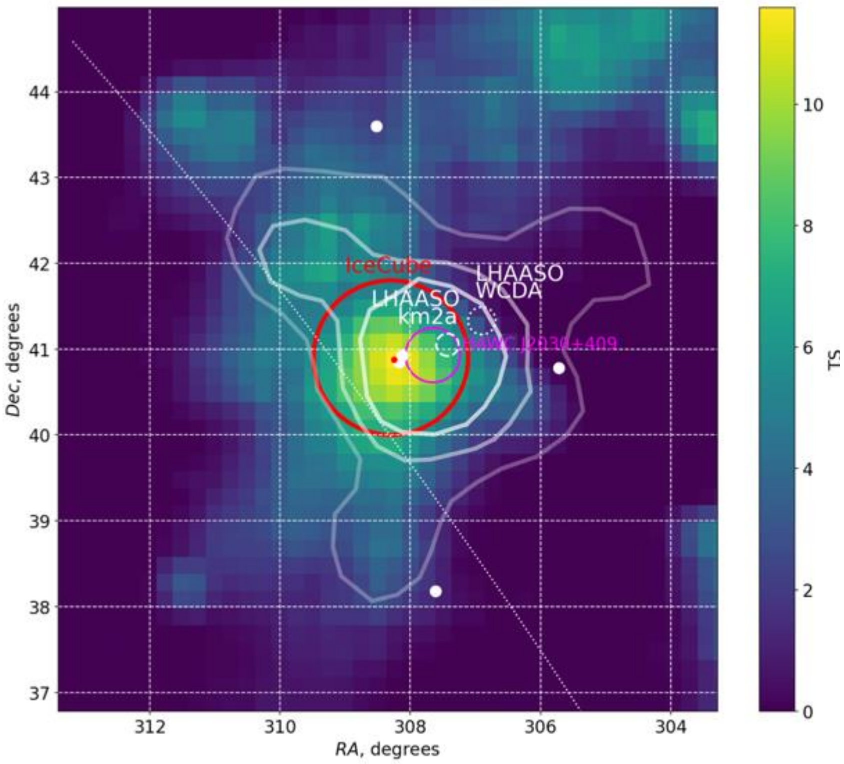

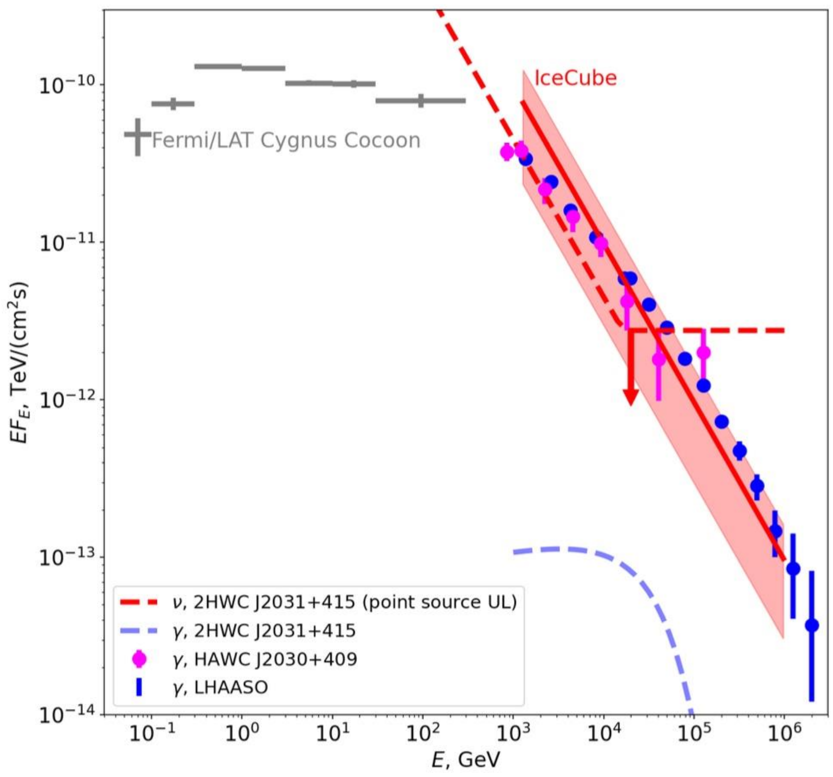

A.Neronov, D.S. and D.Savchenko, arXiv:2311.13711

Micro-quasars

https://arxiv.org/pdf/2410.08988

Micro-quasars

Cygnus X1:

M_BH = $21M_o$

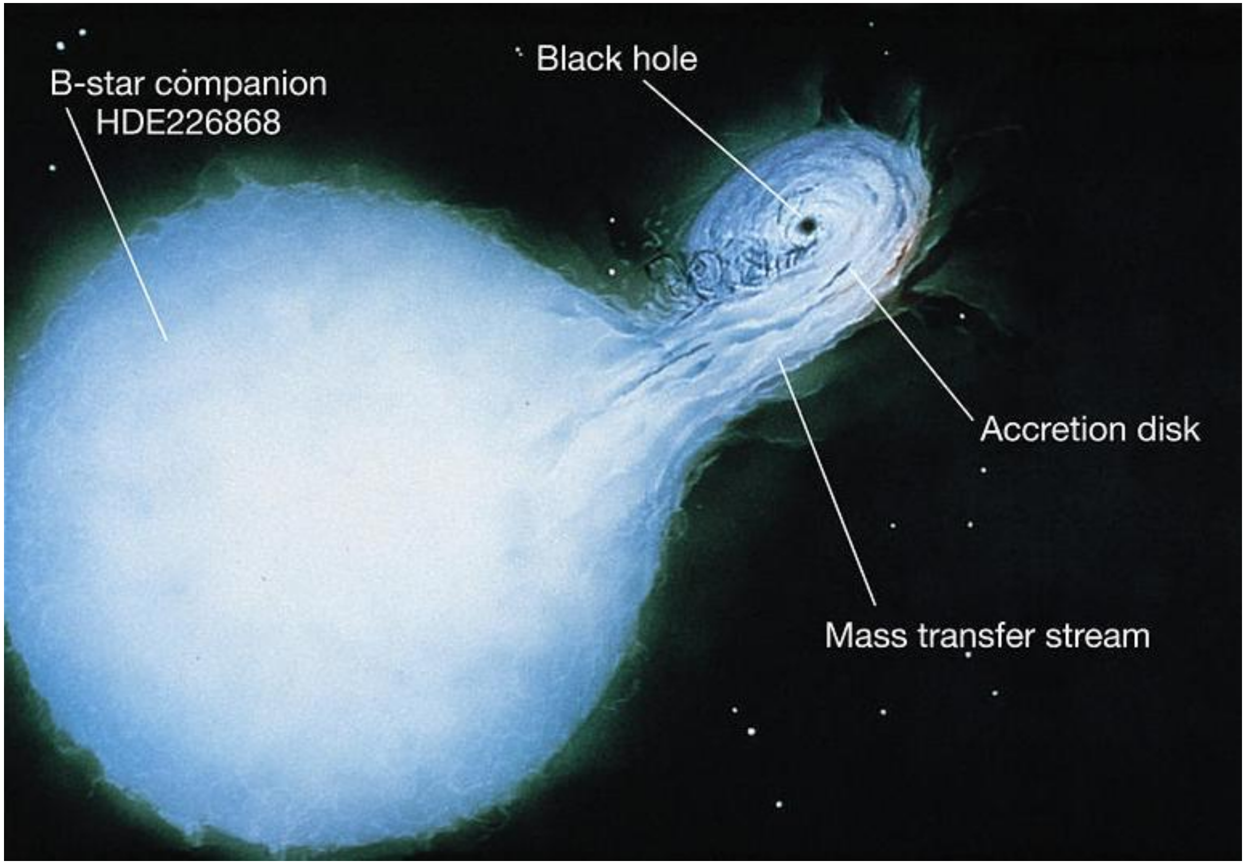

SS 433

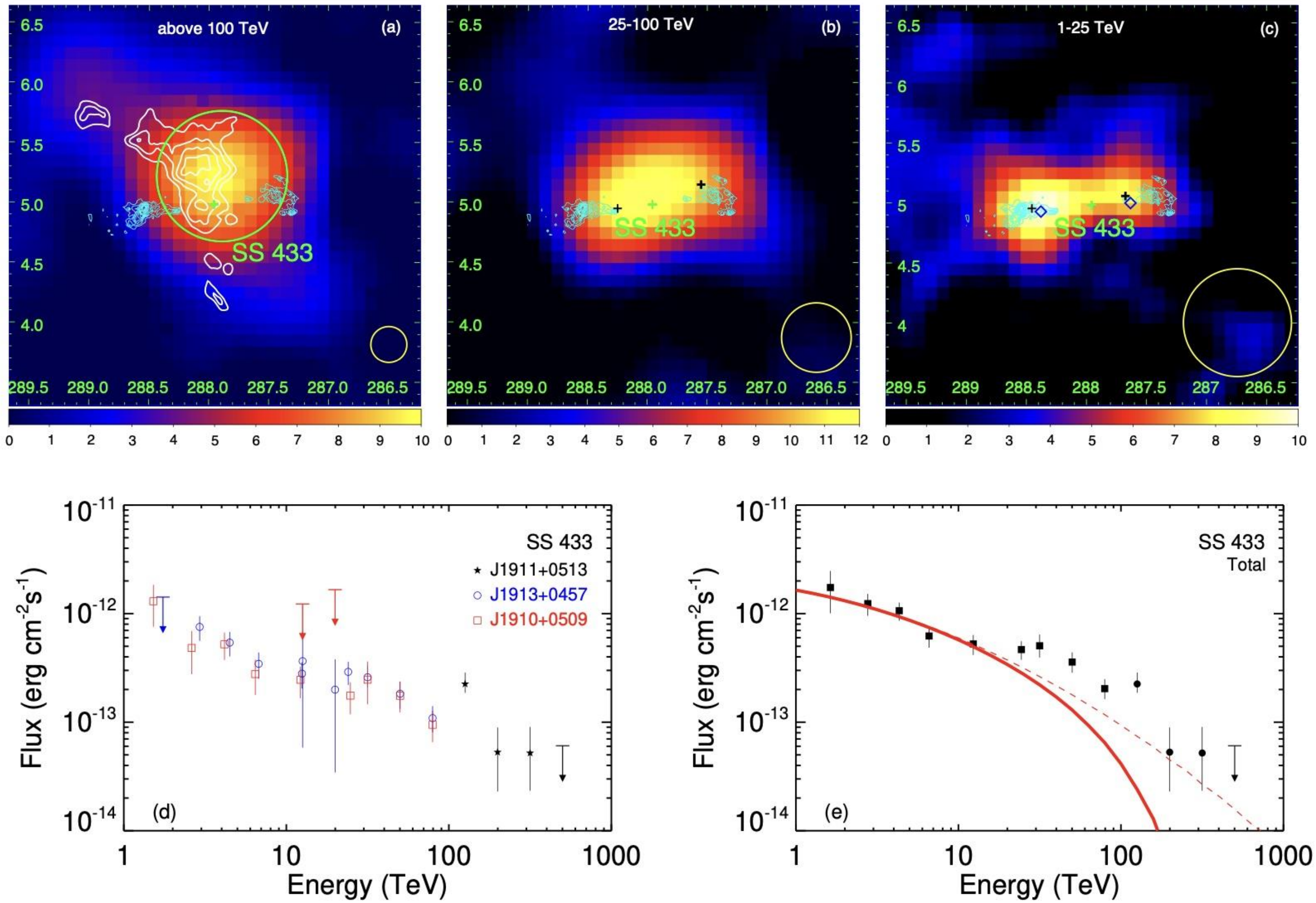

LHAASO collaboration 2410.08988

V4641 Sgr

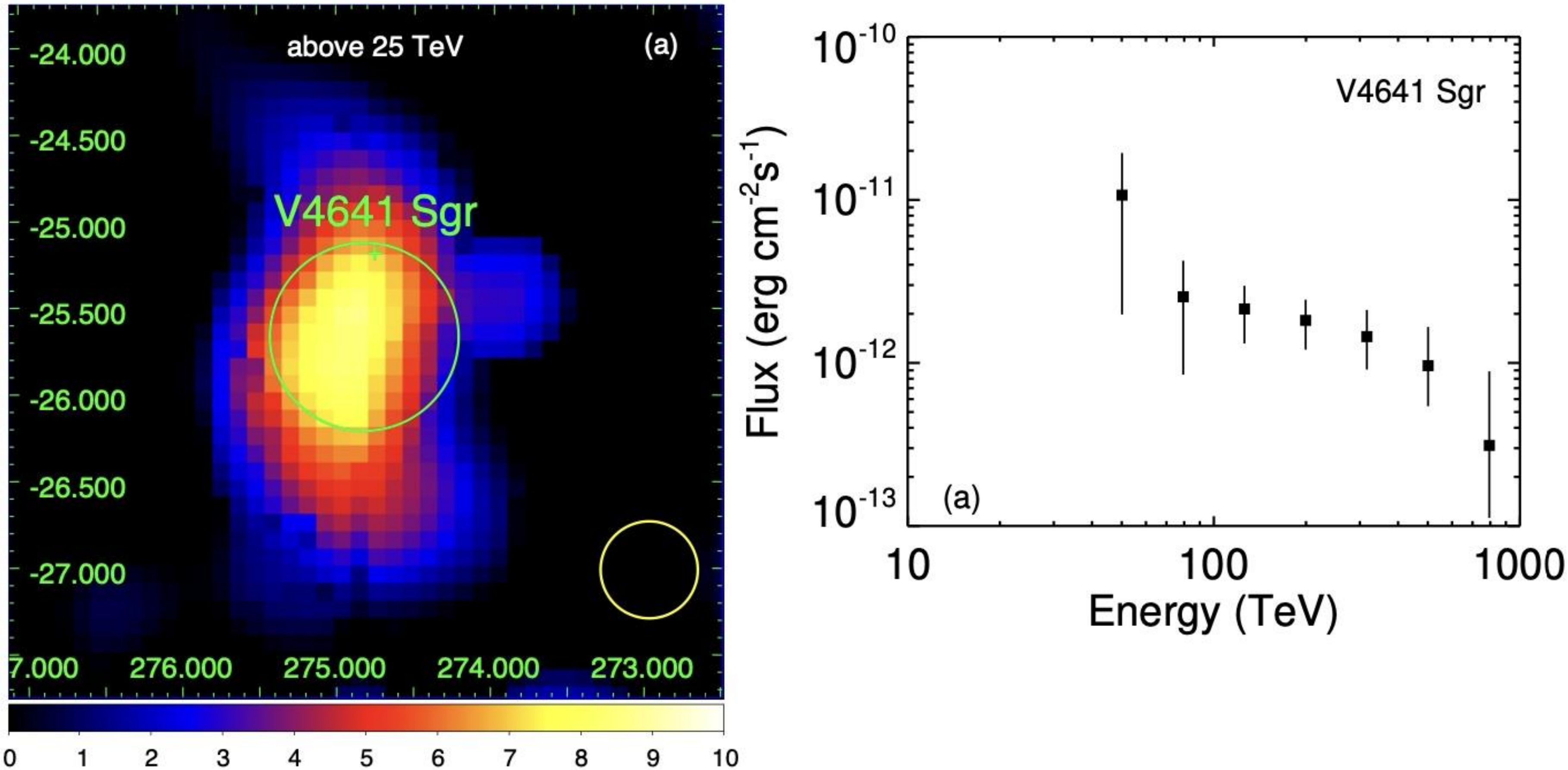

LHAASO collaboration 2410.08988

V4641 Sgr HAWC

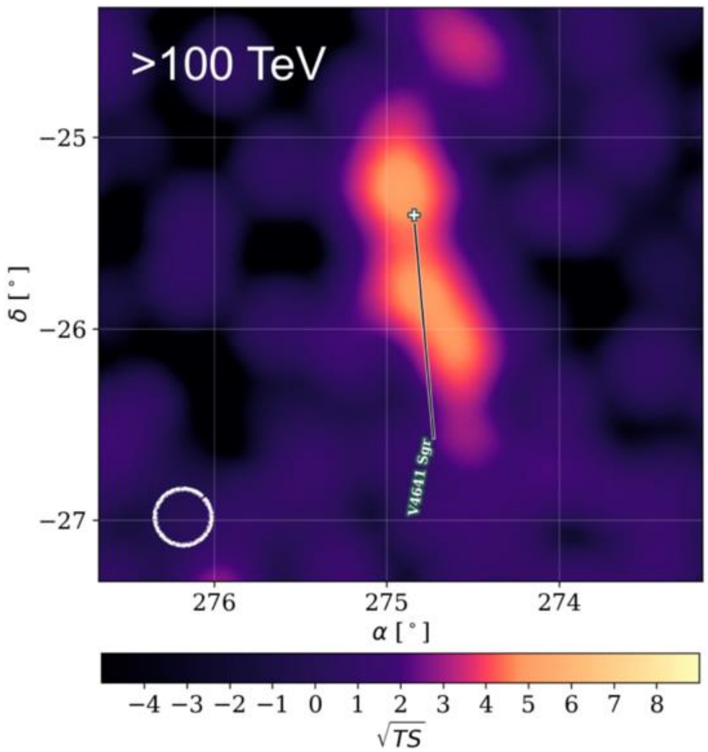

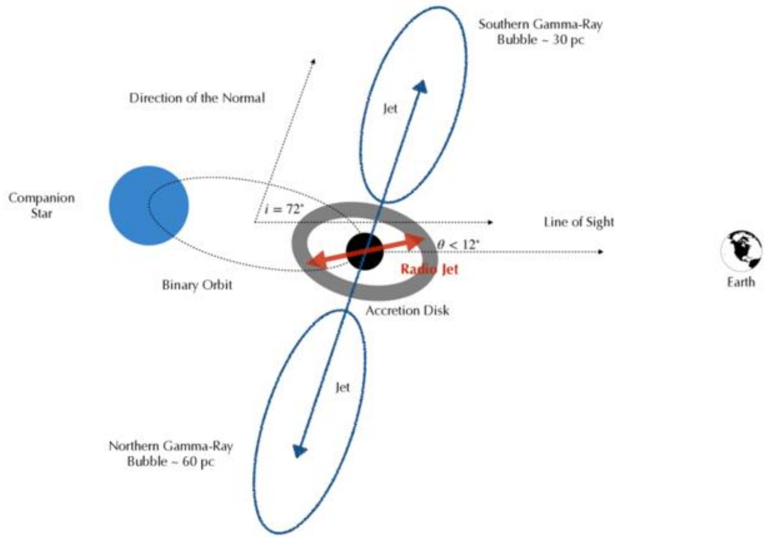

V4641 Sgr model

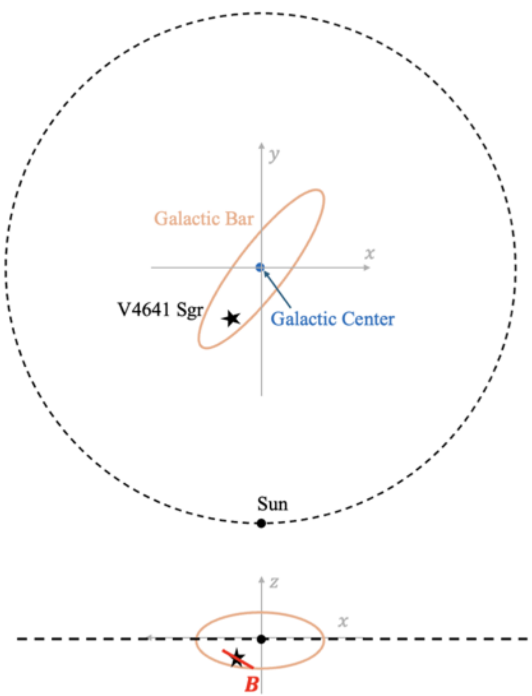

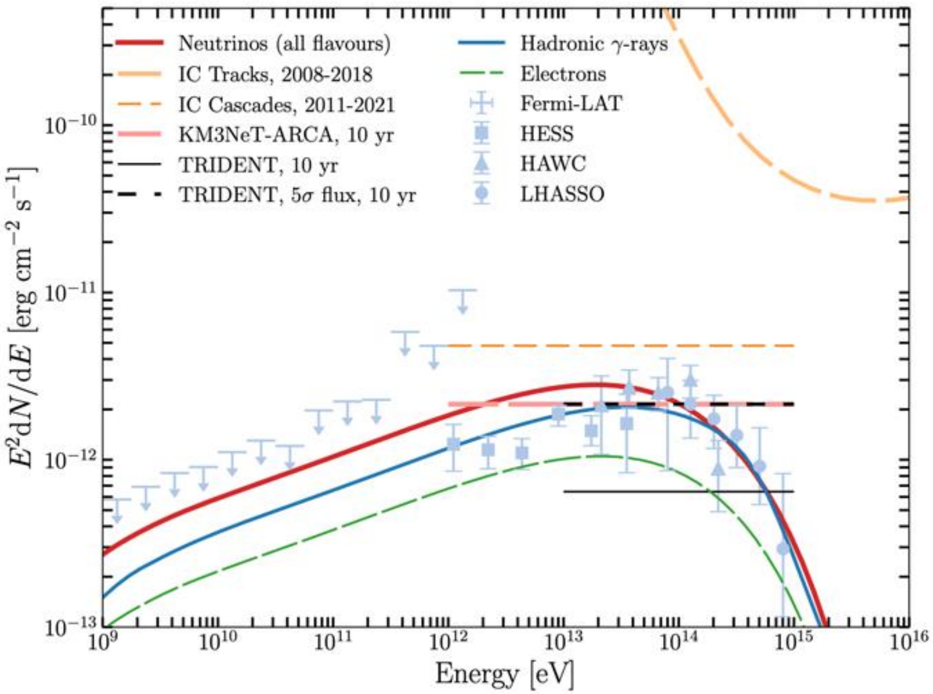

Andrii Neronov, Foteini Oikonomou and D.S., arXiv: 2410.17608

DM limits by LHAASO

DM limits from dwarf galaxies by LHAASO

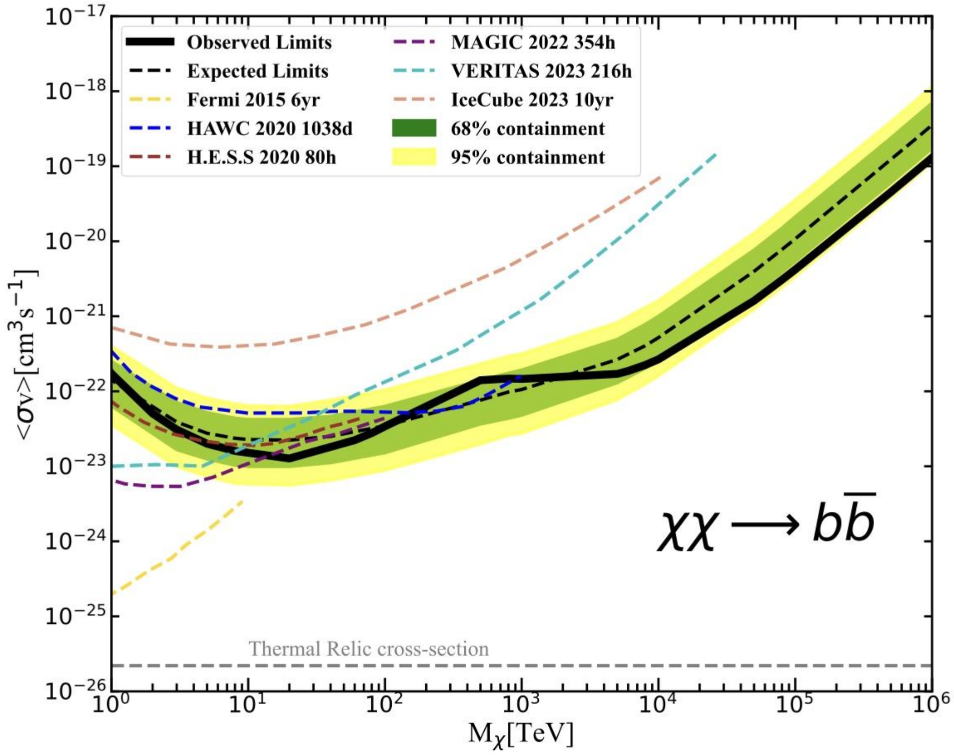

LHAASO collaboration, 2406.08698

LIV from GRB 221009A by LHAASO

Stringent Tests of Lorentz Invariance Violation from LHAASO Observations of GRB 221009A

Zhen Cao,[1,2,3] F. Aharonian,[4,5] Axikegu,[6] Y.X. Bai,[1,3] Y.W. Bao,[7] D. Bastieri,[8] X.J. Bi,[1,2,3] Y.J. Bi,[1,3] W. Bian,[9] A.V. Bukevich,[10] Q. Cao,[11] W.Y. Cao,[12] Zhe Cao,[13,12] J. Chang,[14] J.F. Chang,[1,3,13] A.M. Chen,[9] E.S. Chen,[1,2,3] H.X. Chen,[15] Liang Chen,[16] Lin Chen,[6] Long Chen,[6] M.J. Chen,[1,3] M.L. Chen,[1,3,13] Q.H. Chen,[6] S. Chen,[17] S.H. Chen,[1,2,3] S.Z. Chen,[1,3] T.L. Chen,[18] Y. Chen,[7] N. Cheng,[1,3] Y.D. Cheng,[1,2,3] M.Y. Cui,[14] S.W. Cui,[11] X.H. Cui,[19] Y.D. Cui,[20] B.Z. Dai,[17] H.L. Dai,[1,3,13] Z.G. Dai,[12] Danzengluobu,[18] X.Q. Dong,[1,2,3] K.K. Duan,[14] J.H. Fan,[8] Y.Z. Fan,[14] J. Fang,[17] J.H. Fang,[15] K. Fang,[1,3] C.F. Feng,[21] H. Feng,[1] L. Feng,[14] S.H. Feng,[1,3] X.T. Feng,[21] Y. Feng,[15] Y.L. Feng,[18] S. Gabici,[22] B. Gao,[1,3] C.D. Gao,[21] Q. Gao,[18] W. Gao,[1,3] W.K. Gao,[1,2,3] M.M. Ge,[17] L.S. Geng,[1,3] G. Giacinti,[9] G.H. Gong,[23] Q.B. Gou,[1,3] M.H. Gu,[1,3,13] F.L. Guo,[16] X.L. Guo,[6] Y.Q. Guo,[1,3] Y.Y. Guo,[14] Y.A. Han,[24] M. Hasan,[1,2,3] H.H. He,[1,2,3] H.N. He,[14] J.Y. He,[14] Y. He,[6] Y.K. Hor,[20] B.W. Hou,[1,2,3] C. Hou,[1,3] X. Hou,[25] H.B. Hu,[1,2,3] Q. Hu,[12,14] S.C. Hu,[1,3,26] D.H. Huang,[6] T.Q. Huang,[1,3] W.J. Huang,[20] X.T. Huang,[21] X.Y. Huang,[14] Y. Huang,[1,2,3] X.L. Ji,[1,3,13] H.Y. Jia,[6] K. Jia,[21] K. Jiang,[13,12] X.W. Jiang,[1,3] Z.J. Jiang,[17] M. Jin,[6] M.M. Kang,[27] I. Karpikov,[10] D. Kuleshov,[10] K. Kurinov,[10] B.B. Li,[11] C.M. Li,[7] Cheng Li,[13,12] Cong Li,[1,3] D. Li,[1,2,3] F. Li,[1,3,13] H.B. Li,[1,3] H.C. Li,[1,3] Jian Li,[12] Jie Li,[1,3,13] K. Li,[1,3] S.D. Li,[16,2] W.L. Li,[21] W.L. Li,[9] X.R. Li,[1,3] Xin Li,[13,12] Y.Z. Li,[1,2,3] Zhe Li,[1,3] Zhuo Li,[28] E.W. Liang,[29] Y.F. Liang,[29] S.J. Lin,[20] B. Liu,[12] C. Liu,[1,3] D. Liu,[21] D.B. Liu,[9] H. Liu,[6] H.D. Liu,[24] J. Liu,[1,3] J.L. Liu,[1,3] M.Y. Liu,[18] R.Y. Liu,[7] S.M. Liu,[6] W. Liu,[1,3] Y. Liu,[8] Y.N. Liu,[23] Q. Luo,[20] Y. Luo,[9] H.K. Lv,[1,3] B.Q. Ma,[28] L.L. Ma,[1,3] X.H. Ma,[1,3] J.R. Mao,[25] Z. Min,[1,3] W. Mitthumsiri,[30] H.J. Mu,[24] Y.C. Nan,[1,3] A. Neronov,[22] L.J. Ou,[8] P. Pattarakijwanich,[30] Z.Y. Pei,[8] J.C. Qi,[1,2,3] M.Y. Qi,[1,3] B.Q. Qiao,[1,3] J.J. Qin,[12] A. Raza,[1,2,3] D. Ruffolo,[30] A. Sáiz,[30] M. Saeed,[1,2,3] D. Semikoz,[22] L. Shao,[11] O. Shchegolev,[10,31] X.D. Sheng,[1,3] F.W. Shu,[32] H.C. Song,[28] Yu.V. Stenkin,[10,31] V. Stepanov,[10] Y. Su,[14] D.X. Sun,[12,14] Q.N. Sun,[6] X.N. Sun,[29] Z.B. Sun,[33] J. Takata,[34] P.H.T. Tam,[20] Q.W. Tang,[32] R. Tang,[9] Z.B. Tang,[13,12] W.W. Tian,[2,19] C. Wang,[33] C.B. Wang,[6] G.W. Wang,[12] H.G. Wang,[8] H.H. Wang,[20] J.C. Wang,[25] Kai Wang,[7] Kai Wang,[34] L.P. Wang,[1,2,3] L.Y. Wang,[1,3] P.H. Wang,[6] R. Wang,[21] W. Wang,[20] X.G. Wang,[29] X.Y. Wang,[7] Y. Wang,[6] Y.D. Wang,[1,3] Y.J. Wang,[1,3] Z.H. Wang,[27] Z.X. Wang,[17] Zhen Wang,[9] Zheng Wang,[1,3,13] D.M. Wei,[14] J.J. Wei,[14] Y.J. Wei,[1,2,3] T. Wen,[17] C.Y. Wu,[1,3] H.R. Wu,[1,3] Q.W. Wu,[34] S. Wu,[1,3] X.F. Wu,[14] Y.S. Wu,[12] S.Q. Xi,[1,3] J. Xia,[12,14] G.M. Xiang,[16,2] D.X. Xiao,[11] G. Xiao,[1,3] Y.L. Xin,[6] Y. Xing,[16] D.R. Xiong,[25] Z. Xiong,[1,2,3] D.L. Xu,[9] R.F. Xu,[1,2,3] R.X. Xu,[28] W.L. Xu,[27] L. Xue,[21] D.H. Yan,[17] J.Z. Yan,[14] T. Yan,[1,3] C.W. Yang,[27] C.Y. Yang,[25] F. Yang,[11] F.F. Yang,[1,3,13] L.L. Yang,[20] M.J. Yang,[1,3] R.Z. Yang,[12] W.X. Yang,[8] Y.H. Yao,[1,3] Z.G. Yao,[1,3] L.Q. Yin,[1,3] N. Yin,[21] X.H. You,[1,3] Z.Y. You,[1,3] Y.H. Yu,[12] Q. Yuan,[14] H. Yue,[1,2,3] H.D. Zeng,[14] T.X. Zeng,[1,3,13] W. Zeng,[17] M. Zha,[1,3] B.B. Zhang,[7] F. Zhang,[6] H. Zhang,[9] H.M. Zhang,[7] H.Y. Zhang,[1,3] J.L. Zhang,[19] Li Zhang,[17] P.F. Zhang,[17] P.P. Zhang,[12,14] R. Zhang,[12,14] S.B. Zhang,[2,19] S.R. Zhang,[11] S.S. Zhang,[1,3] X. Zhang,[7] X.P. Zhang,[1,3] Y.F. Zhang,[6] Yi Zhang,[1,14] Yong Zhang,[1,3] B. Zhao,[6] J. Zhao,[1,3] L. Zhao,[13,12] L.Z. Zhao,[11] S.P. Zhao,[14] X.H. Zhao,[25] F. Zheng,[33] W.J. Zhong,[7] B. Zhou,[1,3] H. Zhou,[9] J.N. Zhou,[16] M. Zhou,[32] P. Zhou,[7] R. Zhou,[27] X.X. Zhou,[1,2,3] X.X. Zhou,[6] B.Y. Zhu,[12,14] C.G. Zhu,[21] F.R. Zhu,[6] H. Zhu,[19] K.J. Zhu,[1,2,3,13] Y.C. Zou,[34] and X. Zuo[1,3]

(The LHAASO Collaboration)*

[1] *Key Laboratory of Particle Astrophysics & Experimental Physics Division & Computing Center, Institute of High Energy Physics, Chinese Academy of Sciences, 100049 Beijing, China*
[2] *University of Chinese Academy of Sciences, 100049 Beijing, China*
[3] *Tianfu Cosmic Ray Research Center, 610000 Chengdu, Sichuan, China*
[4] *Dublin Institute for Advanced Studies, 31 Fitzwilliam Place, 2 Dublin, Ireland*
[5] *Max-Planck-Institut for Nuclear Physics, P.O. Box 103980, 69029 Heidelberg, Germany*
[6] *School of Physical Science and Technology & School of Information Science and Technology, Southwest Jiaotong University, 610031 Chengdu, Sichuan, China*
[7] *School of Astronomy and Space Science, Nanjing University, 210023 Nanjing, Jiangsu, China*
[8] *Center for Astrophysics, Guangzhou University, 510006 Guangzhou, Guangdong, China*
[9] *Tsung-Dao Lee Institute & School of Physics and Astronomy, Shanghai Jiao Tong University, 200240 Shanghai, China*
[10] *Institute for Nuclear Research of Russian Academy of Sciences, 117312 Moscow, Russia*
[11] *Hebei Normal University, 050024 Shijiazhuang, Hebei, China*
[12] *University of Science and Technology of China, 230026 Hefei, Anhui, China*
[13] *State Key Laboratory of Particle Detection and Electronics, China*
[14] *Key Laboratory of Dark Matter and Space Astronomy & Key Laboratory of Radio Astronomy, Purple Mountain Observatory, Chinese Academy of Sciences, 210023 Nanjing, Jiangsu, China*
[15] *Research Center for Astronomical Computing, Zhejiang Laboratory, 311121 Hangzhou, Zhejiang, China*
[16] *Key Laboratory for Research in Galaxies and Cosmology, Shanghai Astronomical Observatory, Chinese Academy of Sciences, 200030 Shanghai, China*
[17] *School of Physics and Astronomy, Yunnan University, 650091 Kunming, Yunnan, China*
[18] *Key Laboratory of Cosmic Rays (Tibet University), Ministry of Education, 850000 Lhasa, Tibet, China*
[19] *National Astronomical Observatories, Chinese Academy of Sciences, 100101 Beijing, China*

(Dated: August 27, 2024)

On October 9, 2022, the Large High Altitude Air Shower Observatory (LHAASO) reported the observation of the very early TeV afterglow of the brightest-of-all-time GRB 221009A, recording the highest photon statistics in the TeV band ever obtained from a Gamma-ray burst. We use this unique observation to place stringent constraints on an energy dependence of the speed of light in vacuum, a manifestation of Lorentz invariance violation (LIV) predicted by some quantum gravity (QG) theories. Our results show that the 95% confidence level lower limits on the QG energy scales are $E_{\rm QG,1} > 10$ times of the Planck energy $E_{\rm Pl}$ for the linear, and $E_{\rm QG,2} > 6 \times 10^{-8} E_{\rm Pl}$ for the quadratic LIV effects, respectively. Our limits on the quadratic LIV case improve previous best bounds by factors of 5–7.

LHAASO collaboration, 2402.06009

PBH by LHAASO

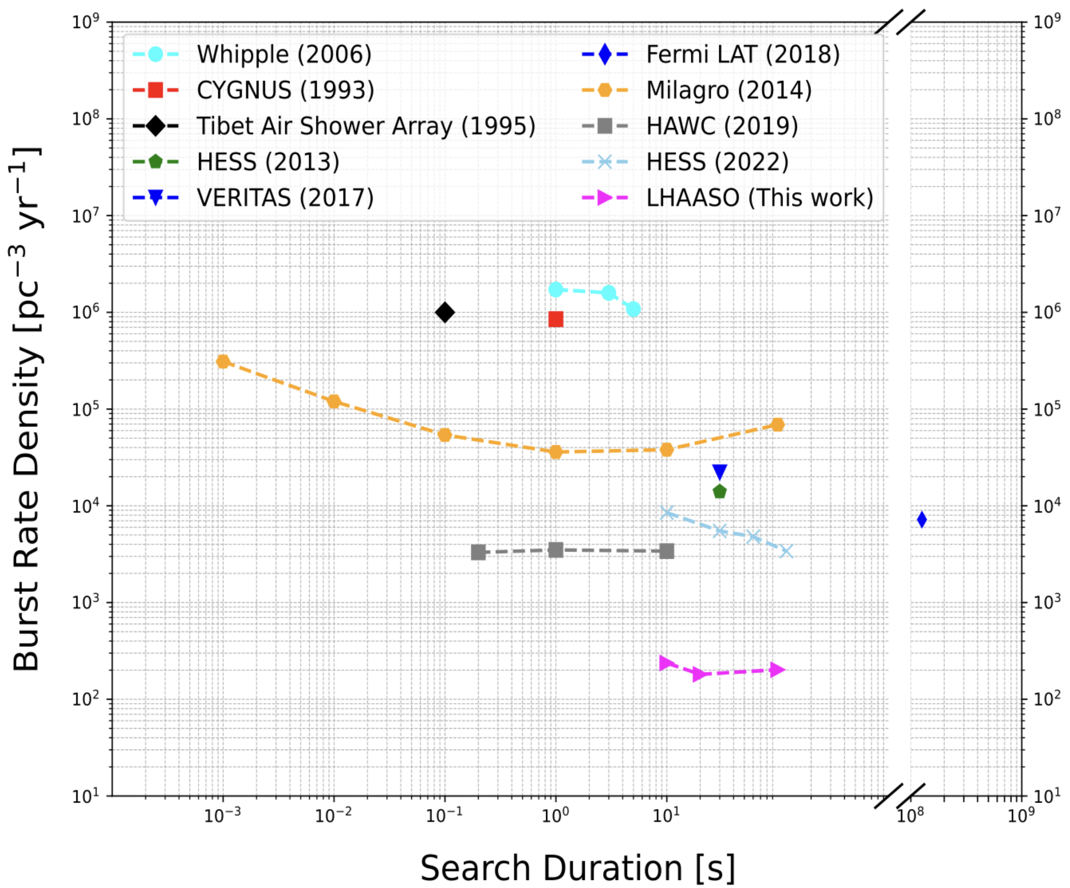

LHAASO collaboration, 2505.24586

Summary

- Construction of LHAASO finished in July 2021. LHAASO operates with almost 100% duty cicle. It's one year sensitivity is better compared to 50 hours for present Cherenkov telescopes above few TeV. Above 20 TeV it is better as compared to future CTA.
- First results on logA of cosmic rays are very promising. For the first time we see proton spectrum at Earth. Combination of proton spectrum, total flux and logA constrain models at knee.
- LHAASO presented first catalog of 90 gamma-ray sources from about 2 first years of observation. 32 are new sources. Number of UHE gamma-ray sources above 100 TeV increased from 4 to 43 by LHAASO observations
  - 35 sources are PWN. Crab, Geminga, milisecond pulsar
  - 7 SNR, gamma-Cygni can not be explained by leptons
  - Star clusters Cygnus, w43
  - AGN: Mkn421, Mkn501, M87 are seen, many more sources in next years

Summary

- Diffuse emission from Galaxy: new models requred
- GRB 221009A: detailed properties of GRB afterglow from 65000 photons in LHAASO WCDA. No new physics in KM2a, but constraints on EBL models/intrinsic spectrum from 10 TeV photons
- Cygnus region: hadronic Pevatron source in central part.
- Micro-quasars: hadronic sources with maximum energy up to 10 PeV
- Dark Matter: limits from dwarf Galaxies improved by 2 orders of magnitude for M_DM=1-10 PeV
- Better limit on PBH evaporation